

Dissertation

Effects of Extracorporeal Photopheresis on White Blood Cells in Patients with acute and chronic Graft versus Host Disease

ausgeführt zum Zwecke der Erlangung des akademischen Grades eines Doktors
der technischen Wissenschaften / der Naturwissenschaften unter der Leitung von

O.Univ.Prof. Dipl.-Ing. Dr.techn. Herbert Stachelberger

Inst. f. Verfahrens- und Umwelttechnik und Techn. Biowissenschaften E166

in Zusammenarbeit mit der

Klinik für Innere Medizin I / Knochenmarktransplantation, MUW Wien

unter der Leitung von

Univ.Prof. Dr. med. Hildegard Greinix

eingereicht an der Technischen Universität Wien

Fakultät für Technische Chemie (E150)

von

Roman Weigl

9327401

Neusiedlgasse 7, 2105 Oberrohrbach, NÖ

Wien, am 9. Oktober 2005



Eidesstattliche Erklärung

Ich erkläre hiermit an Eides statt, dass ich die vorliegende Dissertation selbständig erfasst, andere als die angeführten Quellen und Hilfsmittel nicht benutzt und mich auch sonst keiner unerlaubten Hilfe bedient habe, und dass ich diese Dissertation bisher weder im Inland noch im Ausland in irgendeiner Form als Prüfungsarbeit vorgelegt habe.

Wien, Oktober 2005

Danksagung

An dieser Stelle möchte ich mich recht herzlich bei allen Menschen bedanken, die mich beim Zustandekommen dieser Arbeit direkt oder auch indirekt unterstützt haben.

Zunächst ein Dankeschön an meine Eltern und Großeltern, die immer bemüht waren, mir die bestmögliche Ausbildung zukommen zu lassen. Durch ihre Unterstützung und Vertrauen in meine Fähigkeiten konnte ich wertvolle Kraft für meinen Ausbildungs- und Berufsweg schöpfen.

Für die problemlose Zusammenarbeit der Institute danke ich besonders Prof. Dr. med. Paul Höcker und Prof. Dr. med. Nina Worel (Universitätsklinik für Blutgruppenserologie und Transfusionsmedizin) und Prof. Dr. med. Robert Knobler (Universitätsklinik für Dermatologie).

Prof. DI Dr. Herbert Stachelberger, als Betreuer an der TU Wien, möchte ich in seiner Funktion als betreuender Professor danken.

Prof. Dr.med. Hildegard Greinix, der Leiterin des EU-Projektes TRANS-EUROPE Vienna an der Universitätsklinik für Innere Medizin I / Knochenmarktransplantation, möchte ich in ihrer Funktion als betreuende Professorin besonders danken. Das freundschaftliche Arbeitsklima, inspirative Fachdiskussionen und die fortschrittliche Infrastruktur sind einzigartige Voraussetzungen und waren optimale Stützen für das Zustandekommen dieser Dissertation.

Ein großes Dankeschön auch an die Ärzte, Pfleger und Schwestern aller Universitätskliniken für die Organisation der Blutprobennahme. Vielen Dank auch an meine Kollegen in der Arbeitsgruppe, Karin Feldmann, DI Dr. Elahi Faroborz für ihre Unterstützung und Zusammenarbeit.

Kurzfassung

Grundlagen

Zytokine von T-Helfer Zellen Typ 1 (Th1) scheinen für die Pathogenese von Graft-versus-host Disease (GvHD) mit verantwortlich zu sein. Die Extracorporeale Photochemotherapie (ECP) wird berichtet, verursacht Apoptose in behandelten Leukozyten, beeinflusst das Th1/Th2-Lymphozyten Verhältnis und beeinflusst auch die Balance der zytotoxischen T-Zellen (Tc1/Tc2). Die Entwicklung der dendritischen Zellen (DC) im peripheren Blut scheint eine einfache und reproduzierbare Vorhersage für Rückfälle, GvHD und Überleben nach peripherer Blutstammzellen Transplantation (PBSCT) zu sein.

Ziele

In dieser Studie wurde zur Beschreibung der ECP das Zytokinprofil in peripherem Blut (PB) von Patienten mit akuter und chronischer GvHD bestimmt. Zusätzlich wurden die Leukozytensubpopulationen und DC im PB nach PBSCT bestimmt.

Patienten und Methoden

Insgesamt wurden 64 Patienten und 18 gesunde Freiwillige untersucht. PB wurde vor, während und nach ECP Therapie abgenommen. Die Lymphozyten im PB wurden isoliert, stimuliert und anschließend die intrazelluläre Bildung von Zytokinen bestimmt. Mit fluoreszierenden monoklonalen Antikörpern gegen die Th1-Zytokine IL-2, TNF- α , INF- γ und die Th2-Zytokine IL-4 und IL-10 wurden in den zuvor blockierten CD4+ und CD8+ T-Zellen bestimmt. ECP behandelte Zellen wurden *in vitro* kultiviert und die Vitalität der Lymphozyten mittels AnnexinV und 7-AAD 10 und 24 Stunden nach ECP bestimmt. Die Oberflächenfärbung von DC und Leukozytensubpopulationen wurde mit fluoreszierenden monoklonalen Antikörpern durchgeführt.

Resultate

Wir haben gezeigt, dass ECP eine rasche und signifikante Abnahme der Zytokineproduktion in behandelten CD4+ und CD8+ T Zellen verursacht, die innerhalb 24 Stunden zur Apoptose führt. Die Th1 und Th2 Zytokineproduktion stellte sich jedoch nicht als ein geeigneter Indikator für die Wirksamkeit der ECP Therapie heraus. Unsere Ergebnisse betreffend zirkulierende DC scheinen mit der derzeitigen Theorien über die Pathogenese von GvHD überein zu stimmen. Die Überwachung der Leukozytensubpopulationen von 38 Patienten wurde durchgeführt, jedoch sind für statistisch signifikante Aussagen höhere Fallzahlen erforderlich.

Schlussfolgerungen

Die Fortführung der Überwachung der Entwicklung der peripheren Leukozyten scheint ein geeignetes Instrument zu sein die Therapien zu optimieren.

Abstract

Background

Cytokines derived from T helper (Th)1 lymphocytes are thought to be involved in the pathogenesis of graft-versus-host disease (GvHD). Extracorporeal photopheresis (ECP) has been reported to cause apoptosis in treated leukocytes and affect Th1/Th2 lymphocyte ratios and also influence the balance of cytotoxic T cells (Tc1/Tc2). Dendritic cell recovery in peripheral blood is thought to be a simple and reproducible predictor for clinical outcomes of relapse, GvHD and survival after peripheral blood stem cell transplantation (PBSCT).

Objectives

This study was performed to assess the effect of ECP on the cytokine profile of peripheral blood (PB) lymphocytes from patients with acute and chronic GvHD. The development of leukocyte subsets and circulating dendritic cells after PBSCT was monitored additionally.

Patients and methods

Sixty-four patients and 18 healthy volunteers were studied. Peripheral blood was sampled at baseline, during and after ECP therapy. Intracytoplasmatic cytokine production was assessed in vitro by stimulating PB lymphocytes, inhibiting cytokine release and staining with fluorescein-labeled monoclonal antibodies to Th1-cytokines interleukin (IL)-2, tumor necrosis factor alpha (TNF- α), interferon gamma (IFN- γ) and Th2-cytokines IL-4 and IL-10 on both CD4+ and CD8+ T cells. ECP treated cells were cultured in vitro and apoptosis was assessed with AnnexinV and 7-AAD at 10 and 24 hours. Surface staining of dendritic cells and leukocyte subsets in whole peripheral blood was performed with fluorescein-labeled monoclonal antibodies.

Results

We have shown that ECP causes a rapid and significant decrease of treated cytokine producing CD4+ and CD8+ T cells leading to apoptosis within 24 hours. However, Th1 and Th2 cytokine production was found to be not predictive for the efficacy of ECP. Our findings of circulating dendritic cells appear to be consistent with current theories regarding the pathogenesis of GvHD as decreased production of DC2 might be expected to exacerbate GvHD. Monitoring leukocyte subsets of 38 patients was performed, but further patients are necessary to obtain statistically significant results.

Further monitoring of the development of peripheral white blood subsets has been found to be an adequate instrument for optimizing therapies.

Key words:

Extracorporeal photopheresis, graft-versus-host disease, lymphocytes, apoptosis, tumor necrosis factor alpha, interferon gamma, interleukin-2, interleukin-4, interleukin-10, dendritic cells, NK cells, cytotoxic cells

Table of Contents

Chapter 1 Introduction	1
1. Haematopoietic Stem Cell Transplantation (HSCT)	1
1.1. Classification	1
1.2. Indications for HSCT	2
1.3. Conditioning Regimen	2
1.4. Haematopoietic stem cells for HSCT	4
2. Graft-versus-Host Disease	5
2.1. Classification of GvHD	5
2.2. GvHD Prophylaxis and Therapy	7
2.3. Immunosuppressive Agents	8
3. Extracorporeal Photochemotherapy	10
3.1. Overview	10
3.2. Application	10
3.3. Administration of ECP and 8-methoxypsoralen (8-MOP)	11
3.4. Mechanisms of action of ECP	11
Chapter 2 Aim of Study	13
Chapter 3 Material and Methods	14
1. Patients	14
1.1. Intracytoplasmatic Cytokine Production of stimulated T cells during ECP-Treatment of Patients with acute GvHD	14
1.2. Intracytoplasmatic Cytokine Production of stimulated T cells during ECP-Treatment of Patients with chronic GvHD	15
1.3. Apoptosis of White Blood Cells after Extracorporeal Photochemotherapy of Patients with acute GvHD	15
1.4. Apoptosis of White Blood Cells after Extracorporeal Photochemotherapy of Patients with chronic GvHD	15
2. Extracorporeal Photochemotherapy	16
3. Sample Collection and MNC Separation	17
4. Assessment of Intracytoplasmatic Cytokine Staining	17

5. Assessment of Apoptosis	18
6. Assessment of Circulating Whole Blood Cells	18
7. Flow Cytometry	19
7.1. Overview	19
7.2. The Fluidics System	19
7.3. The Optics System	20
7.4. Fluorescence	22
7.5. Optical Filters and Mirrors	26
7.6. The Electronics System	27
7.7. Acquisition of Flow Cytometric Data	28
8. Statistical Analysis	34
8.1. Intracytoplasmatic Cytokine analyses of Patients with aGvHD	34
8.2. Intracytoplasmatic Cytokine Analyses of Patients with cGvHD	35
8.3. Apoptosis of White Blood Cells after Extracorporeal Photochemotherapy	35
Chapter 4 Results	36
1. Analyses of Patients with acute Graft-versus-Host Disease	36
1.1. Development of Leukocyte Subpopulations of Patients with High Risk of acute GvHD after Haematopoietic Stem Cell Transplantation	37
1.2. CD4/CD8 T cell Ratio in Patients with acute steroid-refractory GvHD during ECP	48
1.3. Intracytoplasmatic Cytokine Production of stimulated T cells during ECP-Treatment of Patients with acute GvHD	51
1.4. Apoptosis of White Blood Cells after Extracorporeal Photochemotherapy of Patients with acute GvHD	57
1.5. Recovery of Dendritic Cells in Patients after Haematopoietic Stem Cell Transplantation	61
2. Analyses of Patients with chronic Graft-versus-Host Disease	68
2.1. Overview	68
2.2. Intracytoplasmatic Cytokine Production of stimulated T cells during ECP-Treatment of Patients with chronic GvHD	68
2.3. Apoptosis of White Blood Cells after Extracorporeal Photochemotherapy of Patients with chronic Graft-versus-Host Disease	75
2.4. Comparison of Apoptosis of Leukocyte Subsets of Patients with aGvHD and cGvHD during ECP	76
Chapter 5 Comparison and Conclusions	79

1. ECP and Apoptosis	79
1.1. General	79
1.2. Comparable Literature	80
1.3. Conclusions	81
1.4. ECP and Immunomodulation	82
1.5. Immunological Aspects of aGvHD	83
1.6. Conclusions	84
2. Immunological Aspects of cGvHD	85
2.1. Effects of ECP on cGvHD	85
2.2. Conclusions	86
3. Development of White Blood Cells after SCT	87
3.1. Development of Leukocytes Subsets after SCT	87
3.2. Development of Dendritic Cells after SCT	89
3.3. Conclusions	91
Abbreviations	93
Appendix A Cell Separation Protocol	97
Appendix B Intracytoplasmatic Cytokine Staining Protocol	98
Appendix C Staining protocol of Whole Blood Cell Subpopulations	105
Appendix D 4-Color Analyses of Intracytoplasmatic Cytokines	109
Appendix E 4-Color-Analyses Protocol of CD4+ and CD8+ T Cells Apoptosis	114
Appendix F 4-Color-Analyses Protocol of NK cells Apoptosis	119
Appendix G 4-Color-Analyses of Dendritic Cells	123
Appendix H 4-Color-Leukocyte Differentiation Analysis	128
Appendix I T Cell Differentiation Analyses	132
References	135

Table of Figures

<i>Figure 1-1: Scheme of Haematopoietic Stem Cell Transplantation.....</i>	<i>3</i>
<i>Figure 1-2: A scheme of the pathogenetic mechanisms of acute GvHD.....</i>	<i>6</i>
<i>Figure 3-1: Scheme of practicing of Extracorporeal Phototherapy.....</i>	<i>17</i>
<i>Figure 3-2: FACScalibur™ Fluid System.....</i>	<i>20</i>
<i>Figure 3-3: Light-Scattering Properties of a Cell.....</i>	<i>21</i>
<i>Figure 3-4: FACScalibur™ Optics System.....</i>	<i>22</i>
<i>Figure 3-5: Excitation and Emission Spectra of FITC, PE, PerCP and APC.....</i>	<i>24</i>
<i>Figure 3-6: Excitation and Emission Spectra of FITC, PE, PE-Cy7 and APC.....</i>	<i>25</i>
<i>Figure 3-7: Excitation and Emission Spectra of FITC, PE, 7-AAD and Cy5.....</i>	<i>26</i>
<i>Figure 4-1: The T-cell receptor complex, CD3, DC4 and CD8 chains.....</i>	<i>38</i>
<i>Figure 4-2: Leukocyte Subpopulations of Healthy Volunteers.....</i>	<i>41</i>
<i>Figure 4-3: Development of CD4/CD8 ratio of patients after HSCT.....</i>	<i>43</i>
<i>Figure 4-4: Development of Leukocytes of patients after HSCT.....</i>	<i>44</i>
<i>Figure 4-5: Development of NK cells of patients after HSCT.....</i>	<i>45</i>
<i>Figure 4-6: Development of T-lymphocytes of patients after HSCT.....</i>	<i>46</i>
<i>Figure 4-7: Development of monocytes of patients after HSCT.....</i>	<i>47</i>
<i>Figure 4-8: CD4/CD8 ratio of peripheral blood of ECP treated patients with aGvHD.....</i>	<i>50</i>
<i>Figure 4-9: IL-2 Production of CD4+ T cells in patients with aGvHD treated with ECP.....</i>	<i>52</i>
<i>Figure 4-10: IL-2 Production of CD8+ T cells in patients with aGvHD treated with ECP.....</i>	<i>52</i>
<i>Figure 4-11: INF-γ Production of CD4+ T cells in patients with aGvHD treated with ECP.....</i>	<i>52</i>
<i>Figure 4-12: INF-γ Production of CD8+ T cells in patients with aGvHD treated with ECP.....</i>	<i>53</i>
<i>Figure 4-13: TNF-α Production of CD4+ T cells in patients with aGvHD treated with ECP.....</i>	<i>53</i>
<i>Figure 4-14: TNF-α Production of CD8+ T cells in patients with aGvHD treated with ECP.....</i>	<i>53</i>
<i>Figure 4-15: IL-4 Production of CD4+ T cells in patients with aGvHD treated with ECP.....</i>	<i>54</i>
<i>Figure 4-16: IL-4 Production of CD8+ T cells in patients with aGvHD treated with ECP.....</i>	<i>54</i>
<i>Figure 4-17: IL-10 Production of CD4+ T cells in patients with aGvHD treated with ECP.....</i>	<i>55</i>
<i>Figure 4-18: IL-10 Production of CD8+ T cells in patients with aGvHD treated with ECP.....</i>	<i>55</i>
<i>Figure 4-19: Cumulative Cytokine Production of CD4+ T cells during ECP.....</i>	<i>56</i>
<i>Figure 4-20: Summarized Cytokine Production of CD8 positive T cells.....</i>	<i>56</i>
<i>Figure 4-21: Overview of Key Apoptotic Events.....</i>	<i>59</i>
<i>Figure 4-22: Interpolated 10-hour-point and 24-hour-point of apoptosis of CD4+ and CD8+ T cells of patients with aGVHD.....</i>	<i>60</i>
<i>Figure 4-23: The pluripotent haematopoietic stem cell gives rise to CD34+ precursors which proliferate and differentiate into DC populations.....</i>	<i>61</i>
<i>Figure 4-24: Healthy volunteers' dendritic cells and basophils.....</i>	<i>64</i>

Figure 4-25: Development of DC1 in patients after HSCT.....	65
Figure 4-26: Development of DC2 in patients after HSCT.....	66
Figure 4-27: Development of total circulating DC in patients after HSCT.....	67
Figure 4-28: Intracytoplasmatic cytokine Production of stimulated CD4+ T cells of seven patients during ECP-treatment.....	71
Figure 4-29: Summarized Cytokine Production of CD4 positive T cells.....	72
Figure 4-30: Intracytoplasmatic cytokine Production of stimulated CD8+ T cells of seven patients during ECP-Treatment.....	74
Figure 4-31: Cumulative Cytokine Production of CD8+ positive T cells.....	75
Figure 4-32: Interpolated 10-hour-point and 24-hour-point within apoptosis kinetics of CD4+ and CD8+ T cells of cGvHD patients.....	76
Figure 4-33: Comparison of interpolated 10-hour-point and 24-hour-point within apoptosis kinetics of CD3 lymphocytes of aGvHD and cGvHD patients.....	77
Figure 4-34: Comparison of interpolated 10-hour-point and 24-hour-point within apoptosis kinetics of CD4+ T cells of aGvHD and cGvHD patients.....	77
Figure 4-35: Comparison of interpolated 10-hour-point and 24-hour-point within apoptosis kinetics of CD8+ T cells of aGvHD and cGvHD patients.....	78
Figure 4-36: Comparison of interpolated 10-hour-point and 24-hour-point within apoptosis kinetics of NK cells of aGvHD and cGvHD patients.....	78
Figure Appendix B-1: Time bars of working steps of Intracytoplasmatic cytokine Analysis.	104
Figure Appendix D-1: Spreadsheet of graphics output of a negative control sample of cytoplasmatic cytokine analysis.	111
Figure Appendix D-2: Spreadsheet of graphics output of a positive sample of cytoplasmatic cytokine analyses.....	112
Figure Appendix E-1: Spreadsheet of graphics output of a negative control analyzing early and late apoptotic CD4+ T cells and CD8+ cytotoxic T cells.....	116
Figure Appendix E-2: Spreadsheet of graphics output of a sample analyzing early and late apoptotic CD4+ T cells and CD8+ cytotoxic T cells.....	117
Figure Appendix F-1: Spreadsheet graphics output of a sample analyzing early and late apoptotic CD3+ T cells and CD3-CD56+ NK cells.	121
Figure Appendix F-2: Spreadsheet graphics output of a negative control analyzing early and late apoptotic CD3+ T cells and CD3-CD56+ NK cells.	122
Figure Appendix G-1: Spreadsheet graphics output of dendritic cell analyses.	125
Figure Appendix G-2: Discrimination of debris in panel 3 (CD3 versus CD45).....	126
Figure Appendix G-3: Density and dot plot of negative control discriminating the gate of CD11c.	126
Figure Appendix H-1: Spreadsheet graphics output of a sample of the leukocyte differentiation analysis.	130
Figure Appendix H-2: Part of the spreadsheet output of a negative control of the leukocyte differentiation analysis.....	131
Figure Appendix I-1: Spreadsheet graphics of a sample analyzing CD4+ and CD8+ T cells.	133

Table Index

<i>Table 4-1: Patient list of leukocyte subpopulation analyses and their categories.....</i>	<i>42</i>
<i>Table Appendix B-0-1: Applied Fluorescence Conjugated Antibodies of Intracytoplasmatic Cytokine Analyses</i>	<i>100</i>
<i>Table Appendix B-0-2: Applied Antibody Specifity and Working Concentrations of Intracytoplasmatic Cytokine Analyses</i>	<i>101</i>
<i>Table Appendix C-0-1: Applied Fluorescence Conjugated Antibodies of Whole Blood Analyses</i>	<i>106</i>
<i>Table Appendix C-0-2: Applied Antibody Specifity and Working Concentrations of Whole Blood Analyses</i>	<i>107</i>
<i>Table Appendix D-0-1: Gate list of Intracytoplasmatic analyses.....</i>	<i>113</i>
<i>Table Appendix G-0-1: Gate List of Dendritic Cell Analyses</i>	<i>127</i>
<i>Table Appendix I-0-1: Spreadsheet data file output of a sample analyzing CD4+ and CD8+ T cells.</i>	<i>134</i>

Chapter 1

Introduction

1. Haematopoietic Stem Cell Transplantation (HSCT)

Today, HSCT is used increasingly for the treatment of patients with haematologic and oncologic diseases and genetic disorders. There are 3 methods to obtain haematopoietic stem cells, bone marrow transplantation (BMT), peripheral blood stem cell transplantation (PBSCT), and cord blood transplantation (CBT) [1].

1.1. Classification

Depending on the source of haematopoietic stem cells, HSCT may be classified into three types:

- (1) Allogeneic transplants, in which a human leukocyte antigen-matched related (e.g., a sibling) or unrelated individual is the donor
- (2) Syngeneic transplants, in which the donor is a monozygotic twin; and
- (3) Autologous transplants, in which the patient's own harvested haematopoietic stem cells are transplanted.

A prerequisite for an allogeneic HSCT is the availability of a human leukocyte antigen (HLA) identical donor. Two sets of HLA antigens of major histocompatibility complex (MHC) Class I (A, B and C loci) and MHC Class II (HLA DR) (two loci each inherited on chromosome 6 from each parent) need to be identical in donor and recipient for a perfect histocompatible match. Molecular methods such as PCR amplification of HLA genes and the use of allele-specific or sequence-specific oligonucleotides, are available to define the suitability of a potential allogeneic donor more accurately.

1.2. Indications for HSCT

Allogeneic HSCT can cure patients suffering from haematologic and oncologic disorders that arise from the bone marrow. This is the case in chronic myelogenous leukaemia, acute myeloid and lymphocytic leukemia, myelodysplastic syndromes and multiple myeloma. In case of inborn or acquired bone marrow aplasia and immunodeficiencies, allogeneic HSCT can restore haematopoiesis and the immune system. Autologous HSCT allows restoration of haematopoiesis in patients with non-Hodgkin's lymphoma, Hodgkin's disease and myeloma after high-dose therapy.

1.3. Conditioning Regimen

Patients must undergo a conditioning regimen before the infusion of haematopoietic stem cells.

1.3.1. Myeloablative Conditioning

In conventional HSCT this conditioning regimen accomplishes several functions. First, it serves to ablate the recipient's bone marrow (=myeloablative conditioning), thereby allowing repopulation of the bone marrow with donor cells. Second, the conditioning regimen may include more rigorous chemotherapy designed to treat malignant cells spread potentially throughout the body (e.g., in the treatment of leukaemia). Finally, it must immunosuppress the host's immune system sufficiently to prevent rejection of the infused allogeneic stem cells, the frequently fatal result of such rejection being engraftment failure. Such conditioning regimens thus typically consist of various chemotherapeutic agents (e.g., cyclophosphamide, busulfan, or cytosine arabinoside) with or without total body irradiation (TBI). The bone marrow becomes aplastic following conditioning with high-dose chemotherapy and/or total body irradiation. Engraftment of donor stem cells and haematologic recovery ensues within 14 to 21 days following infusion of marrow or peripheral blood stem cells. The major causes of morbidity and mortality include infections, graft rejection, venoocclusive disease of the liver, and graft-versus-host disease. In Figure A.1 the scheme of allogeneic HSCT is shown.

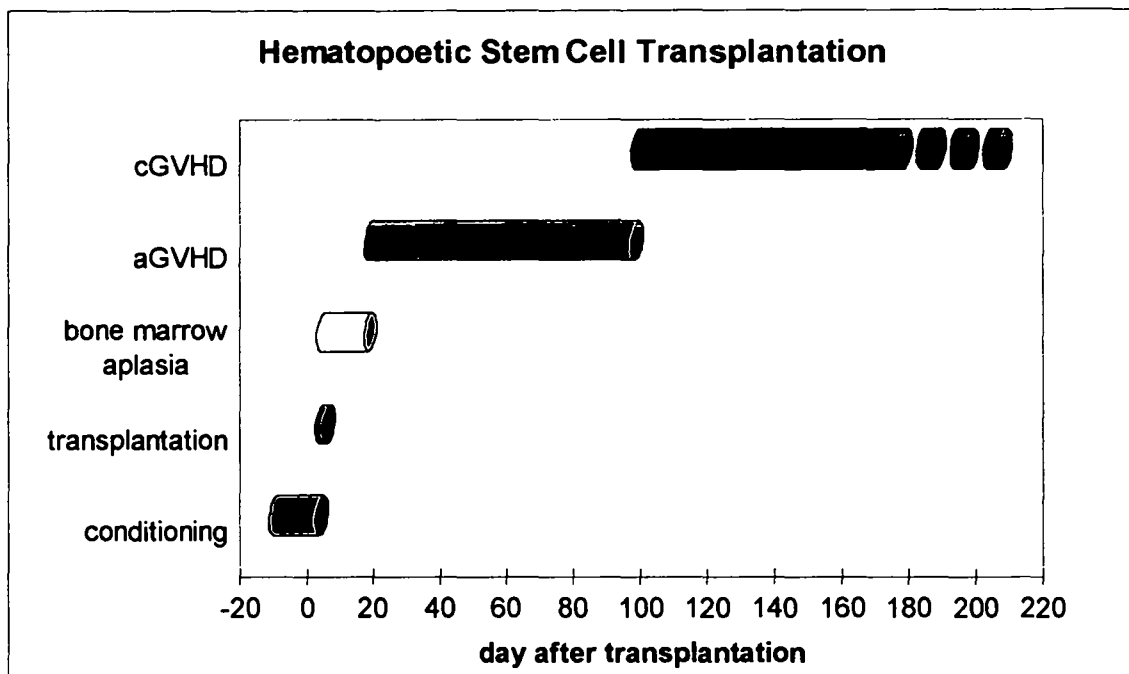


Figure 1-1: Scheme of Haematopoietic Stem Cell Transplantation

1.3.2. Reduced-Intensity Conditioning (RIC)

In the 1990's the emphasis switched to concepts focusing on reducing transplant-related mortality (TRM) and morbidity, with subsequent improvements in quality of life. Better understanding of graft-versus-leukemia (GvL) effects and the factors associated with its induction, the recognition of the capacity of donor lymphocyte infusion to shift the balance between donor and recipient in a predictable way, and preclinical experiments which defined the minimal requirements for stable engraftment led to the introduction of a new concept: Conditioning regimens without primary goal of myeloablation. Initial success was evident. Engraftment with complete donor chimaerism became possible with minimal early toxicity even in patients with advanced age or comorbidities or who received a second HSCT. A wealth of different conditioning regimens followed and new terminology, e.g. "mini"-transplants, "micro"-transplants or non-myeloablative transplants became abundant. Today, the preferred term is "reduced-intensity conditioning" transplants or RIC HSCT. Current data show clearly that the RIC approach is feasible and specifically attractive for patients with advanced age and high risk for TRM [2-4] or to investigate new indications, such as allo-HSCT for solid tumors.

1.4. Haematopoietic stem cells for HSCT

The population of CD34-positive cells contains the very early haematopoietic cells (stem cells) capable of repopulating the ablated bone marrow as well as generating and maintaining long-term haematopoiesis. Therefore, the CD34 antigen is used to measure haematopoietic stem cells for clinical and experimental use. CD34-positive cells can be detected in bone marrow, peripheral blood and cord blood.

1.4.1. Bone Marrow (BM)

Bone marrow contains haematopoietic stem cells and progenitor cells, stromal supportive elements, and other regulatory/facilitating components such as T-lymphocytes and mesenchymal stem cells. BM can be harvested by aspiration through multiple needle punctures of the iliac crest in general anesthesia.

1.4.2. Peripheral Blood Stem Cells (PBSC)

During the last years BM harvests have been replaced in the majority of donors by PBSC collection. In the blood stream, the number of stem cells is about 1/100 of that in the bone marrow. To improve the yield and quality of PBSC, the donor undergoes mobilization of stem cells by receiving subcutaneous injections of the cytokine granulocyte colony-stimulating factor (G-CSF) for four to five days. After *in vivo* cytokine stimulation the donors undergo an apheresis procedure. Thereby, the donor is connected to a cell separator via a needle in each arm. Blood is taken from one arm, circulated through the machine to remove the stem cells, and the remaining blood cells and plasma are returned to the donor through the other arm.

After PBSC transplantation haematologic recovery is faster than after BM infusion. In addition, donors do not have to undergo anesthesia for BM harvest and therefore, prefer PBSC collection.

1.4.3. Cord Blood Stem Cells (CB)

In patients without a suitable BM or PBSC donor, frozen cord blood from an unrelated donor can be used as stem cell alternative for allogeneic HSCT. The main complications of CB transplantation are delayed haematologic recovery with increased rates of infection and graft rejection.

2. Graft-versus-Host Disease

Allogeneic haematopoietic stem cell transplantation is associated with serious side-effects, the most common of which is graft-versus-host disease (GvHD). Despite advances in histocompatibility matching and immunosuppressive drugs, GvHD remains a significant cause of morbidity and mortality after HSCT. Billingham et al [5] defined as prerequisite for the development of GvHD that immunologically competent cells within the graft recognize tissues or cells of a severely immunosuppressed host as foreign. The immunologic event leading to injury of the target organs skin, liver and gut involves activation and clonal expansion of the donor's effector T-cells in response to the patient's disparate major or minor histocompatibility antigens.

2.1. Classification of GvHD

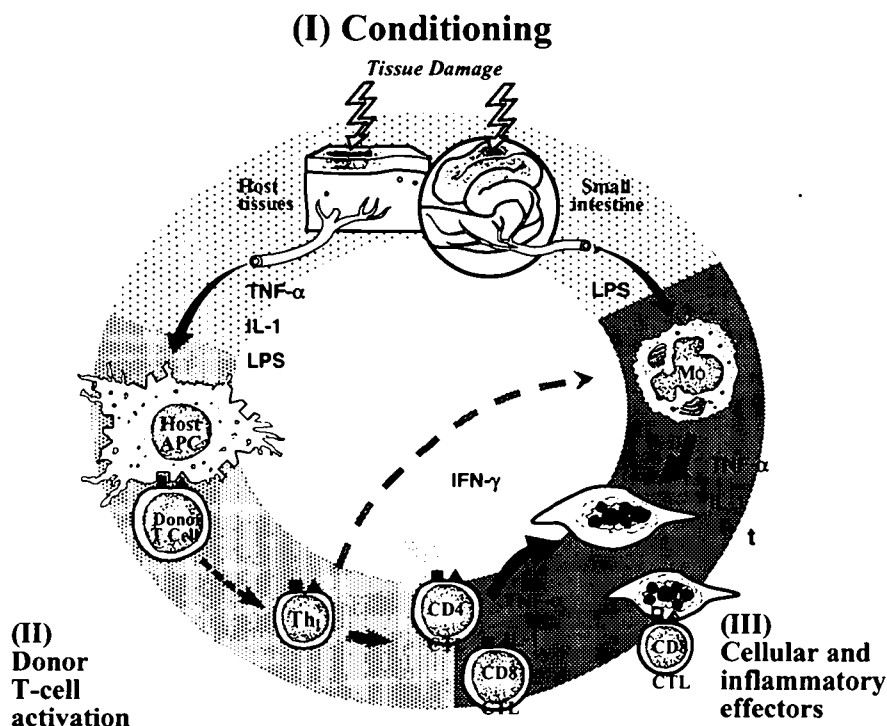
GvHD can be classified as acute or chronic based on timing of onset and clinical features. The two differ in many respects in terms of pathogenesis, reflecting the complexity of the immunological response. The timing of both indications of GvHD is shown in Figure A.1.

2.1.1. Acute GvHD

Acute GvHD (aGvHD) usually develops within the first three months of haematopoietic stem cell transplantation with a median onset of about 3 weeks [6]. Main target organs include the skin, gastrointestinal tract and liver. Acute GvHD is graded from I to IV based on pattern and severity of organ involvement and assessment of clinical performance. Higher grades are associated with increased morbidity and mortality of acute GvHD.

Current evidence suggests that dysregulated cytokine production during sequential monocyte and T-cell activation is responsible for many manifestations of acute GvHD. Damage of host tissues by the conditioning regimen results in the release of the inflammatory cytokines tumor necrosis factor alpha (TNF- α) and interleukins (IL)-1 and -6 which increase the constitutive expression of HLA and other critical adhesion molecules and contribute to increased activation of donor T-cells present in the donor marrow inoculum. The T-lymphocytes secrete predominantly IL-2 and interferon gamma (IFN- γ) inducing cytotoxic T-lymphocyte (CTL) and NK cell responses, and

priming monocytes to produce IL-1 and TNF- α . These inflammatory effectors act in synergy with T and NK-cell mediated cytotoxicity in producing the systemic morbidity of GvHD-associated immunosuppression.



Reddy P.: Hematol Oncol. 2003 Dec;21(4):149-61.

Figure 1-2: A scheme of the pathogenetic mechanisms of acute GvHD

1.1.1 Chronic GvHD

Chronic GvHD develops usually around day 100 after HSCT either as an extension of acute GvHD, after a disease-free interval or with no precedent and may be limited or extensive. Chronic GvHD is a multi-organ autoimmune-like syndrome affecting mainly the skin and/or mucous membranes, liver and the immune system. Patients with extensive chronic GvHD have a high risk for opportunistic infections that can be lethal. Experimental and clinical studies have shown that thymic atrophy, lymphocyte depletion, and the loss of thymic epithelial secretory function may play a role in the pathogenesis of chronic GvHD. Chronic GvHD occurs in approximately 60-80% of those who survive over 100 days after allogeneic hematopoietic stem cell transplantation [7].

2.2. GvHD Prophylaxis and Therapy

For prevention of GvHD donor grafts were depleted of T-cells resulting in substantial reductions in incidence and severity of GvHD but also an increase in graft failure, relapse rates and slow immune reconstitution. Since 1985, *in vivo* immunosuppression after HSCT consisted mainly of the combination of cyclosporine A (CsA) and short-course methotrexate (MTX) which proved to be superior compared to the use of CsA or MTX as single agents.

At some centers, tacrolimus has replaced cyclosporine based on the results of two phase III clinical trials that showed a slight decrease in grade II to IV acute GvHD after prophylaxis with tacrolimus plus methotrexate compared with cyclosporine plus methotrexate.

Despite improvements in posttransplant immunosuppression, up to 30% of HLA-identical sibling graft recipients and up to 90% of patients receiving stem cells from unrelated donors still develop significant acute GvHD. Prednisone has been shown to be effective in the treatment of established acute GvHD. However, patients not responding to corticosteroids are at high risk of death due to overwhelming infections or organ failure. Monoclonal antibodies directed against cytokines, e.g. TNF- α or the IL-2 receptor appeared to be promising but most responses were not of sufficient duration.

Chronic GvHD affects 50% of long-term survivors and is lethal in 20% to 40% of affected patients, despite aggressive treatment. Standard first-line therapy for extensive chronic GvHD includes corticosteroids and CsA or Tacrolimus (FK506). Other therapeutic options are thalidomide, monoclonal antibodies and psoralen and ultraviolet A (PUVA). However, these therapies are often unsuccessful in patients with extensive multiorgan involvement and are associated with significant therapy-related complications.

2.3. Immunosuppressive Agents

Some of the most commonly used immunosuppressive agents for prevention and treatment of both acute and chronic GvHD are cyclosporine A, corticosteroids, tacrolimus, and mycophenolate mofetil.

2.3.1. Cyclosporine A

Cyclosporine A (CsA) is a metabolite obtained from two species of fungi isolated from soil samples collected in the Hardanger highlands of Norway in 1970 [8, 9]. It is a cyclic peptide consisting of 11 amino acid residues.

CsA binds to cyclophilin, and the CsA-cyclophilin complex binds to calcineurin, a calcium/calmodulin-dependent phosphatase (PP2B) and blocks its phosphatase activity [10]. Calcineurin might prevent the deletion of alloantigen reactive T-cells through inhibition of activation-induced cell death [11]. When T-cells were stimulated *in vitro* with PMA and ionomycin, CsA completely blocked the production of IL-10 but enhanced the production of IFN- γ . The later was also seen *in vivo*.

Short term treatment with cyclosporine after bone marrow transplantation was found to promote the development of durable tolerance [12].

Tajima et al [13] investigated the biological effects of CsA on human peripheral blood CD11c⁺ myeloid and CD11c⁻ lymphoid subsets. Addition of CsA substantially inhibited the up-regulation of the glycoprotein B7.1 (CD80) and B7.2 (CD86), but showed no effect on the expression of CD40 and HLA-DQ in either DC subsets. These inhibitory effects of CsA on DC maturation were manifested in a dose-dependent manner. CsA also modulated cytokine production from these DCs.

2.3.2. Corticosteroids

While the immunosuppressive effects of corticosteroids have not yet been fully elucidated, their actions appear to suppress phenotypic and functional dendritic cell maturation, and consequently enhance endocytic capacity mediated by intracellular glucocorticoid receptors (GR) [14, 15]. Steroid-GR complexes form dimers after migration into the nucleus, which are then thought to act as transcription factors that recognize GR binding motifs at target gene promoters, blocking the expression of various cytokines and enzymes [16, 17]. In addition, corticosteroids also appear to suppress transcription factors, such as activation protein-1 (Jun/Fos complex) and

nuclear factor-*kappa*B, thereby inhibiting the expression of molecules dependent on these factors including cytokines and various enzymes and receptors [18-20].

2.3.3. Tacrolimus

Tacrolimus (FK506) is a metabolite isolated from *Actinomyces* spp [21] and, like cyclosporine, forms a complex with a specific protein (FK506-binding protein [FKBP]) that then binds to calcineurin and inhibits its dephosphorylase activity [10]. This prevents the migration of the IL-2 gene transcription factor of activated T cells (NFAT) into the nucleus, therefore blocking subsequent IL-2 biosynthesis [22].

2.3.4. Sirolimus

Sirolimus (Rapamycin) is an immunosuppressive macrocyclic lactone, similar in structure to Tacrolimus. Contrary to expectations, both molecules are not competitive; in fact they appear to be synergistic. Sirolimus is free of nephrotoxicity and neurotoxicity, making combination therapy possible.

Sirolimus suppresses the generation of granulocyte-macrophage colony stimulating factor (GM-CSF)-expanded human monocyte-derived DC populations *in vitro* [23, 24] and the generation of flms-like tyrosine kinase 3 (flt3) ligand-expanded DC populations in mice *in vivo* [25]. Importantly, and in contrast to differentiation inhibitors such as corticosteroids, sirolimus quantitatively reduces growth-factor-induced expansion of DC populations, but does not impair DC differentiation qualitatively. Sirolimus also inhibits DC endocytosis in a DC-maturation-independent manner [25]. At low concentrations, rapamycin impairs macropinocytosis and mannose-receptor-mediated endocytosis of mouse bone-marrow-derived DCs [25]. These effects depend on the interaction of rapamycin with its intracellular receptor FKBP12, as shown by competitive experiments with a molar excess of FK506 (tacrolimus) and can therefore be considered as a specific drug-related effect [25, 24].

2.3.5. Mycophenolate mofetil

Mycophenolate mofetil (MMF), also known as RS-61443, is an ester of mycophenolic acid (MPA) that inhibits the *de novo* synthesis of guanine nucleotides [26]. Following

oral administration, MMF is hydrolyzed by esterase in the intestine and blood to release MPA. MPA exerts a more potent cytostatic effect on lymphocytes than on other cell types, such that its effect on lymphocytes is the principal mechanism of its immunosuppressive activity [27]. MMF in combination with cyclosporine and prednisolone is a useful treatment against GvHD [28], while cyclosporine plus MMF has been shown to be beneficial in GvHD prophylaxis for RIC-HSCT [29].

3. Extracorporeal Photochemotherapy

3.1. Overview

Phototherapy has been used both experimentally and clinically to treat GvHD. Antigen-presenting cells and T-lymphocytes are susceptible to photo-inactivation with a combination of ultraviolet A radiation and a photosensitizing agent such as 8-methoxypsoralen (8-MOP). In clinical practice UVA phototherapy is either administered to the skin surface (PUVA) or to leukocytes isolated from the patient (extracorporeal photochemotherapy or ECP).

3.2. Application

Extracorporeal photochemotherapy (ECP) was developed in the early 1980s and used clinically for the treatment of cutaneous T-cell lymphoma (CTCL) [30]. Nowadays, ECP is being investigated for the treatment of patients with selected autoimmune diseases and rejection after organ transplantation.

At the Medical University of Vienna, Department of Medicine I/BMT ECP has been investigated during the last years for treatment of steroid-refractory severe acute and chronic GvHD demonstrating that ECP can achieve high response rates with excellent overall survival and almost no side effects. Since there was no increase in rate of opportunistic infections or recurrence of neoplastic disease, ECP seems to be not broadly immunosuppressive and does not prevent primary responses to vaccination or other antigenic challenges [31].

3.3. Administration of ECP and 8-methoxypsoralen (8-MOP)

In ECP the patient's peripheral blood is removed and separated into leukocyte-depleted blood, which is returned to the patient, and leukocyte-enriched plasma, which is exposed to ultraviolet light in the presence of extracorporeally administered liquid 8-MOP.

8-MOP is a naturally occurring furocoumarin photoactive substance found in several species of plants, including *psoralea corylifolia*. Without UVA irradiation, the compound is biologically inert. Its reactive sites can be activated by exposure to UVA of the wavelength of 320-400nm. The planar structure of 8-MOP facilitates its intercalation between DNA base pairs and hydrogen-bond formation [32-34]. After the first UVA photon absorption it forms a mono-adduct (covalent bond with a thymine), then it can absorb a second photon and form an inter-strand crosslink between the thymine molecule from the adjacent base pairs (bi-adduct) [35]. Interaction with lipids includes covalent binding of psoralen to unsaturated fatty acids, and oxidation reactions [36]. Proteins like tyrosine, tryptophane, albumin, lysozyme, histone, or ribonuclease can also be affected by ECP with either formation of covalent bonds between two subunits, or by oxidation reactions [37] binding to a variety of cytosolic proteins leading to apoptosis of lymphocytes [38] and activation of antigen-presenting cells (APC) [39].

3.4. Mechanisms of action of ECP

The mechanism of action of ECP is thought to be due to immunomodulatory effects, based on clinical and experimental observations, but many aspects thereof still need to be better understood. It is known that 8-MOP binds to leukocyte DNA after photoactivation, thereby inhibiting DNA synthesis and repair enzymes causing a lethal defect. However, since in one ECP treatment only 2 to 5% of the patient's populations of mononuclear cells are affected, this direct action cannot fully explain the immunomodulatory effect of ECP.

Both in vitro PUVA as well as ECP are known to cause apoptosis of treated cells [40, 41]. About 24 hours after treatment, apoptosis of T-lymphocytes with DNA crosslinking, mitochondrial dysfunction, caspase activation and other cell damage can be found, but monocytes seem to be more resistant to apoptosis [42]. Apoptosis seems to have a crucial role in ECP, but its role may be different in different disorders. In GvHD patients

apoptosis may lead to deletion of graft reactive cells after tolerance induction by donor stem cells. However, in vitro data in GvHD are sparse.

A modulation of dendritic cell subpopulations and a shift in the subsets of effector T-cells from a cytokine profile associated with the T-helper type 1 phenotype to a T-helper type 2-dominated cytokine profile have also been observed.

Recently, Lamioni *et al.* [43] reported an increase in T-cells with a regulatory phenotype and strong suppressive activity after ECP in organ-transplanted patients.

Chapter 2

Aim of Study

For many years patients suffering of extensive chronic and steroid-refractory severe acute GvHD have been treated with extracorporeal photochemotherapy.

Thereby, excellent clinical responses can be achieved with minimal side effects. Despite the frequent use of ECP and the promising results published, the exact mechanisms why ECP works still remain unknown.

The aims of the presented work are

- to analyze the effects of UVA and 8-MOP on white blood cell subsets of patients with acute and chronic GvHD and healthy volunteers.
- to analyze changes in the populations of T-helper type 1 and T-helper type 2 cells of patients with acute and chronic GvHD treated with ECP.
- to find a predictive biomarker for response to ECP by analyzing blood cell subsets prior to and serially during ECP.

Chapter 3

Material and Methods

1. Patients

Informed consent was obtained from all patients and the ethics committee of the Medical University of Vienna approved the study.

Sixty four patients (32 men, 32 women) with a median age of 45 (range, 22 to 66) years receiving haematopoietic stem cell transplantation at our institution, were recruited for all studies. They had received allogeneic haemopoietic marrow (n=4) or blood stem cell transplants (n=60) from related (n=19) or unrelated (n=45) donors for treatment of acute myeloid leukaemia (n=27), acute lymphoblastic leukaemia (n=6), chronic myeloid leukaemia (n=11), myelodysplastic syndrome (n=9), aplastic anemia n=1, Morbus Hodgkin n=1, myeloma (n=2) or lymphoma (n=7).

Additionally a group of 18 volunteers (10 female, 8 men) with a median age of 45 (range, 25 to 66) were analysed at one time point and compared with the analyses.

Because of patients' health, each analysis has a different amount of patients and observations. Further details are shown in the chapter Results.

1.1. Intracytoplasmatic Cytokine Production of stimulated T cells during ECP-Treatment of Patients with acute GvHD

Sixteen patients (7 men, 9 women) with a median age of 40 (range, 22 to 54) years receiving ECP treatment at our institution, were recruited for this study. All patients had acute GvHD grades II to IV according to published criteria and were referred to ECP

because of unresponsiveness to corticosteroids. They had received allogeneic hemopoietic marrow (n=1) or blood stem cell transplants (n=15) from related (n=2) or unrelated (n=14) donors for treatment of acute myeloid leukemia (n=3), acute lymphoblastic leukemia (n=1), chronic myeloid leukemia (n=6), myelodysplastic syndrome (n=3), myeloma (n=2) and lymphoma (n=1). All patients had acute GvHD grades II to IV according to published criteria and were referred to ECP because of unresponsiveness to corticosteroids.

1.2. Intracytoplasmatic Cytokine Production of stimulated T cells during ECP-Treatment of Patients with chronic GvHD

Eight patients (6 men, 2 women) with a median age of 47 (range 22 to 64) years receiving ECP treatment at our institution, were recruited for this study.

All patients had chronic GvHD especially extensive liver (n=1), extensive skin (n=2), oral mucosa (n=1), ocular mucosa (n=1), immune system (n=1), myositis (n=1), extensive lungs (n=1) and were referred to ECP because of unresponsiveness to corticosteroids.

1.3. Apoptosis of White Blood Cells after Extracorporeal Photochemotherapy of Patients with acute GvHD

Eleven patients (5 men, 6 women) with a median age of 45 (range, 33 to 55) years receiving ECP treatment because of aGvHD at our institution, were recruited for this apoptosis study.

1.4. Apoptosis of White Blood Cells after Extracorporeal Photochemotherapy of Patients with chronic GvHD

Five patients (4 men, 1 women) with a median age of 42 (range, 22 to 61) years receiving ECP treatment at our institution, were recruited for this apoptosis study.

2. Extracorporeal Photochemotherapy

At our institution treatments are performed with the UVAR Photopheresis System (Therakos, UK) as shown in **Figure 3-1**. Blood is removed from the patient with an antecubital angiocatheter and passed through the device's centrifuge (apheresis). During the continuous leukapheretic processing, a total of approximately 240 ml of mononuclear cells and 300 ml of plasma are collected and diluted with 200ml of heparinized saline solution. 8-MOP (0.2 mg; UVADEX, Ben Venue Laboratories, Bredford OH, USA) is added to the final enriched lymphocyte solution containing 6×10^9 cells with a haematocrit of approximately 2.5 percent. The solution is passed as a 1-mm thick film through a disposable plastic device and exposed to a UVA radiation source ($2 \text{ J/cm}^2/\text{cell}$). The exposure time is dependent on the volume and haematocrit of the buffy coat (approx. 15-60 min). The cells are immediately reinfused after treatment [30]. ECP is performed on two consecutive days at 1 to 4 week intervals for varying lengths of time.

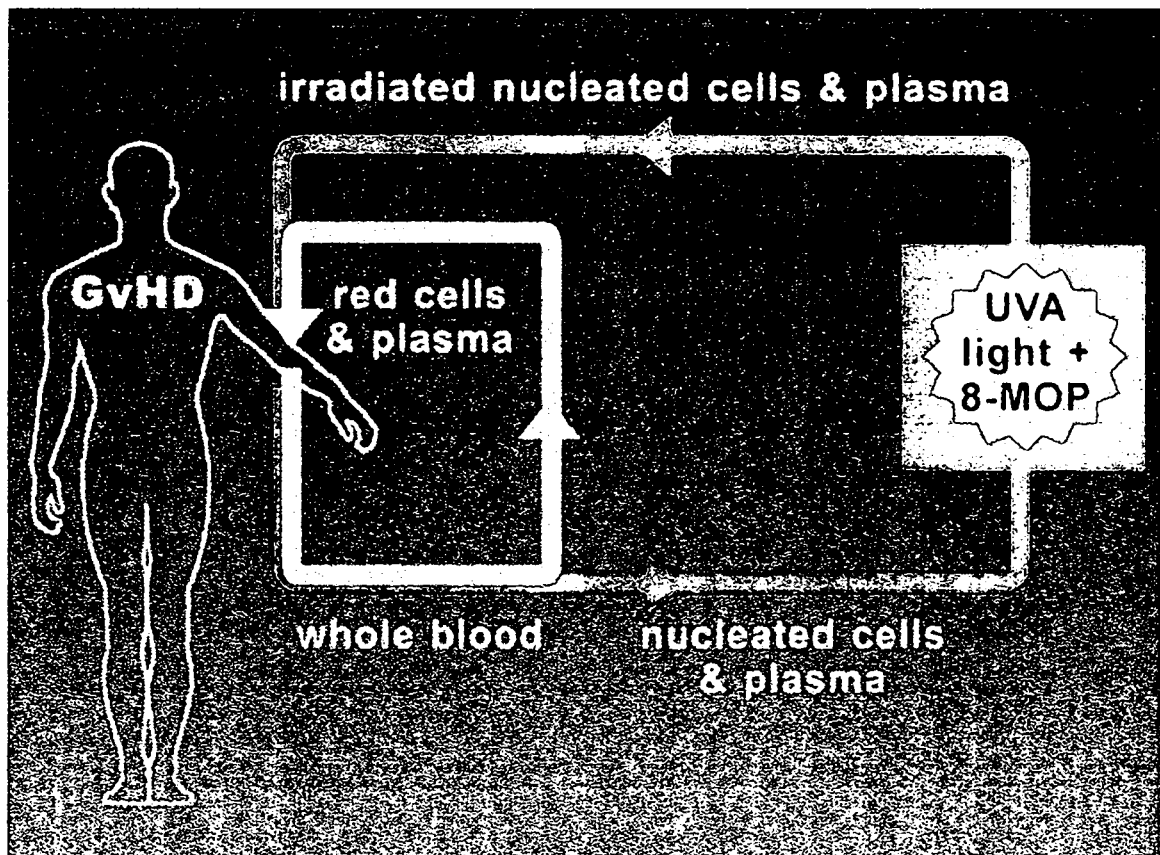


Figure 3-1: Scheme of practicing of Extracorporeal Phototherapy

3. Sample Collection and MNC Separation

Three heparinized PB samples were taken from each patient undergoing ECP therapy. The first was taken as venous blood immediately prior to ECP (PB), the second from the leukocyte collection before 8-MOP was added (PRE-ECP), the third from the bag after ECP treatment before reinfusion into the patient (POST-ECP).

Mononuclear cells (MNC) were separated using a density gradient (Biocoll; Biochrom AG, Germany), and washed with phosphate buffered saline (PBS, Gibco, Invitrogen, USA).

The protocol for MNC separation is included in Appendix A.

4. Assessment of Intracytoplasmatic Cytokine Staining

For intracellular cytokine measurement 3×10^6 MNC/ml were cultured in serum free culture medium (AIMV; Gibco), supplemented with 2mM L-Glutamin, 10µg/ml gentamycin sulphate, 50µg/ml streptomycin sulphate and 3.5µl/l 2-mercapto-ethanol (all Sigma, St. Louis, USA). Cells were stimulated in a volume of 5 ml with 10 ng/ml phorbol-12-myristate 13-acetate (PMA, Sigma) and 1.25 µg/ml ionomycin (Sigma) in a 25cm²-culture flask for 4 hours at 37°C in 5% CO₂. 10 µg/ml brefeldin A (Sigma) were added for cytoplasmic cytokine transport. Thereafter, cells were harvested, washed twice with PBS, and stained for the surface antigens CD4 (anti-CD4-APC, BD Bioscience, San Jose, CA, USA) and CD8 (anti-CD8-PE, Beckman Coulter, Fillerton, CA, USA) by antibody-incubation for 20 min at 4°C. Then, cells were washed in PBS, their plasma membrane was permeabilized and stained as described by the manufacturer (IntraPrep Permeabilization Reagent Kit, Beckman Coulter). Briefly, cells were fixed in 5.5% formaldehyde for 15 min at room temperature, washed with PBS and incubated in saponin solution for 5 min. Samples were incubated in the dark for 15 min at room temperature with cytokine-specific antibodies including IFN-γ-FITC, IL-2-PE, IL-4-PE, IL-10-PE, and TNF-α-PE (all purchased from Pharmingen, San Diego, USA). Samples were washed again with PBS and were finally resuspended in PBS.

The staining protocol and reagents are included in Appendix B.

IL-10-PE, and TNF- α -PE (all purchased from Pharmingen, San Diego, USA). Samples were washed again with PBS and were finally resuspended in PBS.

The staining protocol and reagents are included in Appendix B.

5. Assessment of Apoptosis

After density-gradient separation MNCs were washed in PBS and cultured at 0.5×10^6 cells/ml in 6 well plates in RPMI medium containing 10% fetal calf serum, L-glutamin (300mg/L) (all Gibco), Penicillin (100 U/ml), and Streptomycin (100 μ g/ml) (both Sigma) in the dark at 37°C in 5% CO₂.

In proper intervals after UVA irradiation one well was harvested by rigorously shaking on a vortex, MNCs were washed in PBS and incubated in blocking solution (Sigma) for 10 min at 4°C. Then, MNCs were incubated with monoclonal antibodies (mAB) against CD4-FITC, CD8-PE, CD3-FITC, CD56-PE (all antibodies BD Bioscience) for 20 min at 4°C. Then, cells were washed once with PBS, resuspended in a Calcium-Puffer (BD Bioscience) containing 5 μ g/ml 7-Aminoactinomycin D (7-AAD) (Sigma), and 1 μ l/sample Annexin V-Cy5 Reagent (Bio Vision, CA, USA), and incubated for 10 min at room temperature in the dark. Then cells were diluted 1:15 with ice-cold Calcium-buffer, kept on ice and measured within one hour.

The detailed protocols are shown in Appendix E and Appendix F.

6. Assessment of Circulating Whole Blood Cells

Heparinized PB samples were taken in the morning from patient after transplantation and also from patients before undergoing ECP therapy in proper intervals. In 5 different panels antibodies to identify CD3⁺ (positive) lymphocytes' subsets CD4⁺ and CD8⁺ T cells, DC1 and DC2, CD14⁺ monocytes and NK cells were directly added to a small blood volume. After 15 minutes incubation time at room temperature in the dark, erythrocytes were then lysed by adding 1X FACS Lysing Solution (BD Bioscience, San Jose, CA, USA). After 10 minutes incubation time cells were centrifugated and washed once with PBS.

The detailed protocol is shown in Appendix A and Appendix C.

7. Flow Cytometry

7.1. Overview

Flow cytometry uses the principles of light scattering , light excitation, and emission of fluorochrome molecules to generate specific multi-parameter data from cells ranging in size from 0.5 μ m to 40 μ m diameter. Cells are hydro-dynamically focused in a sheath of PBS before intercepting an optimally focused light source (See Figure 3-2). Lasers (*light amplification by stimulated emission of radiation*) are used as a light source in flow cytometry.

The FACSCalibur™ (BD Bioscience, San Jose, USA) flow cytometer is made up of three main systems: fluidics, optics, and electronics. In Figure 3-4 the 3 systems and their interactions are shown.

7.2. The Fluidics System

The fluid system transports cells in a stream of sheath fluid to the laser beam for interrogation. After laser intercept the fluid stream goes to the waste.

Flow cytometers use the principle of hydrodynamic focusing for presenting cells to a laser. The sample is injected into the center of a sheath flow. The combined flow is reduced in diameter, forcing the cell into the center of the stream. Then the laser illuminates one cell at a time. For an illustration of hydrodynamic focusing in a FACSCalibur™ flow chamber (flow cell) see Figure 3-2.

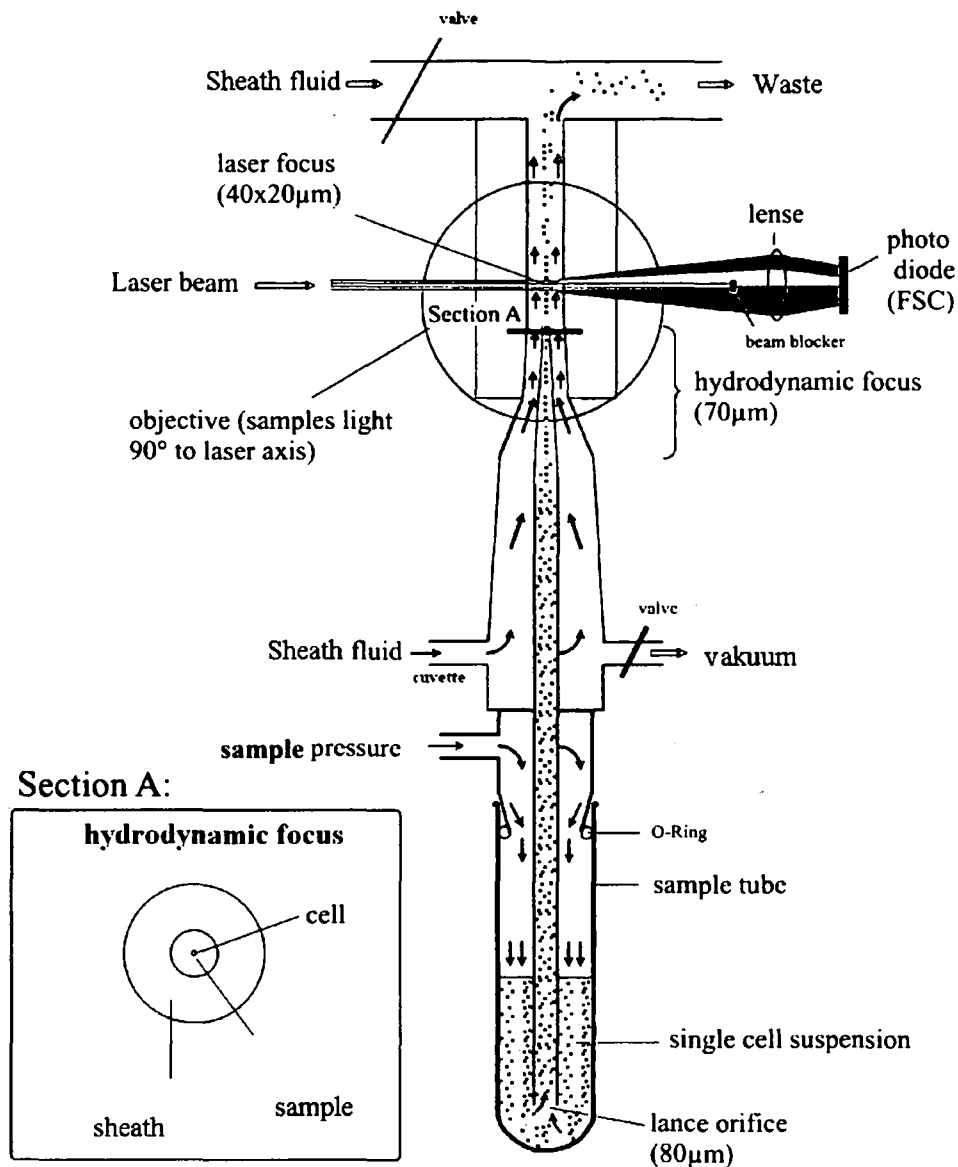


Figure 3-2: FACScalibur™ Fluid System

7.3. The Optics System

The optics system consists of 2 lasers, an Argon Laser emitting at 488nm and a Red Diode Laser emitting at ~635nm. Collimated (parallel light waveforms) light is picked up by confocal lens focused at the intersection point of hydro-focused cell stream and the light beam. Light is split by different mirrors and sent to different optical filters to direct the resulting light signals to the appropriate detectors (photomultiplier tube, PMT).

7.3.1. Light Scatter

Light scattering occurs when a particle deflects incident laser light. The extent to which this occurs depends on the physical properties of a particle, namely its size and internal complexity. Factors that affect light scattering are the cell's membrane, nucleus, and any granular material inside the cell. Cell shape and surface topography also contribute to the total light scatter.

7.3.2. Forward-scattered light (FSC)

FSC is proportional to cell-surface area or size. FSC is a measurement of mostly diffracted light and is detected just off the axis of the incident laser beam in the forward direction by a photodiode. FSC provides a suitable method for detecting particles greater than a given size independent of their fluorescence and is therefore often used in immunophenotyping to trigger signal processing.

7.3.3. Side-scattered light (SSC)

SSC is proportional to cell granularity or internal complexity. SSC is a measurement of mostly refracted and reflected light that occurs at any interface within the cell where there is a change in refractive index (Figure 3-3). SSC is collected at approximately 90 degrees to the laser beam by a collection lens and then redirected by a beam splitter to the appropriate detector.

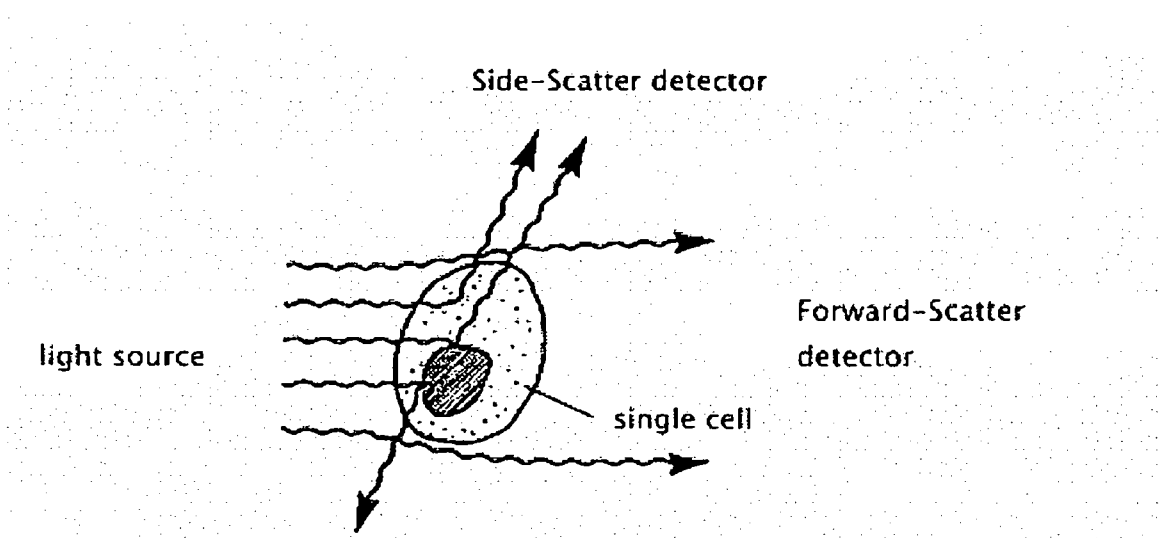


Figure 3-3: Light-Scattering Properties of a Cell.

Correlated measurements of FSC and SSC allow the differentiation of cell types in a heterogeneous cell population. Main leukocyte subpopulations can be differentiated using FSC and SSC.

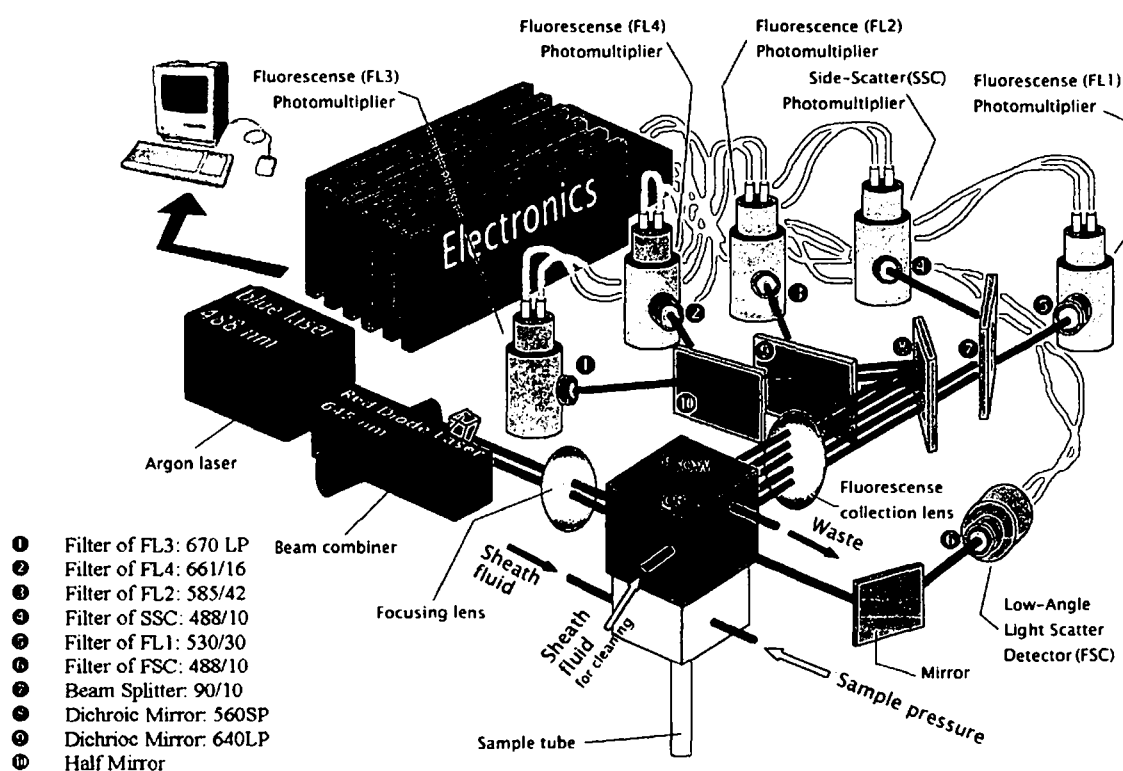


Figure 3-4: FACSCalibur™ Optics System

7.4. Fluorescence

A fluorescent compound absorbs light energy over a range of wavelengths that is characteristic for that compound. This absorption of light causes an electron in the fluorescent compound to be raised to a higher energy level. The excited electron quickly decays to its ground state, emitting the excess energy as a photon of light. This transition of energy is called fluorescence.

The range over which a fluorescent compound can be excited is termed its absorption spectrum. As more energy is consumed in absorption transitions than is emitted in fluorescent transitions, emitted wavelengths will be longer than those absorbed and each compound has a characteristic emission spectrum.

The argon ion laser is used in flow cytometry because the 488-nm light that it emits, excites the fluorochromes fluorescein isothiocyanate (FITC) and phycoerythrin (PE) by different peak emission wavelengths. These peak emission wavelengths are far enough apart (40 nm) so that each signal can be detected by a separate detector. The amount of fluorescent signal detected is proportional to the number of fluorochrome molecules on the particle. Two further fluorochromes, allophycocyanin (APC) and the Peridinin-chlorophyll-protein Complex (PerCP) have nearly the same peak emission. But APC is excited by the Red Diode Laser at 635nm and PerCp is excited by 488nm. The different emission light can only be distinguished by the time delay between both laser beams and is controlled by software (laser compensation). The excitation and emission spectra of both alternatives are shown in Figure 3-5 (FITC, PE, PerCP, APC) suitable for the FASCcalibur™.

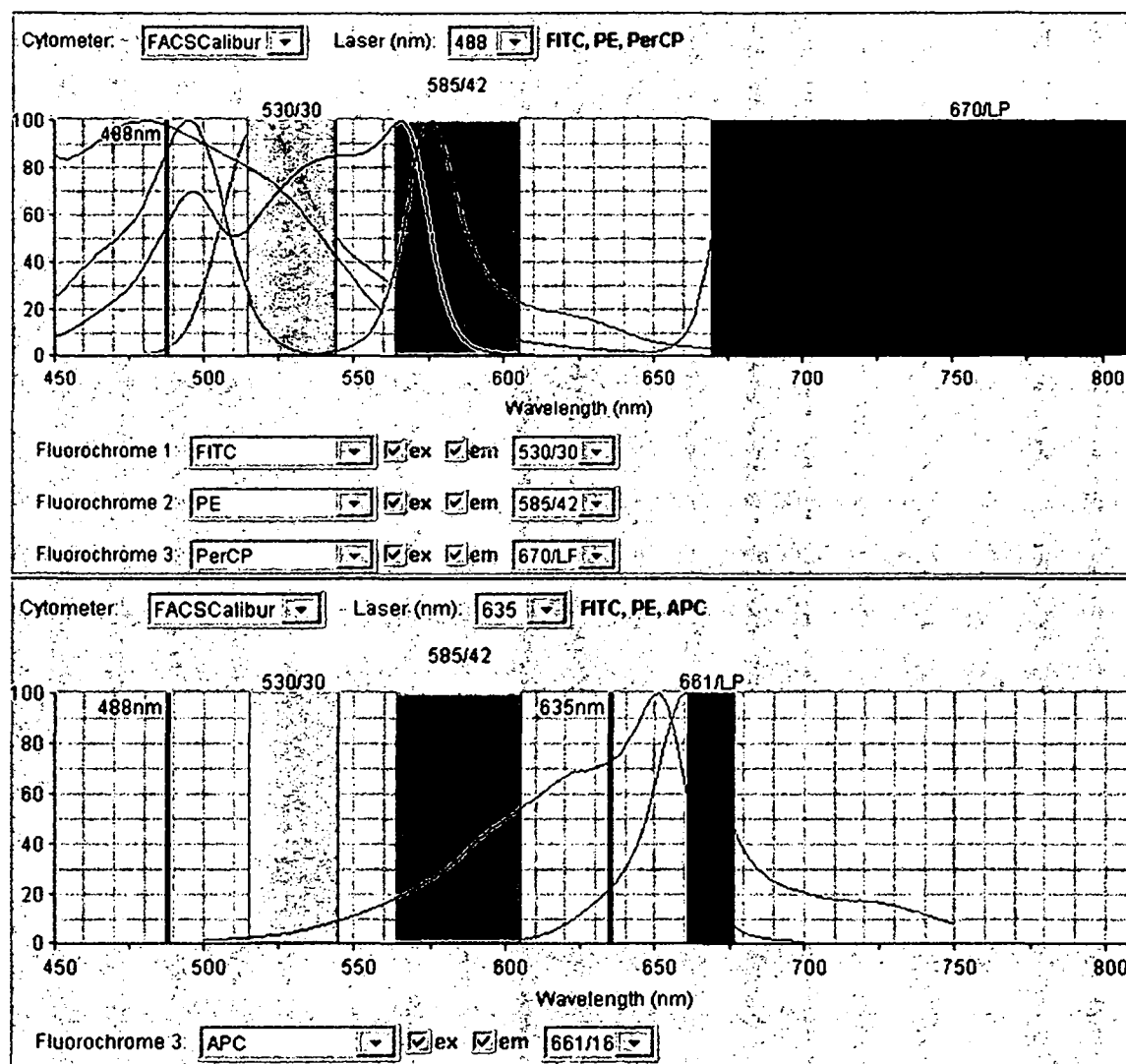


Figure 3-5: Excitation and Emission Spectra of FITC, PE, PerCP and APC

As an alternative to the weak emission light of PerCp, the tandem fluorochrome PE-Cy7 needs only minimal cross-beam compensation, which is required when used simultaneously with APC. PE-Cy7 is also excited by an argon laser and the resonance energy is transferred from PE molecule to Cyanin 7 (Cy7) at an emission wavelength of 760nm. The excitation and emission spectra of both alternatives are shown in Figure 3-6 (FITC, PE, PE-Cy7, APC) suitable for the FACSCalibur™.

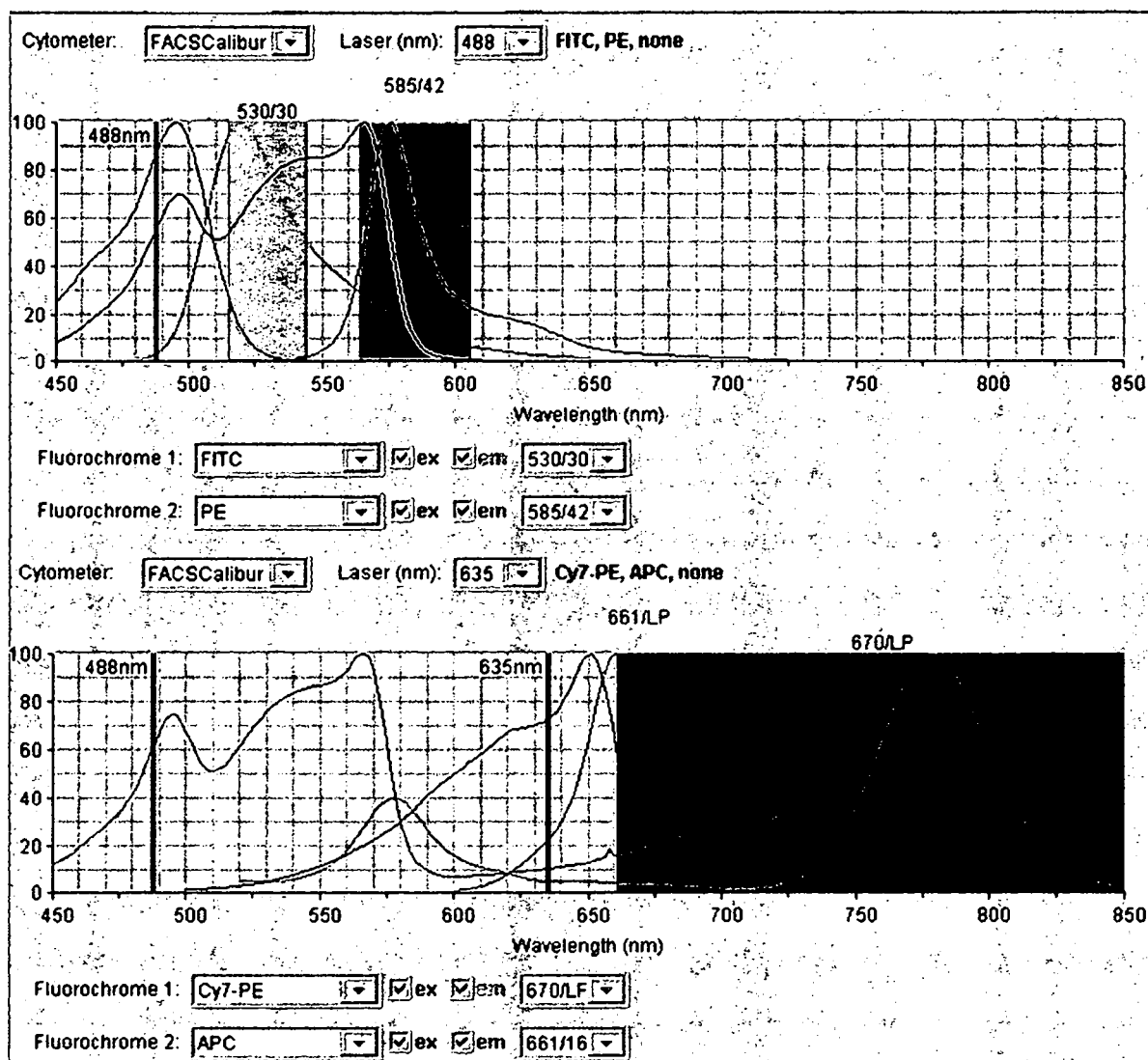


Figure 3-6: Excitation and Emission Spectra of FITC, PE, PE-Cy7 and APC

FITC and PE can also be combined with DNA dye 7-AAD (excitation wavelength of 633nm; emission wavelength of 670nm) and the fluorochrome Cyanin 5 (Cy5) (excitation wavelength of 488nm; emission wavelength of 647nm). In this case the laser compensation is necessary. In Figure 3-7 the excitation and emission spectra demonstrate the optics of the FACSCalibur™.

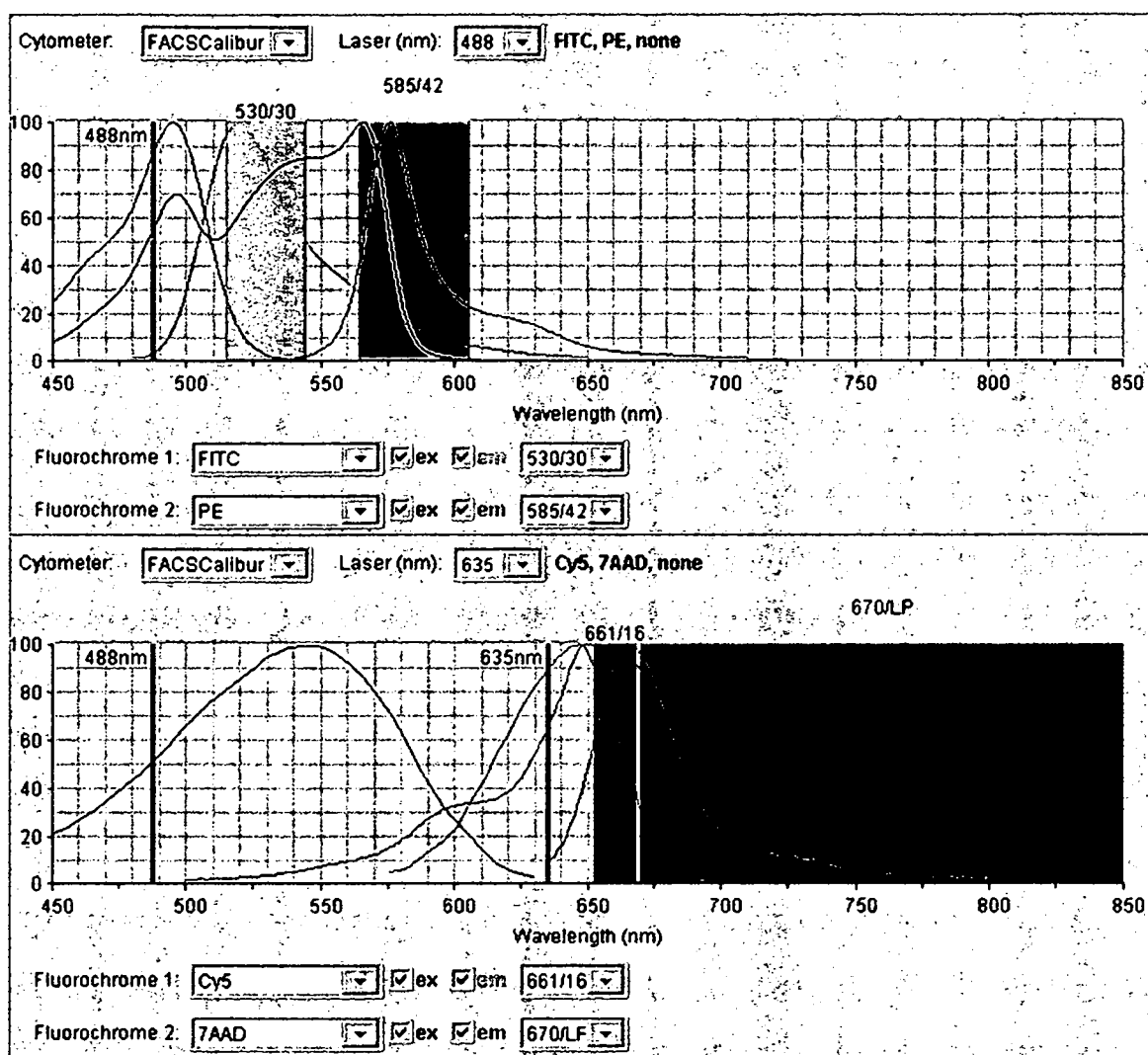


Figure 3-7: Excitation and Emission Spectra of FITC, PE, 7-AAD and Cy5

When a fluorescent dye is conjugated to a monoclonal antibody, it can be used to identify a particular cell type based on the individual antigenic surface markers of the cell. In a mixed population of cells, different fluorochromes can be used to distinguish separate subpopulations. The staining pattern of each subpopulation, combined with FSC and SSC data, can be used to identify which cells are present in a sample and to count their relative percentages.

7.5. Optical Filters and Mirrors

Once a cell or particle passes through the laser light, emitted weak SSC and fluorescence signals are diverted to the PMTs and a photodiode collects the amplified FSC signals.

The specificity of a detector for a particular fluorescent dye is optimized by placing a filter in front of the PMT, which allows only a narrow range of wavelengths to reach the detector. This spectral band of light is close to the emission peak of the fluorescent dye.

Such filters are called bandpass (BP) filters as shown in Figure 3-2 ②, ③, ④, ⑤, ⑥. For example, the filter used in front of the FL1 detector in Figure 3-2 ⑤ is labeled 530/30. This number gives the characteristics of the spectral band transmitted: 530 ± 15 nm, or wavelengths of light that are between 515 nm and 545 nm.

Other filters used in the flow cytometer are shortpass (SP) filters ③, which transmit wavelengths of light equal to or shorter than a specified wavelength, and longpass (LP) filters ①, which transmit wavelengths of light equal to or longer than a specified wavelength.

Beam splitters as shown in Figure 3-2 ⑦ are devices that direct light of different wavelengths in different directions.

Dichroic mirrors are a type of beam splitter. The 560 SP dichroic mirror shown in Figure 3-2 ⑧ transmits wavelengths of light 560 nm or shorter. Wavelengths of light longer than 560 nm are reflected at 45 degrees.

7.6. The Electronics System

A voltage pulse is created when a particle enters the laser beam and starts to scatter light or fluorescence. The photodiode is less sensitive to light signals than the PMTs and thus is used to detect the stronger FSC signal. PMTs are used to detect the weaker signals generated by SSC and fluorescence (FL1-FL4).

Once the light signals, or photons, strike one side of the PMT or the photodiode, they are converted into a proportional number of electrons that are multiplied, creating a greater electrical current.

The electrical pulses originating from scattered and emitted light are then processed by an Analog to Digital Converter (ADC). The ADC converts a 0–1,000 mV pulse to a digital number representing 0–1,000 mV channels. The channel number is then transferred to the computer. The light signal is then displayed in an appropriate position on the data plot.

Logarithmic amplification is most often used to measure fluorescence in cells. This type of amplification expands the scale for weak signals and compresses the scale for “strong” or specific fluorescence signals.

Flow cytometry data outputs are stored in the form of computer files using the FCS 3.0 standard.

7.7. Acquisition of Flow Cytometric Data

7.7.1. Common Parameters

Instrument Settings were taken from the current FACS Comp protocol (updated about every 7 days) to adjust the PMT voltages and fluorescence compensation and to check the sensitivity of the instrument.

All acquisitions were done with CellQuest Pro™ software on the FACSCalibur.

FSC and SSC amplifier are adjusted manually to view the proper cell populations in the dot plot.

7.7.2. Assessment of Intracytoplasmatic Cytokines by Flow Cytometry

The production of cytokines of peripheral blood leukocytes can be detected as mRNA or as translated protein. Several comparisons of mRNA and their proceeding protein have shown that not every mRNA leads to a right folded and functional protein. In most cases the analyses concerned on total protein amounts of all heterogen blood cells. The challenge was to derive new theses from clone and animal cell line experiments to *ex vivo* analyses of human cells. This circumstances leads to new methods analysing several proteins simultaneously, to receive information about a shift of cytokine syntheses within one cell population [44]. Some of these methods are ELISPOT (Enzyme Linked ImmunoSorbent SPOT-Assay), limiting dilution analyses and *in situ* hybridisation. In 1991 Sander et al [45] published a method to combine intracellular cytokines detection with phenotyping single T cells using a fluorescence microscope. In 1993 Jung et al [46] set the next step by transforming the phenotyping and intracytoplasmatic cytokine (ICC) detection of single cells to flow cytometry. This revolutionary method has the additional benefit to analyze specific cytokines of large numbers of cells by relatively low efforts. Intracytoplasmatic cytokine analyses in

combination with flow cytometry established to the most common analyses in hematological diseases.

For four-color analysis, samples were analyzed on a FACSCalibur (BD Bioscience). The intracytoplasmatic analyses program was created with CellQuestPro™ and described in Appendix D.

Briefly 10000 target cells were collected per sample and the subpopulations CD4 and CD8 were further analyzed in two different dot plots for their cytokine expression of IL-2, IL-4, IL-10, TNF- α combined with INF- γ . Appropriate intracellular isotype controls were used; extracellular unspecific staining was prevented by the blocking solution.

Results were presented as total number of cells as well as the percentage of cytokine producing cells.

Brefeldin A (BfA)

Brefeldin A is a unique fungal metabolite of a 13-membered macrocyclic lactone ring and has an inhibitory effect on virus multiplication. Mitsumi et al [47] first described the effect of total protein synthesis and secretion inhibition on cultured rat hepatocytes. They had analyzed that the albumin secretion was inhibited in a dose-dependent manner. In the presence of 1 μ g/ml BfA the secretion was almost completely blocked until 1 hour. After that time, the newly synthesized albumin was rapidly secreted into the medium, reaching about 90% of normally secreted level at 3 h of chase. At higher concentrations of brefeldin A, the complete blockade of secretion continued for 2h (5 μ g/ml) or a longer period (10 μ g/ml). Exposures of rat hepatocytes for 4 h to a concentration of 10 μ g/ml BfA showed markedly dilated endoplasmatic reticulums with or without ribosomes containing morphologous materials, which may be possibly secretory proteins within the lumen [47].

PMA and Ionomycin

PMA, phorbol-12-myristate-13-acetate, induces prolonged protein kinase C (PKC) activation and together with ionomycin the downregulation of the TCR-CD3 complex and expression of the IL-2R and secretion of IL-2 itself [48].

PMA mimics the signal through the TCR/CD3 complex. PMA is an analog of diacylglycerol (DAG), a second messenger normally produced by phospholipase C (PLC). DAG causes release of calcium from intracellular stores, activates the phosphatase calcineurin, and ultimately triggers nuclear import of the NFAT transcription factor. Ionomycin is a calcium ionophore that efficiently shuttles Ca^{2+} ions into the cell and further augments signaling [49].

Ramson et al [50] analyzed that the addition of PMA to cultures induces B cell membrane depolarization but fails to induce an increase in Ca^{2+} more or less he suggested a slight decrease in Ca^{2+} . Plasma membrane depolarization has been shown to be an initial and pivotal event in activation and entry into the mitotic cycle of T and B lymphocytes [50]. CD69 has been shown to function as a co-stimulatory molecule in conjunction with PMA. PMA stimulation (10 ng/ml) led to activation of both T- and NK cells between 1 and 2 h post incubation. There was no difference between the rate of CD4 or CD8 responsiveness on PMA [51].

Saponin

Saponin, is a herbal glycoside and solubilizes cholesterol and leaves much of the cell structure intact. The cells being treated retained sufficient integrity to enable differentiation of cell types and the basis of morphology. Moreover the membrane expression of most antigens is not altered which is of particular interests for the simultaneous detection of membrane and intracellular structures [52].

7.7.3. Assessment of Apoptosis by Flow Cytometry

As with viability, no single parameter fully defines cell death in all systems. Therefore it is often advantageous to use several different approaches when studying apoptosis.

Assessment of asymmetric phospholipid distribution is most sensitive and meaningful when carried out utilizing single-cell assays such as microscopy and flow cytometry, which examine large numbers of individual cells and can therefore identify and quantify subpopulations of apoptotic cells. The normal phospholipids distribution is one in which phosphatidylcholine and sphingomyelin are present mainly in the external leaflet, while most of the phosphatidylethanolamine and all of the phosphatidylserine (PS) are located in the internal leaflet [53, 54]. Abolition of the normal lipid distribution

requires inactivation of the aminophospholipid translocase, the enzyme responsible for maintaining lipid asymmetry, and activation of a membrane protein called the scramblase, which catalyzes transbilayer movement of all classes of phospholipids [55]. Loss of lipid asymmetry, through randomization of lipids across the bilayer, results in exposure of PS on the cell surface. Also during cellular activation, the scramblase is activated, but because there is no corresponding downregulation of aminophospholipid translocase activity [56], any resulting asymmetry is soon rectified.

Annexin-Cy5 Reagent

Annexin V (AxV)-Cy5 is a bright fluorescent conjugated reagent for detecting the externalization of PS [57]. Annexin V has a strong, Ca^{2+} -dependent affinity for PS (K_d of $\sim 5 \times 10^{-2}$) [58] and therefore serves as a probe for detecting apoptosis. Cy5 fluorescent dye conjugates produce an intense signal in the far-red region of the spectrum and therefore it is very useful for multiple labelling of cells with green and red coloured fluorescent probes. Cy5 is excitable with a Helium-Neon Laser at $\lambda_{\text{max}} = 649 \text{ nm}$ and yields fluorescence with a λ_{max} emission of 670 nm.

7-AAD Viability Dye

Actinomycins are biologically active compounds containing a 2-amino-4,6 dimethylphenoxazone-3 chromophore and two cyclic pentapeptides [59]. Actinomycins form stable complexes with double-stranded DNA but neither with double-stranded RNA, nor with RNA-DNA hybrids or with single-stranded DNA or RNA [59, 60].

7-Amino-Actinomycin D (7-AAD), an analogue of actinomycin D contains a substituted- amino group at the 7-position of the chromophore. 7-AAD intercalates between cytosine and guanine bases of the DNA [60].

The spectral properties of 7-AAD make this molecule particularly suitable for flow cytometry analysis [61]. The maximum absorption of the complex (7-AAD / DNA) is situated in the green spectral region and thus is suitable for argon laser equipped-cytometer (excitation wavelength of 488 nm) [60]. The deep red fluorescence emission of 7-AAD (635 to 675 nm) make the use of this probe in combination with FITC and PE [61].

Apoptotic, necrotic cells and / or damaged cells are source of interference in the analysis of viable cells by flow cytometry. Nonviable cells can be evaluated and discriminated following 7-AAD positive labeling when viable cells remain unstained (negative) [62].

For four-color apoptosis acquisition, 8 000 target cells were measured but all cells within acquisition were stored with a FACSCalibur, Becton Dickinson.

Apoptosis of CD4 and CD8 T Cells

CD4 and CD-positive cells (FL1 / FL2 or FL1/SSC and FL2/ SSC) were compared with the Isotype plot (FL1 / FL2) and gated excluding background. Target cells were further expressed in an Annexin/ 7-AAD plot (FL3 / FL4) and analyzed using quadrant statistics. Double CD4+CD8+ cells were excluded from analyses.

The T cell analyses program was created with Attractors™ (BD Biosciences) and is described in Appendix E.

Briefly the program monitors early (AxV) and late (7-AAD) apoptosis of T helper cells (CD4+) and cytotoxic T cells (CD8+) and creates a printable layout, which makes it possible to recapitulate the region settings.

Apoptosis Analyses of T Cells (CD3) and NK Cells (CD3-CD56+)

The T cell analyses program was created with Attractors™ (BD Biosciences) and is described in Appendix F.

The program monitors early (AxV) and late (7-AAD) apoptosis of CD3-T cells, CD3+CD56+ T cells and CD4-CD56+ NK cells and creates a printable layout, which makes it possible to recapitulate the region settings.

7.7.4. Assessment of Whole Blood Cells by Flow Cytometry

For four-color whole blood acquisition FSC and SSC are prepared to monitor all blood cells. 100 000 total cells are acquired and stored with a FACSCalibur. The whole blood analyses include the detection of dendritic cells, Monocytes, NK cells, and the T cell subpopulations.

Flow Cytometry Analyses of DC1 and DC2

Dendritic cells were negative for lineage marker in FL1 (CD3, CD14, CD16, CD19, CD20, CD56) and HLA-DR+ in FL3. DC1 were CD11c-(FL4), and DC2 were CD123+(FL2).

Appropriate negative control instead of CD11c and CD123 were used to define gates. Results of DC1 and DC2 were presented as absolute number (DC/ μ L), determined by multiplying the percentage of DC1 and DC2 with the total number of leukocytes per μ L. Total number of leukocytes were received from routine analyses of the patients at our institute.

The dendritic cell analyses program was created with CellQuestPro™ and described in Appendix G. Briefly the program arranges fixed cell determinations of DC1, DC2 and basophils for all patients of different immune status and creates a printable layout, which shows all chosen settings.

Leukocyte Differentiation Analyses

Leukocytes are characterized as a large CD45+ population in peripheral blood, containing most immunomodulating cells. Within this large population lymphocytes (CD3), monocytes (CD14+) and natural killer cells (CD3-CD56+) are gated and describes as percentage of CD45 leukocytes. Isotype control is performed to exclude unspecific CD56 staining.

The leukocyte analyses program was created with Attractors™ (BD Biosciences) and is described in Appendix H. Briefly the program arranges fixed cell determinations of leukocyte subpopulations for all patients of different immune status. The program creates a printable layout, which makes it possible to recapitulate the region settings.

T cell Subpopulation Analyses

The CD3- T cells are further analyzed by their fraction of T helper cells (CD4+), cytotoxic cells (CD8+) and double positive CD4+CD8+. These subpopulations are described as percentage of CD3 T cells. Additional a CD4/CD8 ratio is derived.

The T cell analyses program was created with Attractors™ (BD Biosciences) and is described in Appendix I. Briefly the program arranges fixed cell determinations of CD3-

(neg.) T cells subpopulations for all patients of different immune status. The program creates a printable layout, which makes it possible to recapitulate the region settings.

7.7.5. Data Preparation for Statistical Analyses

Raw data generated by the CellQuestPro™ analyses programs

Working with the Cell Quest Batch System is handicapped in undoing a data export. In case of repeated analysis every batch resume click generates doubles in the Output file. The raw data file must be cleaned manually.

The shape of the data file is shown in Appendix D and G. Briefly, each batch resume generates small tables of figures from each plot, which are arranged by their top variables, but vertical table characteristics are summarized in frequent columns.

The procedure to generate a consistent data file with one character in one column is applied by Enterprise Guide 2.0. Although SAS is known for high capacity of importing different data-formats, several experts have given in to assist in generating a general import mask. Besides several characters generated by CellQuestPro™ (e.g. date format) are rejected by SAS and must be adjusted before import.

The alternative to an import mask was to filter the data file by variables and their particular characteristics and generate smaller sub-files with new variable descriptions. At least all sub-files are merged to one file.

Raw data generated by the Attractors™ Analyses Programs

In contrast to Cell Quest raw data files Attractors raw data files are already sorted by their characters. Therefore filtering and joining of data is not necessary as described in by CellQuestPro™.

8. Statistical Analysis

8.1. Intracytoplasmatic Cytokine analyses of Patients with aGvHD

Data set was done with SAS 8.2 and statistic work was performed with Enterprise Guide 2.0 to compare any differences in the medians in PB, Pre-ECP and Post ECP samples

using the descriptive analysis. To test the change of all 5 cytokines we calculated the ANOVA with the fixed factor cytokine and the random factor patient ID and the interaction between time and patient ID. The test was repeated using the Turkey-Kramer Method and only p-values lower than 0.05 in both tests were interpreted as significant. P-values of ANOVA are mentioned.

8.2. Intracytoplasmatic Cytokine Analyses of Patients with cGvHD

Data set was done with SAS 8.2 and statistic work was performed with Enterprise Guide 2.0 to compare any differences in the medians in PB, Pre-ECP and Post ECP samples using the descriptive analysis. Any further analyses are not possible due to fewer patients.

8.3. Apoptosis of White Blood Cells after Extracorporeal Photochemotherapy

Each plot, comparing PB, Pre-ECP and Post-ECP samples, at 10 and 24 hours was first tested with the Friedman Test in order to see if there is at least one difference between the groups. Because of multiple testing, the p-values were further corrected by the Bonferroni stepdown method. Significant plots were described by p-values.

In plots with a corrected $p < 0.05$ the differences between PRE-ECP and POST-ECP were tested with the Wilcoxon Signed Rank Test and the resulting p-values were corrected again.

Chapter 4

Results

1. Analyses of Patients with acute Graft-versus-Host Disease

There is convincing evidence that T-cells contained in the donor graft or subsequently derived from donor SC react to host Antigen-presenting cells (APCs) (alloreactivity), causing target organ damage that are recognised as clinical manifestations of GvHD. The immunobiology of aGvHD is complex. Three sequential phases of cytokine dysregulation are responsible for the manifestations of acute GvHD [63]: The first phase depends on host conditioning. Donor T-cells are infused into a host that has been profoundly damaged by underlying disease, infections and particularly by the conditioning regimen, all of which result in activation of host cells with secretion of proinflammatory cytokine such as TNF- α and IL-1 and nitric oxide [64]. As a consequence, expression of MHC Ag and adhesion molecules is increased, thus enhancing the recognition of host alloantigens. The second phase was described by the secretion of predominantly IL-2 and INF- γ of donor CD4 (Th1) and CD8 (Tc1) T cells after interaction with host APCs [65, 66]. These cytokines are pivotal mediators of aGvHD and amplify the immune response by priming monocytes to produce the proinflammatory cytokines IL-1 and TNF- α [67, 68]. Based on the observation that IL-4 and IL-10 gene expression in PBMC was suppressed in patients with severe GvHD compared to those without severe GvHD [69] arose the thesis, that phase 3 of aGvHD is culminating in a cytokine dysregulation in synergy with T- and natural killer (NK) cell-mediated cytotoxicity, producing the systemic morbidity of GvHD-associated immunosuppression. Finally, the inflammatory response, together with the CTL and NK components, leads to target tissue destruction, via target cell apoptosis, in the transplant host.

This leads to the considerable evidence that a type 1 → type 2 immune deviation after allogeneic transplantation is associated either with decreased acute GvHD or with the development of a 'chronic' GvHD syndrome that is characterized by decreased lethality and autoantibody formation [70-73].

Differential activation of donor T-cell subsets has been evoked in the immunopathogenesis of various other autoimmune, infectious, and immunodeficiency diseases [74, 75] and there is thus a significant interest in the potential relevance of the Th1/Th2 paradigm for acute GvHD and the positive effects of ECP. There is now considerable evidence that a type 1 → type 2 immune deviation after allogeneic transplantation is associated either with decreased acute GvHD or with the development of a "chronic" GvHD syndrome that is characterized by decreased lethality and autoantibody formation.

1.1. Development of Leukocyte Subpopulations of Patients with High Risk of acute GvHD after Haematopoietic Stem Cell Transplantation

1.1.1. Overview

The T-Cell Receptor Complex and CD3

The T-cell receptor complex (TCR) is a transmembrane molecule with short cytoplasmatic tail and is expressed on the surface of T cells in non covalent association with the transmembrane polypeptides known as CD3 complex. The CD3 complex is composed of six polypeptides with usually four different chains: γ CD3, δ CD3, ϵ CD3 and ζ CD3. Three different dimmers ($\gamma\epsilon$, $\delta\epsilon$, and $\zeta\zeta$) constitute the CD3 complex. The CD3 polypeptide chains are members of the Ig superfamily. Unlike CD3 and the TCR, the CD3 ζ chain is not T-cell specific, exhibit independent metabolism and regulation of expression of CD3- $\gamma\delta\epsilon$ chains. In the absence of CD3 ζ , the TCR-CD3 complex can not be expressed on the cell surface. The CD3 ζ chain is indeed expressed on the cell surface of T cells even in the absence of the surface TCR dimer-CD3 complex [76]. NK cells express CD3 chains only in the cytoplasm [77]. CD3 and ζ chain polypeptides do not bind antigen. Each chain of the CD3 complex contains one tyrosine-containing sequence referred to as an immunoreceptor tyrosine-based activation motif (ITAM) and the ζ chain contains three [78]. Following antigen binding to the α and β chains of the TCR, the activation signals of

the associated CD3 and ζ chains mediate tyrosin kinases to phosphorylate ITAM causing the activation of ZAP-70 which is bound to the phosphorylated ITAM [49] . Thus, CD3 and ζ chain play a crucial role as transducer molecules after antigen binding to the TCR. When T cells are activated, the whole TCR-CD3 complex is rapidly internalized and thus T cells become functionally unresponsive. The di-leucine motif within the cytoplasmic region of CD3 γ has been shown to be important for internalization of the TCR-CD3 complex upon stimulation with phorbol myristate acetate (PMA) as a protein kinase C (PKC)-dependent activation [79] .

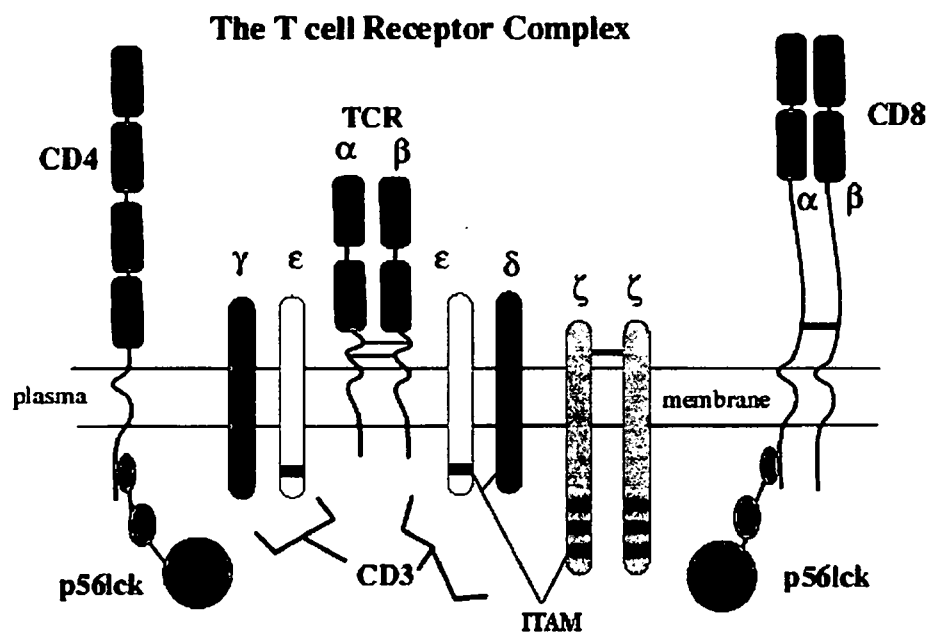


Figure 4-1: The T-cell receptor complex, CD3, CD4 and CD8 molecules

CD16^{dim}/neg. These NK subsets are functionally distinct with the immunoregulatory CD56^{bright} cells producing abundant cytokines and the cytotoxic CD56^{dim} cells likely functioning as efficient effectors of natural and antibody-dependent target cell lysis [87]. CD8 are present on ~30% to 40% of NK cells and. The density of CD8 antigen on NK cells is lower than that on T cells [88].

Cell surface receptors that inhibit and/or activate NK cells to lyse target cells have been characterized, including killer cell immunoglobulin-like receptors (KIRs), lectins, and natural cytotoxicity receptors (NCRs) [89-91]. CD56^{dim} NK cells, express both KIR and C-type lectin NK receptors at relatively high surface density along with an abundance of cytolytic granules packaged in the cytoplasm [92].

CD14- The Monocyte Cell Marker

CD14, a glycosylphosphatidyl inositol-linked glycoprotein present on mononuclear and polymorphonuclear phagocytes. CD14 acts as a high-affinity receptor for complexes of LPS and LPS-binding protein [93]. The binding of lipopolysaccharide (LPS) to CD14 and then to toll receptor-4 results in the production of key proinflammatory cytokines, including IL-1, IL-6, IL-8, and TNF- α , which mediate inflammatory reactions. Surprisingly, intestinal macrophages lack CD14 [94, 95], and colonic macrophages express low levels of CD14 [96, 97]. The downregulated expression of CD14 on intestinal macrophages likely serves to dampen the LPS-induced response of intestinal macrophages to luminal bacteria and their LPS.

1.1.2. Assessment of Leukocyte Subpopulations of healthy Volunteers

A group of healthy volunteers (8 female, 10 men) with a median age of 40 (range, 20 to 62) were analysed at one time point. The mean leukocyte population was 6.55×10^6 /ml. I analysed median populations of 446.85 CD14⁺ monocytes/ μ l, 174.39 NK cells per μ l, 27.53 cytotoxic cells per μ l and 1067.55 CD3⁺ T cells per μ l. Within the CD3⁺ T cell population 357.86 CD8⁺ T cells/ μ l and 660.86 CD4⁺ T cells/ μ l leading to a median CD4/CD8 ratio of 2.14.

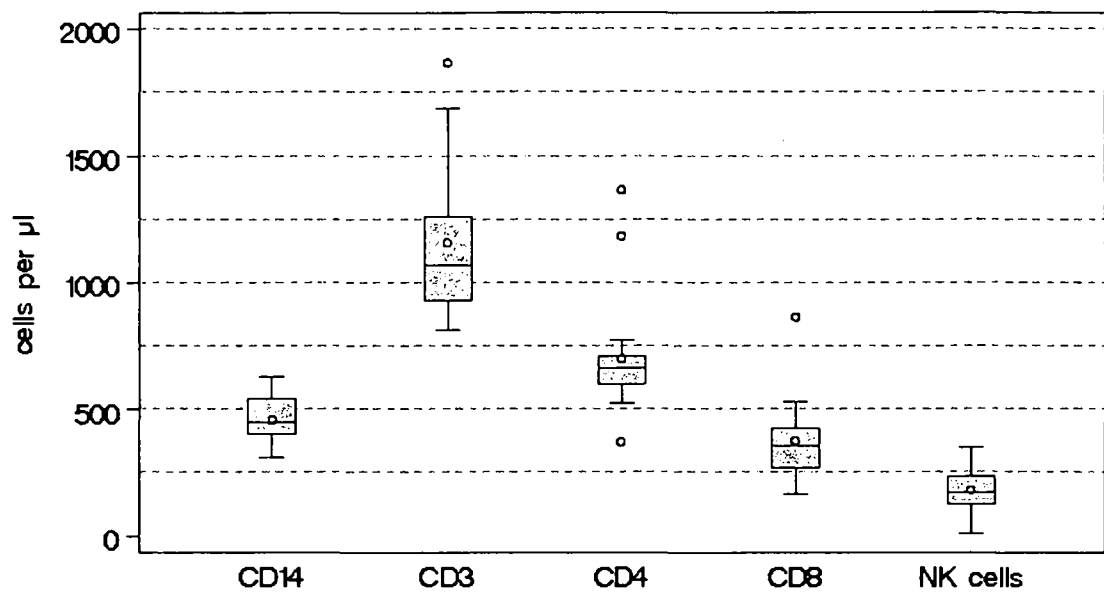


Figure 4-2: Leukocyte Subpopulations of Healthy Volunteers

Total T cells (CD3) and its two sub-fractions CD4, CD8 T cells, monocytes (CD14) and basophils of the healthy group are shown in box plots. Outliers are marked as points. Points within the boxes show the mean.

1.1.3. Assessment of Leukocyte Subpopulations of patients after HSCT

We have analyzed leukocytes of 30 patients after HSCT for 200 days. These patients are further divided in 6 categories depending on post-transplanted diagnoses namely 'no problems', 'acute GvHD', 'chronic GvHD', 'Infections', 'TRM' and 'Relapse'. Table 4-1 shows the patients ID and their post-transplanted diagnosis.

Patient ID	Diagnoses/ Categories
20	relapse
21	relapse
22	infections, TRM
23	chronic GVHD
24	no problems
25	infections
26	infection, chronic GVHD
27	no problems
28	acute GVHD, chronic GVHD
29	chronic GVHD
33	no problems
38	no problems
39	acute GVHD, TRM
40	acute GVHD, chronic GVHD
41	acute GVHD
46	acute GVHD
47	acute GVHD
48	acute GVHD, relapse
50	no problems
51	acute GVHD, relapse
52	no problems
70	chronic GVHD
71	infection, chronic GVHD
79	acute GVHD
80	relapse
100	no problems
102	chronic GVHD
103	no problems
107	relapse
108	acute GVHD

Table 4-1: Patient list of leukocyte subpopulation analyses and their categories

We assessed the production of CD4+ and CD8+ T cells and derived the ratio of CD4 to CD8. Results are shown in Figures 4-3 whereas all categories have different patient numbers as shown in the legend.

Additionally we assessed the leukocyte population of the same patients. Results of the same patients are shown in Figure 4-4. Of the same patient group we assessed the leukocyte subpopulations, NK cells, CD3+ T-lymphocytes, and monocytes. Results of NK cells are shown in Figure 4-5, results of T- lymphocytes are shown in Figure 4-6 and results of monocytes in Figure 4-7.

Results

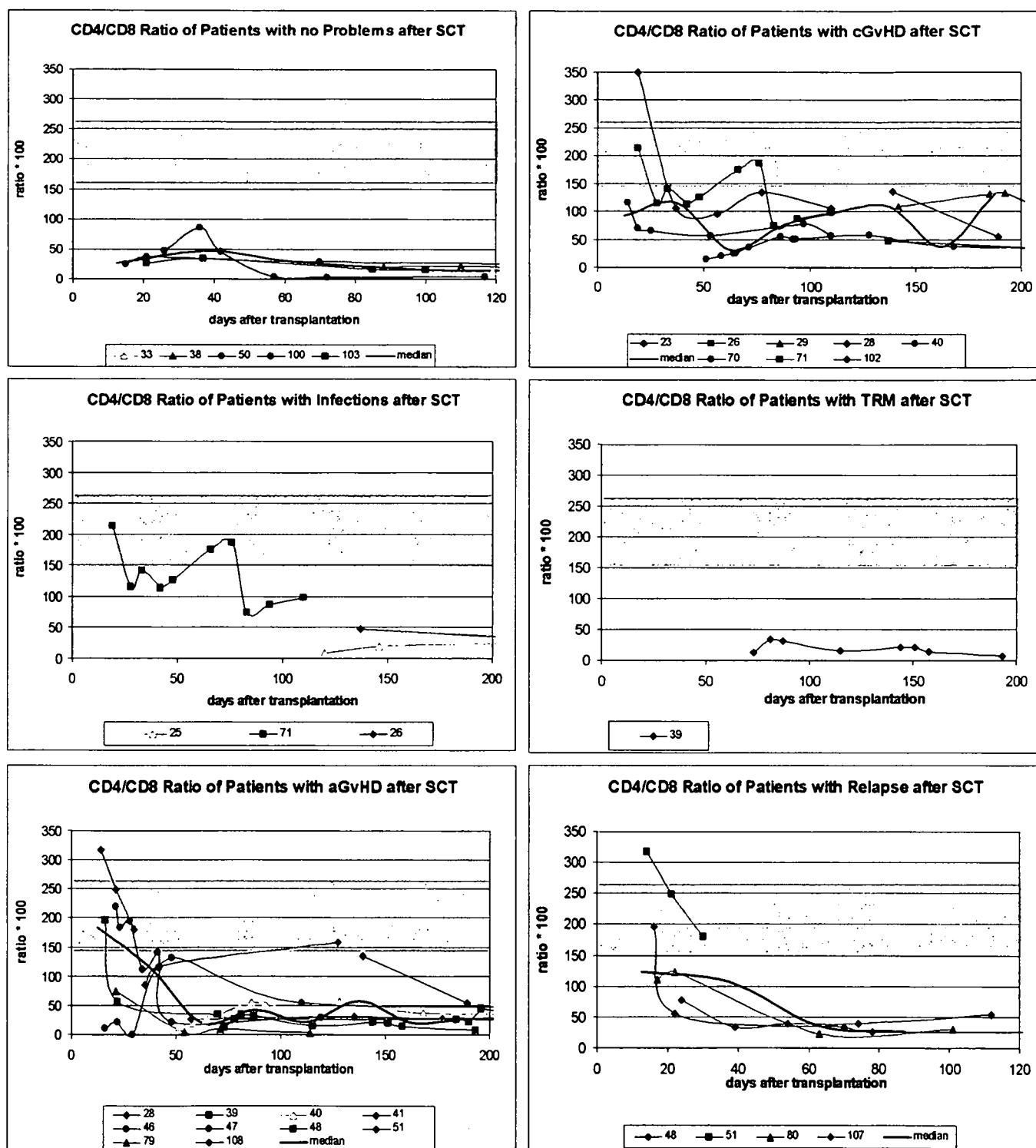


Figure 4-3: Development of CD4/CD8 ratio of patients after HSCT

Patients with multiple diagnoses as described in Table 4-1 are plotted several times in the 6 graphics. The black median line is calculated by cumulating all measurements within 25-day-intervals. The median is plotted in the middle of each interval. In case of fewer than 3 values the median is dropped. The green bar in the graphics is the inter-quartile range of the healthy volunteer group (1.5-2.6) as shown in Figure 4-2.

Results

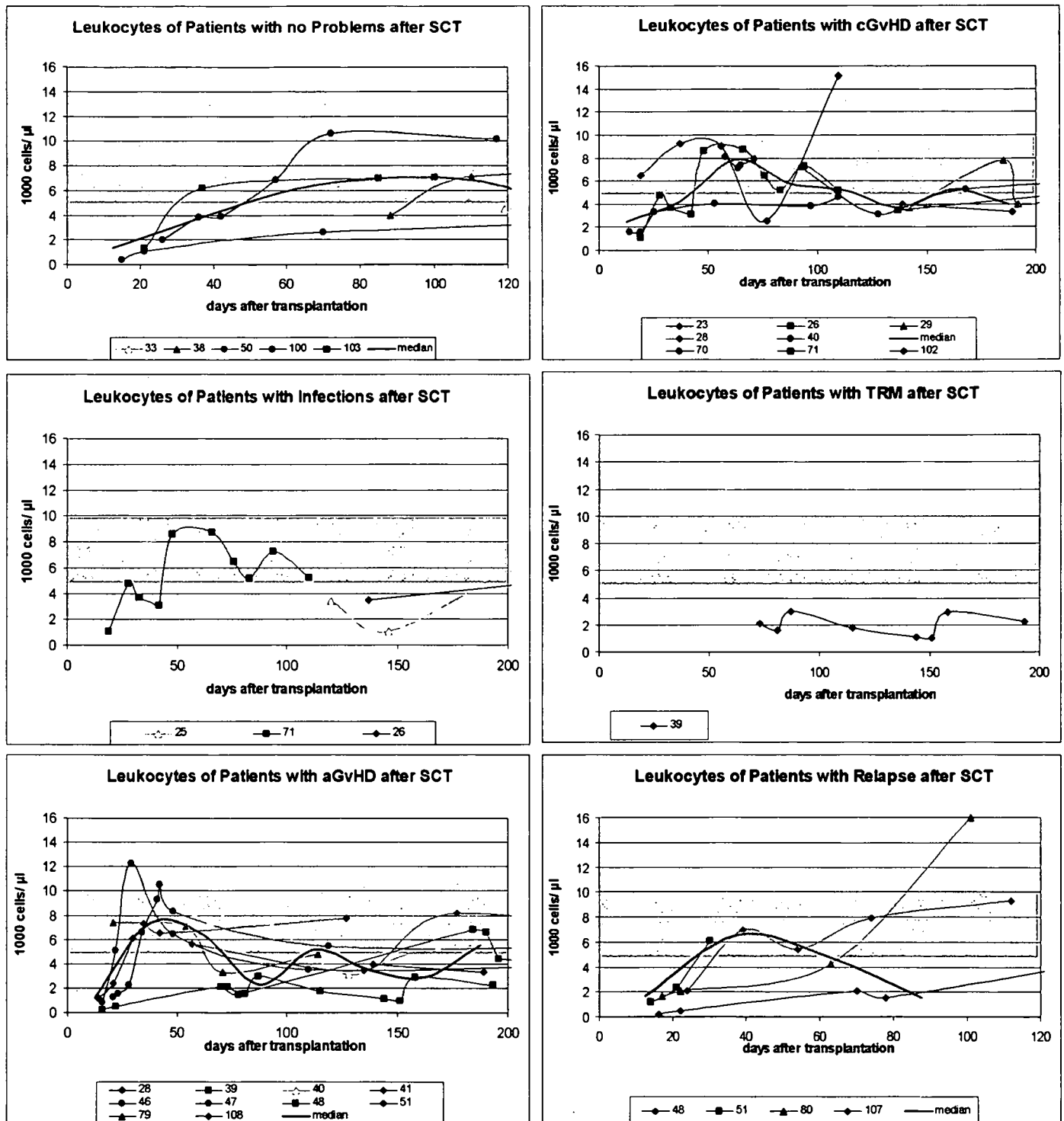


Figure 4-4: Development of Leukocytes of patients after HSCT

Patients with multiple diagnoses as described in Table 4-1 are plotted several times in the 6 graphics. The black median line is calculated by cumulating all measurements within 25-day-intervals. The median is plotted in the middle of each interval. In case of fewer than 3 values the median is dropped. The green bar in the graphics is the inter-quartile range of the healthy volunteer group as shown in Figure 4-2. Leukocytes range of healthy people (4.8-10) was taken from literature [98].

Results

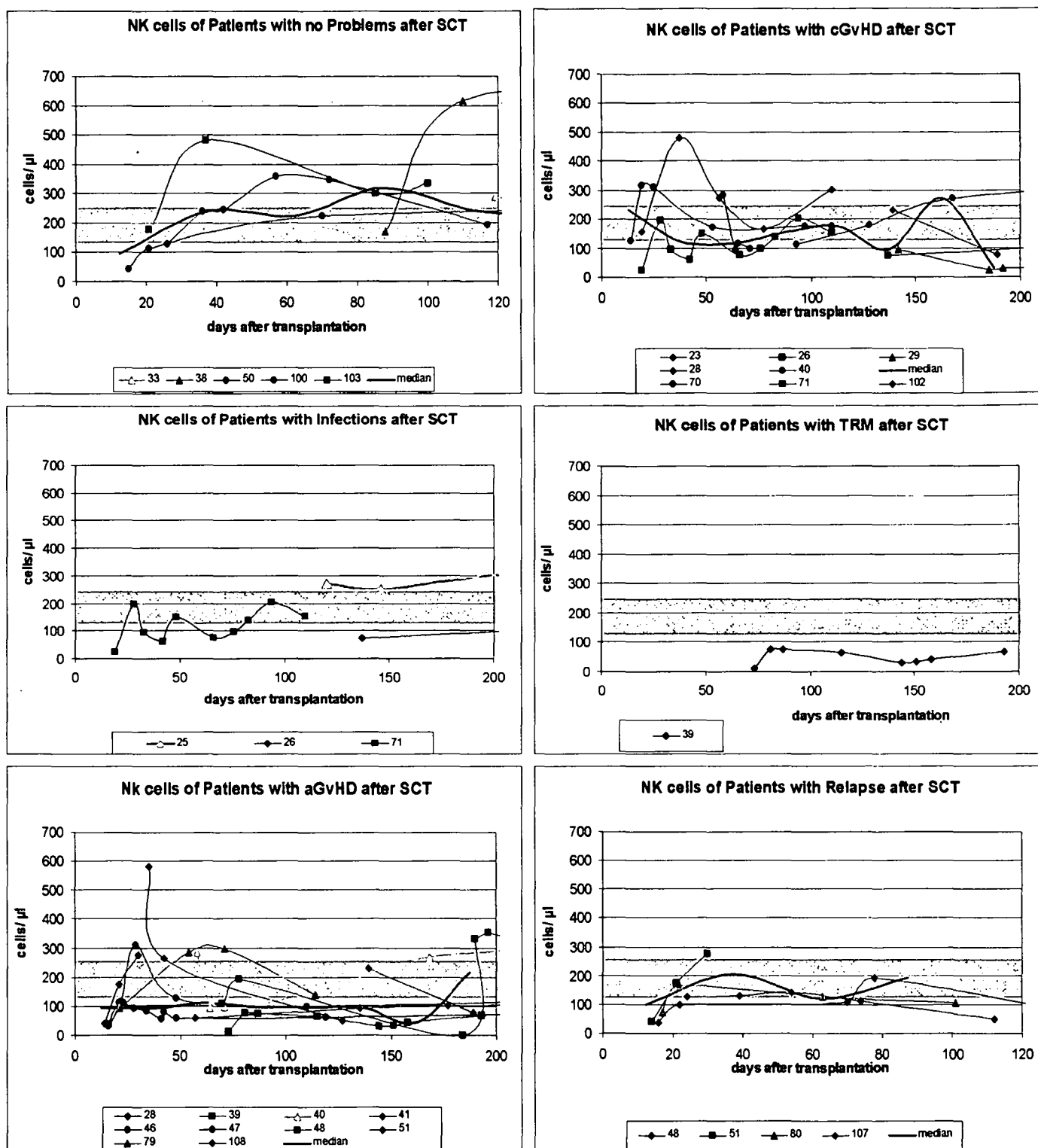


Figure 4-5: Development of NK cells of patients after HSCT

Patients with multiple diagnoses as described in Table 4-1 are plotted several times in the 6 graphics. The black median line is calculated by cumulating all measurements within 25-day-intervals. The median is plotted in the middle of each interval. In case of fewer than 3 values the median is dropped. The green bar in the graphics is the inter-quartile range of the healthy volunteer group (124-234) as shown in Figure 4-2.

Results

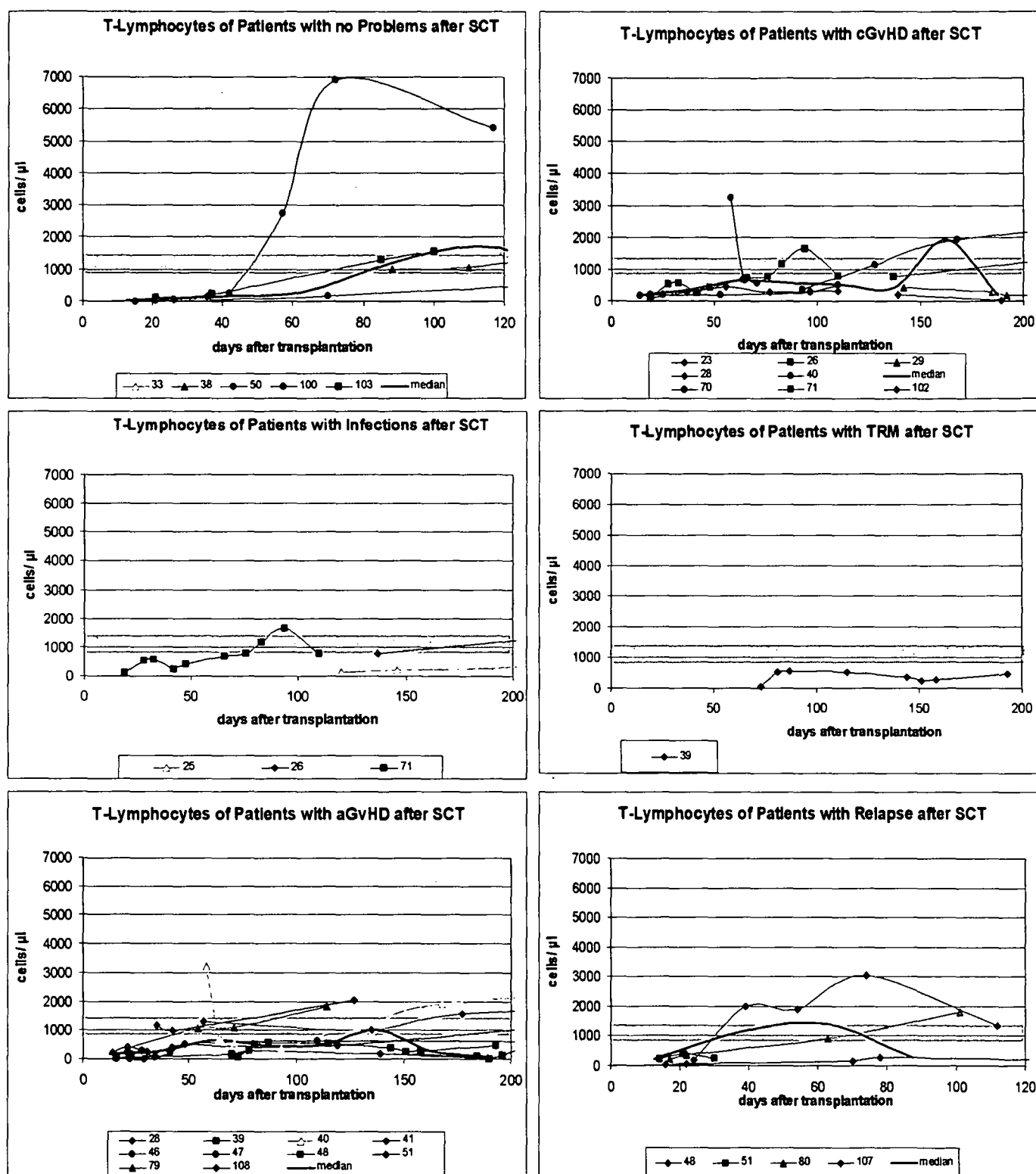


Figure 4-6: Development of T-lymphocytes of patients after HSCT

Patients with multiple diagnoses as described in Table 4-1 are plotted several times in the 6 graphics. The black median line is calculated by cumulating all measurements within 25-day-intervals. The median is plotted in the middle of each interval. In case of fewer than 3 values the median is dropped. The green bar in the graphics is the inter-quartile range of the healthy volunteer group (932-1261) as shown in Figure 4-2.

Results

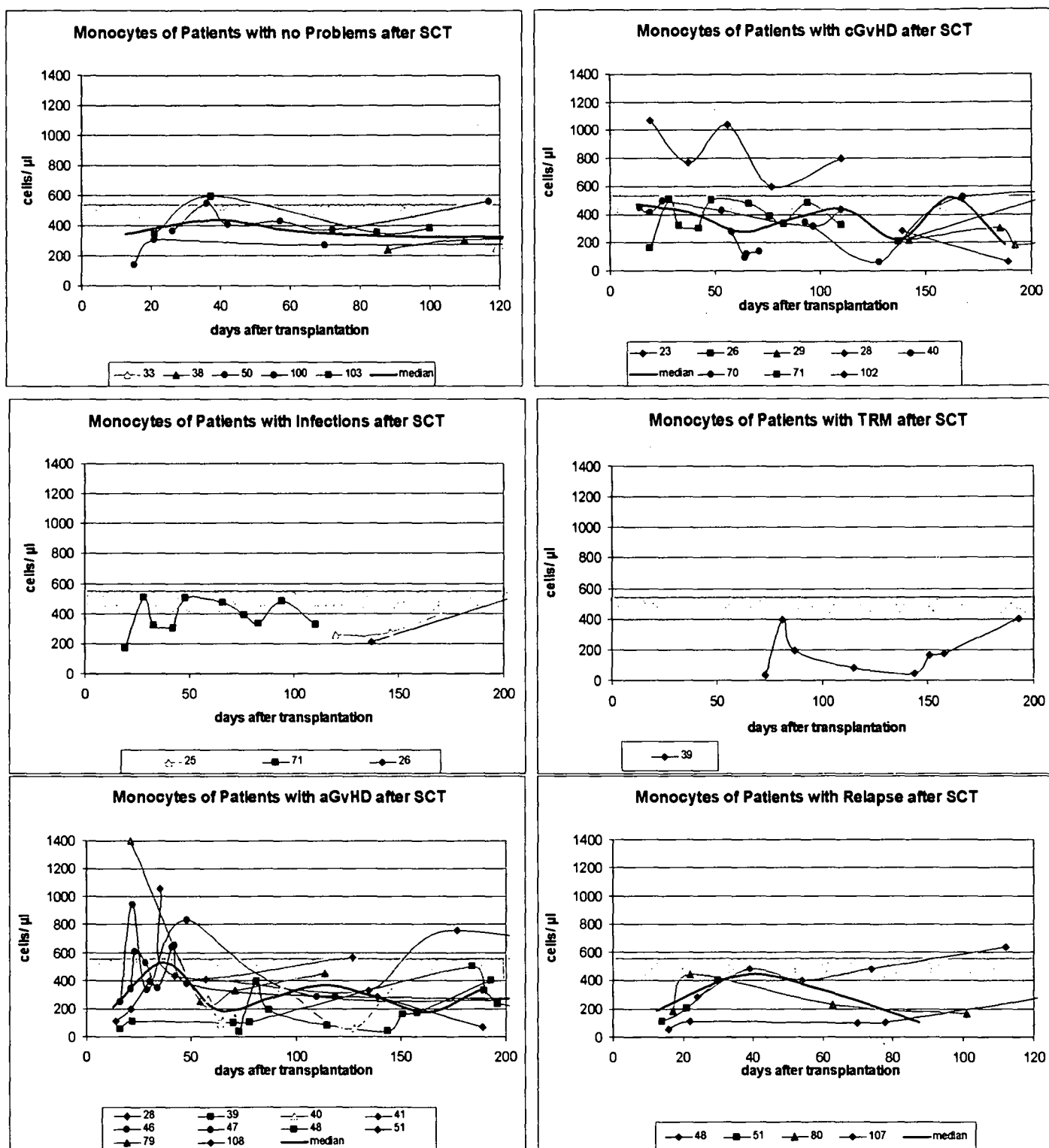


Figure 4-7: Development of monocytes of patients after HSCT

Patients with multiple diagnoses as described in Table 4-1 are plotted several times in the 6 graphics. The black median line is calculated by cumulating all measurements within 25-day-intervals. The median is plotted in the middle of each interval. In case of fewer than 3 values the median is dropped. The green bar in the graphics is the inter-quartile range of the healthy volunteer group (400-545) as shown in Figure 4-2.

1.2. CD4/CD8 T cell Ratio in Patients with acute steroid-refractory GvHD during ECP

1.2.1. Overview

Most T cells are either CD4⁺ CD8⁻ or CD4⁺CD8⁺. Coreceptor molecule expression splits the T-cell population into one of two major subsets, either CD4⁺ CD8⁻ or CD4⁺CD8⁺. Immature T cells at a specific stage of differentiation in the thymus and a very small population in the peripheral blood are CD4⁺CD8⁺. In blood and most tissues, the ratio of CD4⁺ to CD8⁺ T cells is normally a little greater than 2 to 1.

CD4 – T Cell Marker

The CD4 molecule is a cell surface glycoprotein of 55000 Mr. It is mainly expressed by the T-cell lineage (the T lymphocyte subset that recognizes antigens associated with self major histocompatibility complex (MHC) class II molecules, thymocyte subsets) but also by peripheral blood monocytes and tissue macrophages. The extracellular region of CD4 consists of four Ig-like domains. The cytoplasmic domain of CD4 associates with p56lck, a Src-like protein tyrosine kinase, allowing CD4 to transducer intracellular signals when triggered by ligand binding. In Figure 4-1 the CD4 molecule is shown in association with the TCR-CD3 complex.

CD4 interacts with class II MHC proteins (MHC II) [99, 100] and acts as a co-receptor in antigen recognition of peptides associated with MHC II. CD4 appears to contact non-polymorphic regions of MHC II [100, 101] leading to the formation of a ternary complex with the T-cell receptor (TCR). During the antigen recognition process by TCR, MHC II molecules are engaged in simultaneous interaction with TCR and CD4, leading to the coclustering of CD4 and TCR and to T-cell activation.

Conversely, when preceded by ligation of CD4 with anti-CD4 antibodies or other ligands, the signaling through TCR results in T-cell unresponsiveness due to the induction of activation-dependent cell death by apoptosis [102]. Finally, in the absence of antigen recognition and TCR-mediated signaling, the interaction of CD4 with MHC II molecules has been shown to generate a signal inhibiting the T-B lymphocyte adhesion [103].

Mechanism of CD4 T cells

CD4 effector T cells act mainly through the production of cytokines and membrane-associated proteins, and their actions are therefore directed at cells bearing MHC class II

molecules and expressing receptors for these proteins. Activated CD4⁺ T cells are divided in two functional types Th1 and Th2.

Th1 cells are specialized to activate macrophages that are infected by or have ingested pathogens; they secrete IFN- γ to activate the infected cell, as well as other effector molecules. They can also express membrane-bound CD40 ligand and/or Fas ligand. Th2 cells are specialized for B cell activation; they secrete the B-cell growth factors IL-4, IL-5, IL-9, and IL-13. The principal membrane-bound effector molecule expressed by Th2 cells is CD40 ligand, which binds to CD40 on the B cell and induces B-cell proliferation and isotype switching.

CD8 – Cytotoxic T Cell Marker

CD8 is a cell surface glycoprotein expressed on thymocytes and T cells that are specific for antigen presented by MHC class I molecules. CD8 consists of two disulfide-linked chains that form α/α homodimers ($\gamma\delta$ T cells and NK cells) and α/β heterodimers. Both CD8 α and CD8 β have a typical immunoglobulin variable region-like domain in an N-terminal extracellular portion that makes them members of the immunoglobulin gene superfamily. In Figure 4-1 the CD8 molecule is shown in association with the TCR-CD3 complex.

By interacting with the non-polymorphic ($\alpha 3$) domain of the same MHC class I molecules that interact with the T-antigen receptor, CD8 can mediate a function as a coreceptor in TCR-ligand binding and T-cell activation [104]. In the intracytoplasmic domain, CD8 α associates with the intracellular tyrosine kinase p56lck, that may contribute to the successful progress of the activation cascade [105]. Another study shows the involvement of protein kinase C in CD8-mediated signalling [106]. Studies with CD8 knockout mice demonstrated the important roles of CD8 in positive selection within the thymus [107, 108].

Mechanism of Cytotoxic T cell Action

The principal mechanism of cytotoxic T cell action is the calcium-dependent release of specialized lytic granules upon recognition of antigen on the surface of a target cell. These granules are modified lysosomes that contain at least three distinct classes of cytotoxic effector protein. Such proteins are stored in the lytic granules in an active form, but conditions within the granules prevent them from functioning until after their release. One of these cytotoxic proteins, known as perforin, polymerizes in target-cell membranes to

form transmembrane pores. Another class of cytotoxic proteins comprises at least three proteases called granzymes, which belong to the same family of enzymes the serine proteases as the digestive enzymes trypsin and chymotrypsin. The third cytotoxic protein, granulysin, is able to induce apoptosis in target cells and also has antimicrobial action.

1.2.2. Analysis of CD4/CD8 Ratio

We derived the CD4/CD8 ratio of the MNC on both consecutive days during all 4 ECP treatment cycles of 12 patients who achieved complete response (CR) one patient with partly response (PR) and one patient with no response (NR) to ECP.

In Figure 4-8 we have compared results of 12 patients with CR (boxes) with the result of a patient with NR (line with squares) and PR (line with stars). During ECP no significant change of the CD4/CD8 ratio was observed.

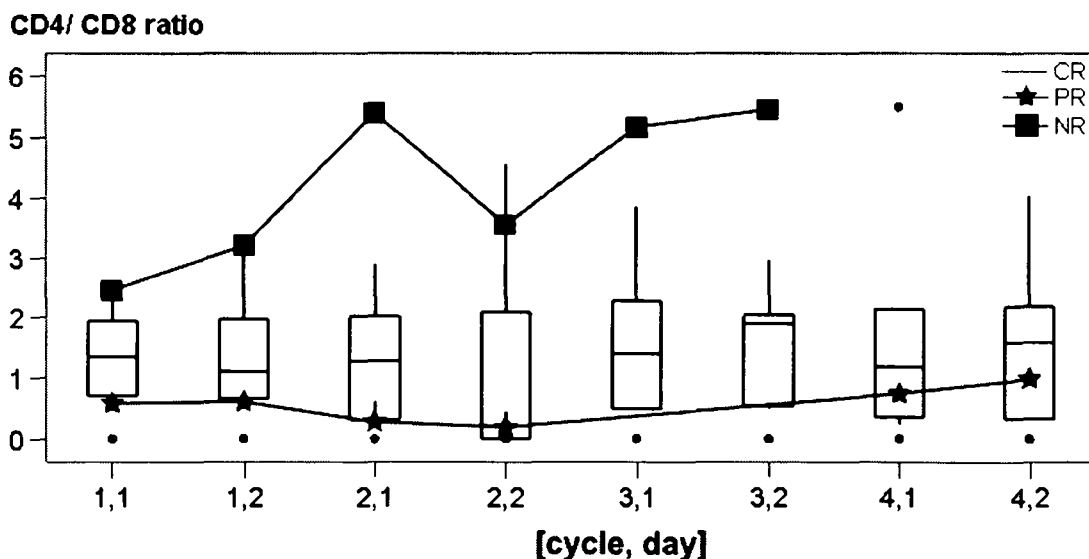


Figure 4-8: CD4/CD8 ratio of peripheral blood of ECP treated patients with aGvHD

The outliers of the boxes are shown as small points. On the X-axes the number of ECP cycles given on day 1 and day 2 are shown [cycle, day]. The following numbers were performed: 1,1 n=10; 1,2 n=8; 2,1 n=6; 2,2 n=6; 3,1 n=10; 3,2 n= 7; 4,1 n=7; 4,2 n=7.

1.3. Intracytoplasmatic Cytokine Production of stimulated T cells during ECP-Treatment of Patients with acute GvHD

1.3.1. Overview

In 1986 Mosmann *et al.* [65] first described the existence of subpopulations of CD4 cells known as T helper type 1 (Th1) and T helper type 2 (Th2) lymphocytes in mice. Initial studies in mice and later in man showed that Th1 cells produce interleukin 2 (IL-2), interferon γ (INF- γ) and tumor necrosis factor α (TNF- α). Th2 cells produce IL-4 as well as IL-5, IL-9, IL-10 and IL-13. All T helper lymphocytes start out as naïve Th0 cells, which, after being activated, are capable of differentiating into either Th1 or Th2 effector cells.

In both mice and humans, a cytokine storm related to the Th1 phenotype has been found to correlate with the development of aGvHD. Thereby, IL-2 and INF- γ mature T lymphocytes. IL-4 and IL-10 produced by Th2 prevent the secretion of INF- γ and this way may help to suppress GvHD [109].

1.3.2. Decrease in Th1 Cytokines during ECP

We assessed the production of the Th1-cytokines IL-2, INF- γ and TNF- α in CD4+ and CD8+ T cells prior to and after ECP therapy in all 16 patients. Results are shown in Figures 4-9 to 4-14. The decrease of IL-2, TNF- α and INF- γ in Post-ECP samples compared to PB and Pre-ECP samples is highly significant ($p < 0.001$) in both CD4+ T cells as well as CD8+ T cells. A significant decrease between PB and Pre-ECP is only seen for IL-2 in CD4 ($p=0.0002$) and CD8 T cells ($p=0.0461$). Additionally, we found a significant decrease in TNF- α between PB and Pre-ECP in CD8 T cells ($p=0.0104$).

Results

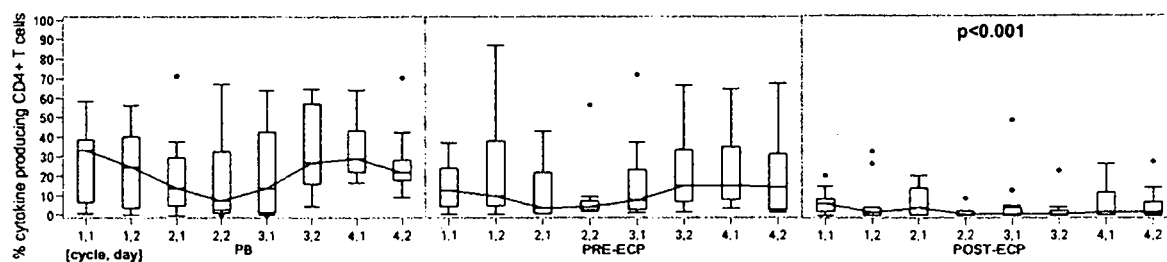


Figure 4-9: IL-2 Production of CD4+ T cells in patients with aGvHD treated with ECP

On the X-axes the number of ECP cycles given on day 1 and day 2 are shown [cycle, day].

The following ECP therapy events are performed for each patient:

In PB 1,1: n=13, 1,2: n=12, 2,1 n=8, 2,2: n=6, 3,1: n=11, 3,2: n=8, 4,1: n=8; 4,2: n=9.

In PRE-ECP and POST-ECP 1,1: n=13, 1,2: n=12, 2,1 n=8, 2,2: n=8, 3,1: n=12, 3,2: n=8, 4,1: n=8; 4,2: n=9 CD4 analyses and CD8 analyses, as well as all 5 cytokines have the same falling numbers.

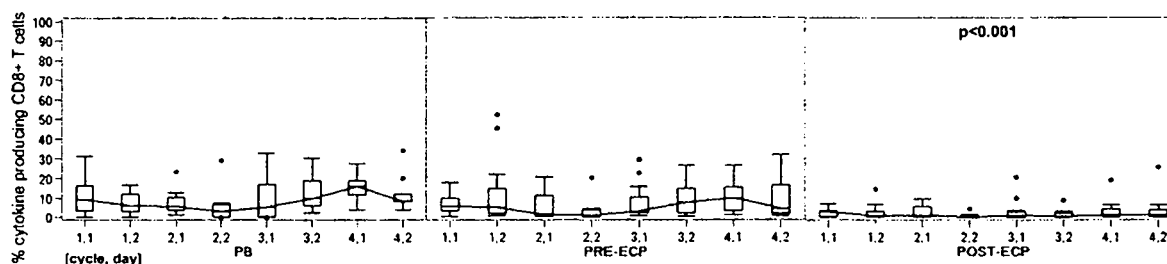


Figure 4-10: IL-2 Production of CD8+ T cells in patients with aGvHD treated with ECP

On the X-axes the number of ECP cycles given on day 1 and day 2 are shown [cycle, day].

The following ECP therapy events are performed for each patient:

In PB 1,1: n=13, 1,2: n=12, 2,1 n=8, 2,2: n=6, 3,1: n=11, 3,2: n=8, 4,1: n=8; 4,2: n=9.

In PRE-ECP and POST-ECP 1,1: n=13, 1,2: n=12, 2,1 n=8, 2,2: n=8, 3,1: n=12, 3,2: n=8, 4,1: n=8; 4,2: n=9 CD4 analyses and CD8 analyses, as well as all 5 cytokines have the same falling numbers.

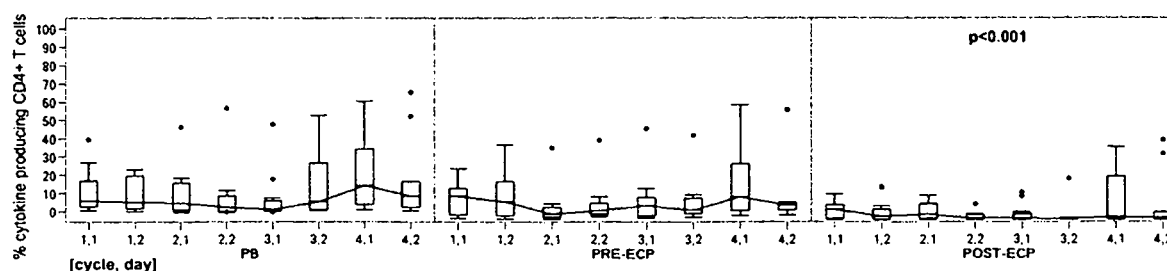


Figure 4-11: INF-γ Production of CD4+ T cells in patients with aGvHD treated with ECP

On the X-axes the number of ECP cycles given on day 1 and day 2 are shown [cycle, day].

The following ECP therapy events are performed for each patient:

In PB 1,1: n=13, 1,2: n=12, 2,1 n=8, 2,2: n=6, 3,1: n=11, 3,2: n=8, 4,1: n=8; 4,2: n=9.

In PRE-ECP and POST-ECP 1,1: n=13, 1,2: n=12, 2,1 n=8, 2,2: n=8, 3,1: n=12, 3,2: n=8, 4,1: n=8; 4,2: n=9 CD4 analyses and CD8 analyses, as well as all 5 cytokines have the same falling numbers.

Results

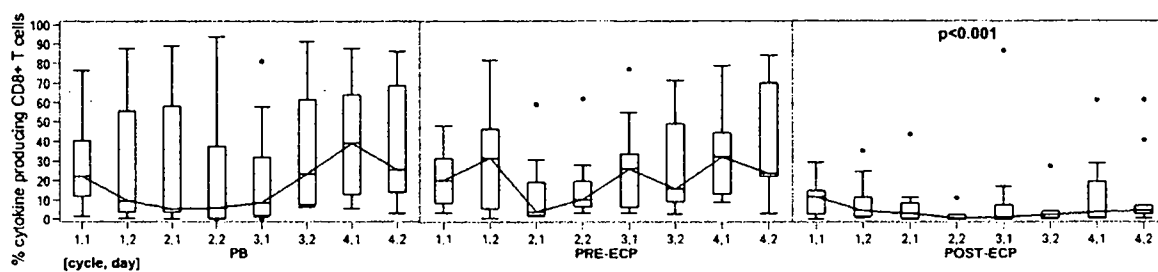


Figure 4-12: INF- γ Production of CD8+ T cells in patients with aGvHD treated with ECP

On the X-axes the number of ECP cycles given on day 1 and day 2 are shown [cycle, day].

The following ECP therapy events are performed for each patient:

In PB 1,1: n=13, 1,2: n=12, 2,1 n=8, 2,2: n=6, 3,1: n=11, 3,2: n=8, 4,1: n=8; 4,2: n=9.

In PRE-ECP and POST-ECP 1,1: n=13, 1,2: n=12, 2,1 n=8, 2,2: n=8, 3,1: n=12, 3,2: n=8, 4,1: n=8; 4,2: n=9 CD4 analyses and CD8 analyses, as well as all 5 cytokines have the same falling numbers.

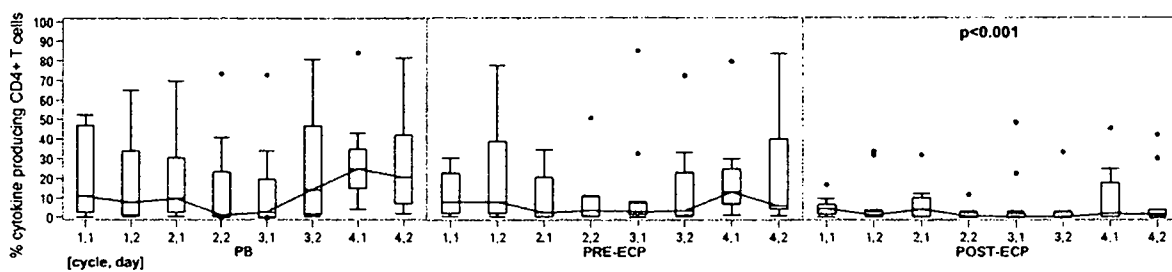


Figure 4-13: TNF- α Production of CD4+ T cells in patients with aGvHD treated with ECP

On the X-axes the number of ECP cycles given on day 1 and day 2 are shown [cycle, day].

The following ECP therapy events are performed for each patient:

In PB 1,1: n=13, 1,2: n=12, 2,1 n=8, 2,2: n=6, 3,1: n=11, 3,2: n=8, 4,1: n=8; 4,2: n=9.

In PRE-ECP and POST-ECP 1,1: n=13, 1,2: n=12, 2,1 n=8, 2,2: n=8, 3,1: n=12, 3,2: n=8, 4,1: n=8; 4,2: n=9 CD4 analyses and CD8 analyses, as well as all 5 cytokines have the same falling numbers.

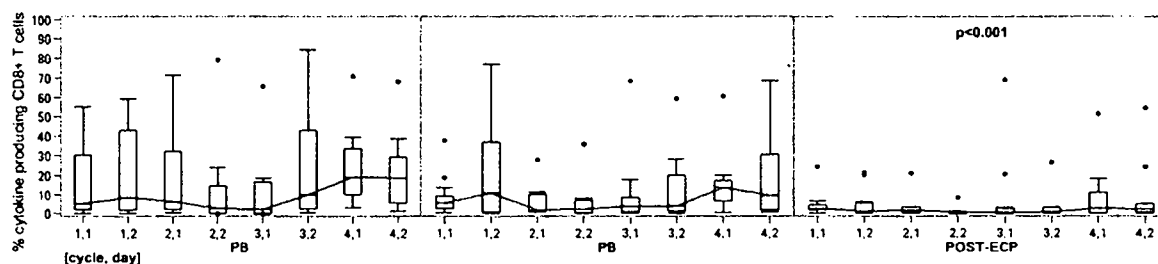


Figure 4-14: TNF- α Production of CD8+ T cells in patients with aGvHD treated with ECP

On the X-axes the number of ECP cycles given on day 1 and day 2 are shown [cycle, day].

The following ECP therapy events are performed for each patient:

In PB 1,1: n=13, 1,2: n=12, 2,1 n=8, 2,2: n=6, 3,1: n=11, 3,2: n=8, 4,1: n=8; 4,2: n=9.

In PRE-ECP and POST-ECP 1,1: n=13, 1,2: n=12, 2,1 n=8, 2,2: n=8, 3,1: n=12, 3,2: n=8, 4,1: n=8; 4,2: n=9 CD4 analyses and CD8 analyses, as well as all 5 cytokines have the same falling numbers.

1.3.3. No Increase in Th2 Cytokines during ECP

We analyzed the production of the Th2-cytokines IL-4, and IL-10 in CD4+ T cells and CD8+ T cells prior to and after ECP therapy in all 16 patients. Results are shown in Figures 4-15 to 4-18.

The decrease of IL-4 after ECP compared to PB and PRE-ECP is highly significant in CD4+, highly significant in CD8+ only between PB and Post-ECP T cells ($p < 0.001$) and significant in CD8+ between Pre-ECP and Post-ECP ($p < 0.0385$). The measured IL-10 amounts were low and thus, changes in production difficult to assess. In both CD4+ and CD8+ T cells a significant decrease of IL-10 was seen after ECP compared to PB prior to ECP ($p=0.0026$ and 0.0158).

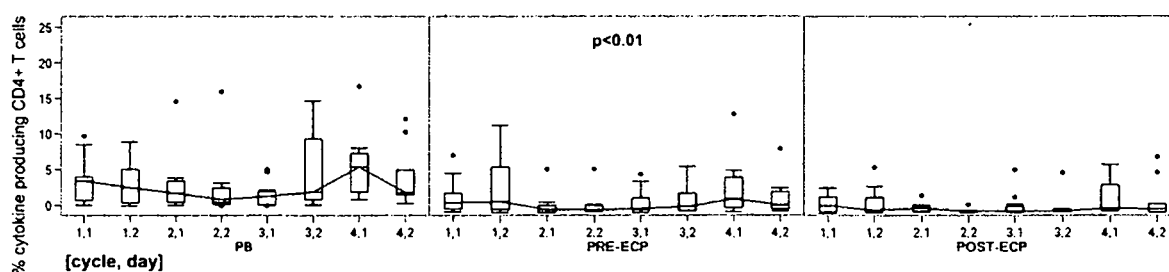


Figure 4-15: IL-4 Production of CD4+ T cells in patients with aGvHD treated with ECP

On the X-axes the number of ECP cycles given on day 1 and day 2 are shown [cycle, day].

In PB 1,1: n=13, 1,2: n=12, 2,1: n=8, 2,2: n=6, 3,1: n=11, 3,2: n=8, 4,1: n=8, 4,2: n=9.

In PRE-ECP and POST-ECP 1,1: n=13, 1,2: n=12, 2,1: n=8, 2,2: n=8, 3,1: n=12, 3,2: n=8, 4,1: n=8, 4,2: n=9

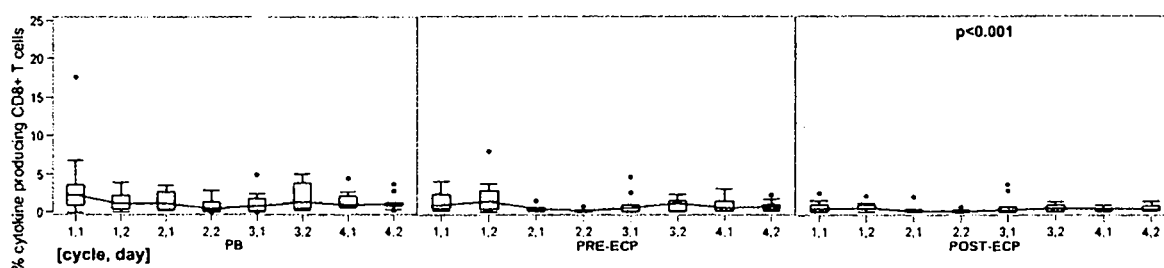


Figure 4-16: IL-4 Production of CD8+ T cells in patients with aGvHD treated with ECP

On the X-axes the number of ECP cycles given on day 1 and day 2 are shown [cycle, day].

In PB 1,1: n=13, 1,2: n=12, 2,1: n=8, 2,2: n=6, 3,1: n=11, 3,2: n=8, 4,1: n=8, 4,2: n=9.

In PRE-ECP and POST-ECP 1,1: n=13, 1,2: n=12, 2,1: n=8, 2,2: n=8, 3,1: n=12, 3,2: n=8, 4,1: n=8, 4,2: n=9

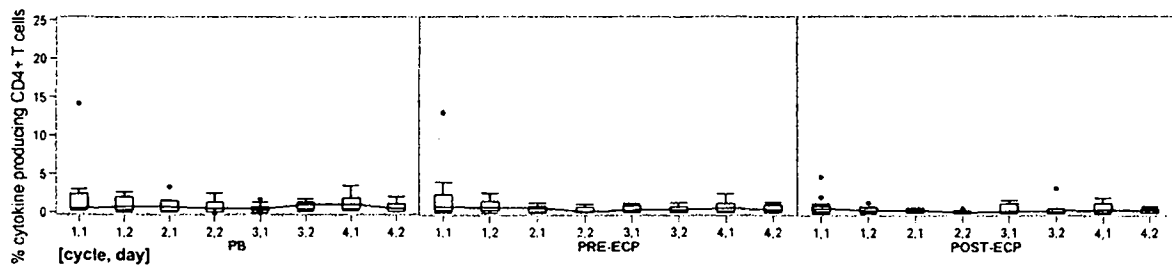


Figure 4-17: IL-10 Production of CD4+ T cells in patients with aGvHD treated with ECP

On the X-axes the number of ECP cycles given on day 1 and day 2 are shown [cycle, day].

In PB 1,1: n=13, 1,2: n=12, 2,1: n=8, 2,2: n=6, 3,1: n=11, 3,2: n=8, 4,1: n=8; 4,2: n=9.

In PRE-ECP and POST-ECP 1,1: n=13, 1,2: n=12, 2,1: n=8, 2,2: n=8, 3,1: n=12, 3,2: n=8, 4,1: n=8; 4,2: n=9

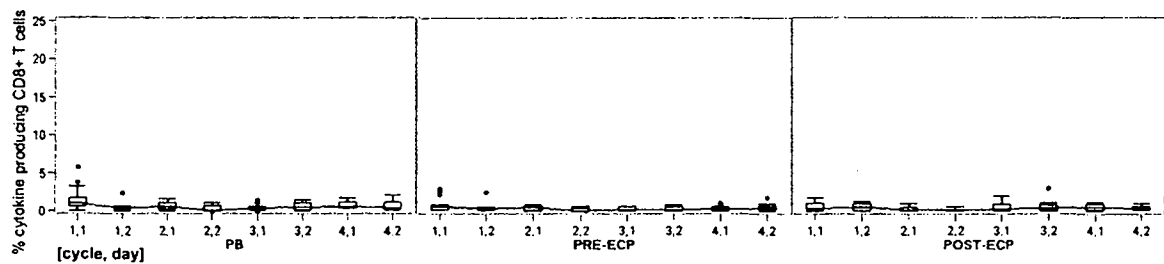


Figure 4-18: IL-10 Production of CD8+ T cells in patients with aGvHD treated with ECP

On the X-axes the number of ECP cycles given on day 1 and day 2 are shown [cycle, day].

In PB 1,1: n=13, 1,2: n=12, 2,1: n=8, 2,2: n=6, 3,1: n=11, 3,2: n=8, 4,1: n=8; 4,2: n=9.

In PRE-ECP and POST-ECP 1,1: n=13, 1,2: n=12, 2,1: n=8, 2,2: n=8, 3,1: n=12, 3,2: n=8, 4,1: n=8; 4,2: n=9

1.3.4. Correlation of Treatment Response with Cytokine Production

During the time of analyses, we had only 2 patients with PR and NR confronting 12 patients with CR to ECP. We found a difference in CD4/CD8 ratio of one NR patient as shown in Figure 4-3. A comparison of cytokine production between all PB, PRE-ECP and POST-ECP in CD4+ and CD8+ T cells of 12 CR patients PB (n=79), PRE-ECP (n=82), POST-ECP (n=82) shows Figure 4-19 and Figure 4-20. Because of insufficient amount of patients with diagnosed NR and PR, a comparison to CR patients was not possible.

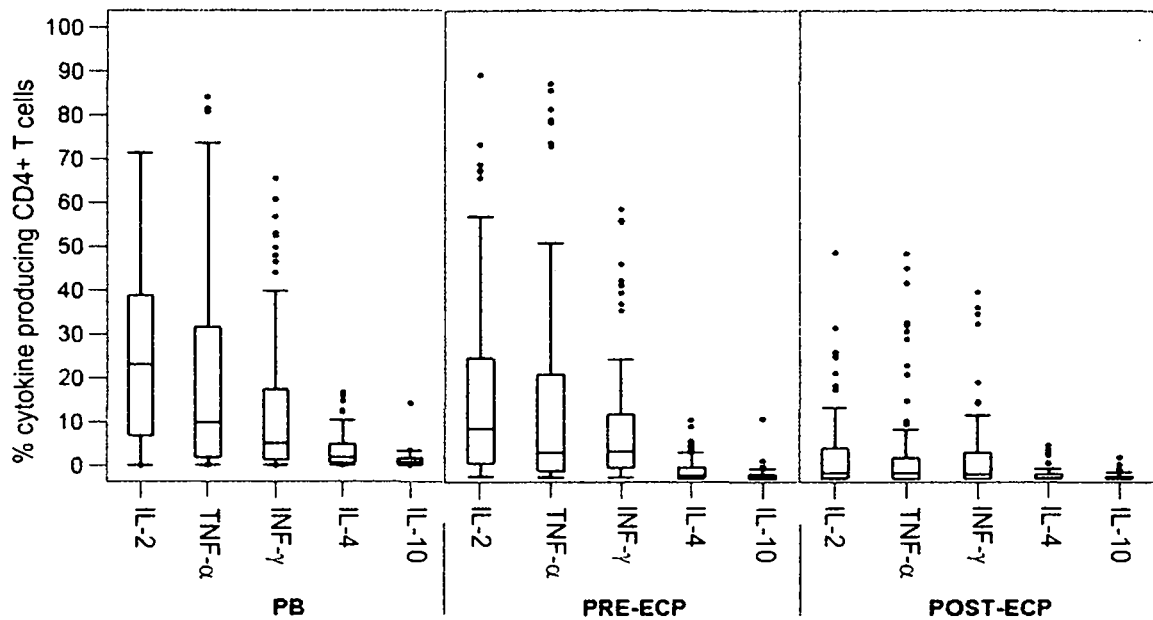


Figure 4-19: Cumulative cytokine production of CD4+ T cells during ECP

Cytoplasmatic cytokine producing cells are shown in percent of total CD4 T cells population. For each sample of PB (n=79), Pre-ECP (n=82) and Post-ECP (n= 82) the 5 cytokines (IL-2, TNF-α, INF-γ, IL-4, IL-10) are cumulated in one box. Outliers are signed as points.

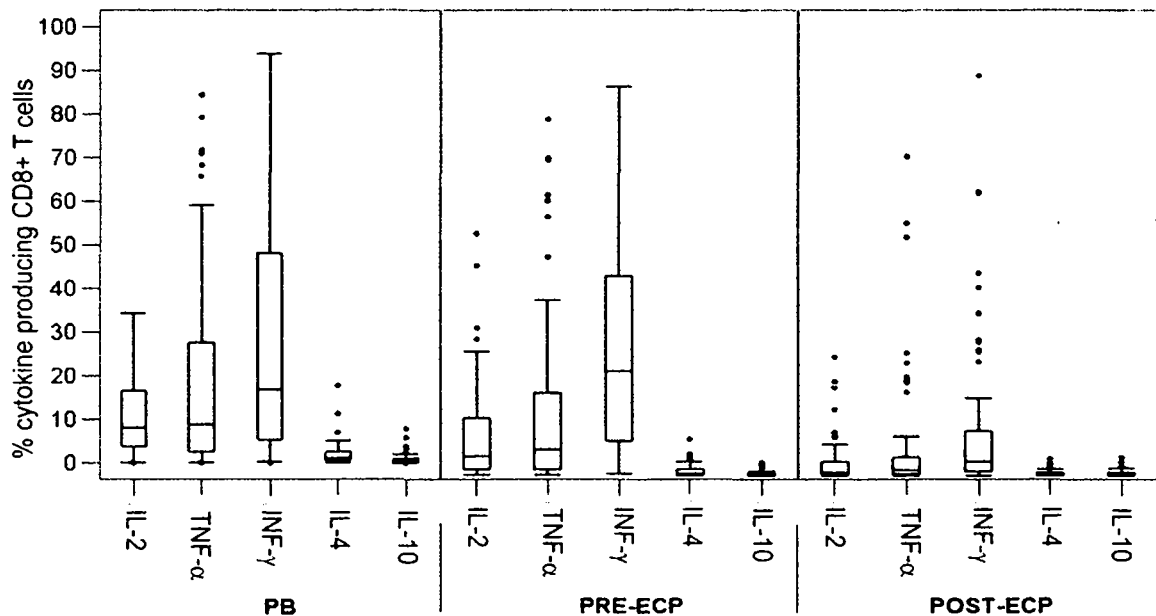


Figure 4-20: Cumulative cytokine production of CD8+ T cells during ECP

Cytoplasmatic cytokine producing cells are shown in percent of total CD8 T cells population. For each sample of PB (n=79), Pre-ECP (n=82) and Post-ECP (n= 82) the 5 cytokines (IL-2, TNF-α, INF-γ, IL-4, IL-10) are cumulated in one box. Outliers are signed as points.

1.4. Apoptosis of White Blood Cells after Extracorporeal Photochemotherapy of Patients with acute GvHD

1.4.1. Overview

Each day the bone marrow produces many millions of new neutrophils, monocytes, red blood cells, and lymphocytes, and this production must be balanced by an equal loss of these cells. Regulated loss of all these blood cells occurs by apoptosis. Apoptosis is the genetically controlled ablation of cells during normal development and is distinct from necrosis in both the biochemical and the morphological changes that occur [110-112].

Fas and Fas ligand

Lymphocytes are special since they do not receive survival signals and become self-reactive undergoing programmed cell death. The Fas antigen is expressed on many cells but is especially prominent on activated T-lymphocytes. Activation of Fas (CD95) by the Fas ligand (CD178) of cytotoxic T cells has profound consequences for the cell since Fas contains a 'death domain' in its cytoplasmic tail, which can initiate an activation cascade that leads to apoptotic cell death [113]. Fas is important in maintaining T-lymphocyte homeostasis.

1.4.2. Steps of Apoptosis

In contrast to necrotic cells, apoptotic cells are characterized morphologically by compaction of the nuclear chromatin, shrinkage of the cytoplasm and production of membrane bound apoptotic bodies. Biochemically, apoptosis is distinguished by fragmentation of the genome and cleavage or deregulation of several cellular proteins. In Figure 4-21 the steps of apoptosis are shown in an overview.

Loss of the mitochondrial inner transmembrane potential is often associated with the early stages of apoptosis and may be one of the central features of the process [114]. Collapse of this potential is thought to coincide with the opening of the mitochondrial permeability transition pores, allowing passage of ions and small molecules. The resulting equilibration of ions leads in turn to the decoupling of the respiratory chain and subsequently to the release of cytochrome c into the cytosol.

Caspases are a key component of the apoptotic machinery of cells, participating in an enzyme cascade that results in cellular disassembly. The recognition site for caspases is marked by three to four amino acids followed by an aspartic acid residue, with the

cleavage occurring after the aspartate. These proteases are typically synthesized as inactive precursors. Inhibitor release or cofactor binding activates the caspase through cleavage at internal aspartates through autocatalysis or by the action of another protease. Caspase 3 is a key effector in the apoptosis pathway, amplifying the signal from initiator Caspases (such as caspase-8) and signifying full commitment to cellular disassembly. In addition to cleaving other caspases in the enzyme cascade, caspase-3 has been shown to cleave poly(ADP-ribose) polymerase (PARP), DNA-dependent protein kinase, protein kinase Cd and actin [115, 116].

Changes in the cell cytosol also occur during apoptosis, with variations in cellular ion concentration (e.g. Ca^{2+}), pH, and level of reactive oxygen species (ROS) [117, 118].

In viable cells, PS is located on the cytoplasmic surface of the cell membrane. As cells undergo apoptosis, PS is translocated to the outer leaflet of the plasma membrane and exposed to the extracellular environment [119].

As apoptosis progresses, the permeability of a cell's membrane gradually increases in discrete stages [120].

Cells undergoing apoptosis display an increase in chromatin condensation. Morphologically, the nuclei of apoptotic cells become smaller than those of normal cells and become hyperfluorescent when labeled with some nuclear stains.

DNA fragmentation has long been used to distinguish apoptosis from necrosis, and is among the most reliable methods for detection of apoptotic cells [121]. When DNA strands are cleaved or nicked by nucleases, 3'-hydroxyl ends are exposed. The hydroxyl groups can then serve as a starting point for terminal deoxynucleotidyl transferase (TdT), which adds deoxyribonucleotides in a template-independent fashion.

A cell undergoing apoptosis rapidly condenses into small enclosed fragments (apoptotic bodies), which can then be phagocytosed [122]. Dying peripheral blood cells are phagocytosed by specialized macrophages in the liver and spleen.

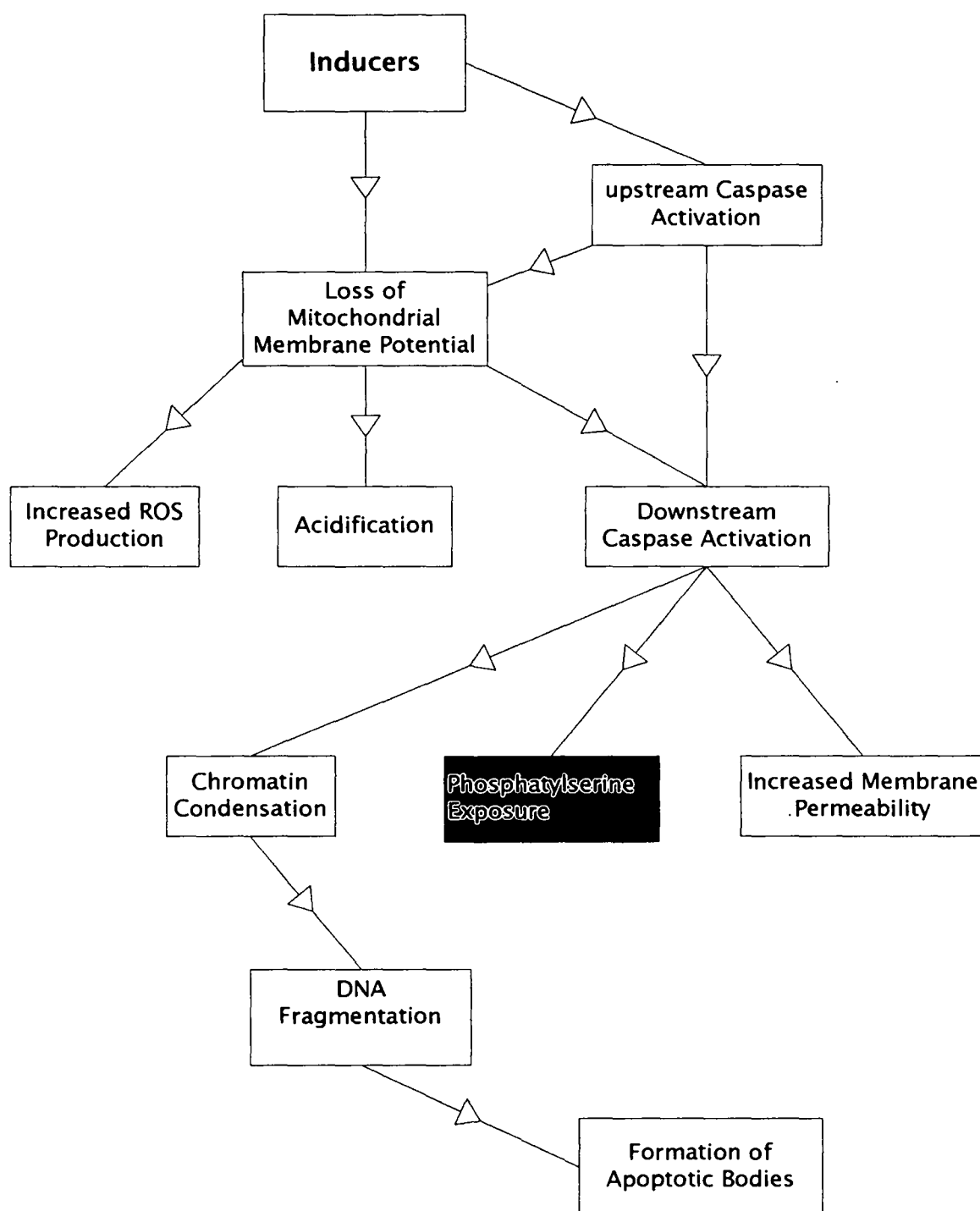


Figure 4-21: Overview of key apoptotic events

1.4.3. Assessment of Apoptosis in PB of aGVHD Patients

PB samples of 11 patients with aGVHD were analyzed for apoptosis. PB was taken from the first of the 2 consecutive days and CD4⁺ T cells and CD8⁺ T cells were analyzed separately.

Figure 4-22 shows the percentage of viable CD4+ and CD8+ T cells in PB, Pre-ECP and Post-ECP blood samples 10 hours and 24 hours after irradiation. The viability of CD4+ T cells in PB and pre-ECP did not significantly change between 10 and 24 hours of culture whereas in post-ECP samples at 10 and 24 hours only 50% and 15% of CD4+ T cells were vital.

CD8+ T cells nearly have the same rapidly decreasing tendency of 49% vital cells at 10 hours decreasing to 18% at 24 hours. The loss of viability of CD4+ and CD8+ T cells in post-ECP samples at 24 hours was found to be statistically significant compared with pre-ECP samples. The particular p-values are shown within Figure 4-22. Pre-ECP CD8+ T cells have a drop of vitality of 5% compared to PB at both time points. The same tendency is shown by CD4+ T cells at 10 hours, but Pre-ECP CD4+ T cells at 24 hours have an increased vitality of 6% compared to PB.

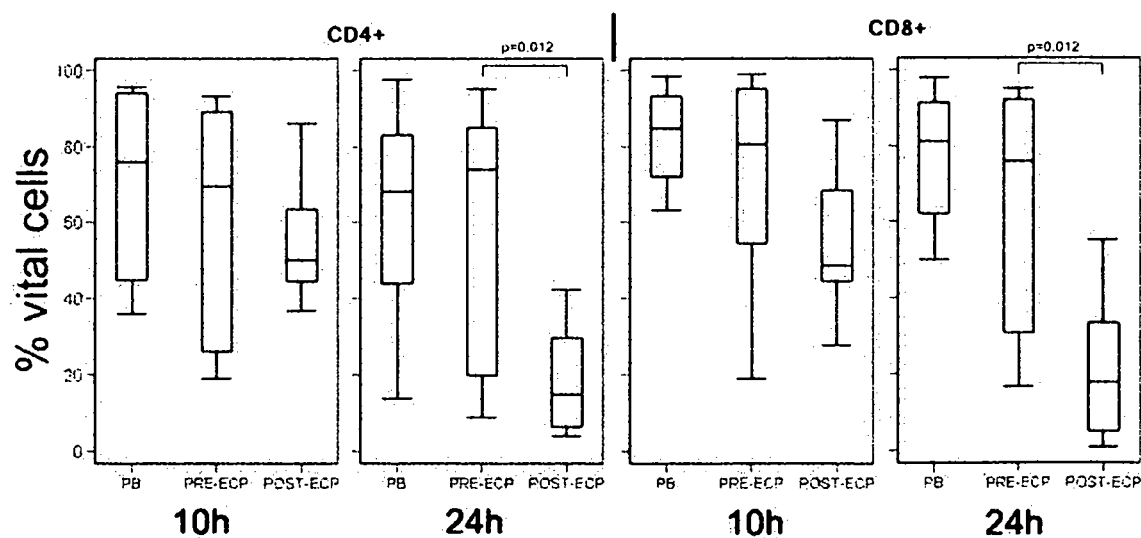


Figure 4-22: Interpolated 10-hour-point and 24-hour-point of apoptosis of CD4+ and CD8+ T cells of patients with aGVHD.

The following numbers of analyses were performed: The patient group differed by PB (n=8), Pre-ECP (n=10) and Post-ECP (n=13), but was kept equal for both subpopulations.

1.5. Recovery of Dendritic Cells in Patients after Haematopoietic Stem Cell Transplantation

1.5.1. Overview

Dendritic Cells (DC) represent populations of leukocytes (Figure 4-23) derived from BM progenitor cells, which have specialist APC functions and as such, they link the innate and adaptive immune systems.

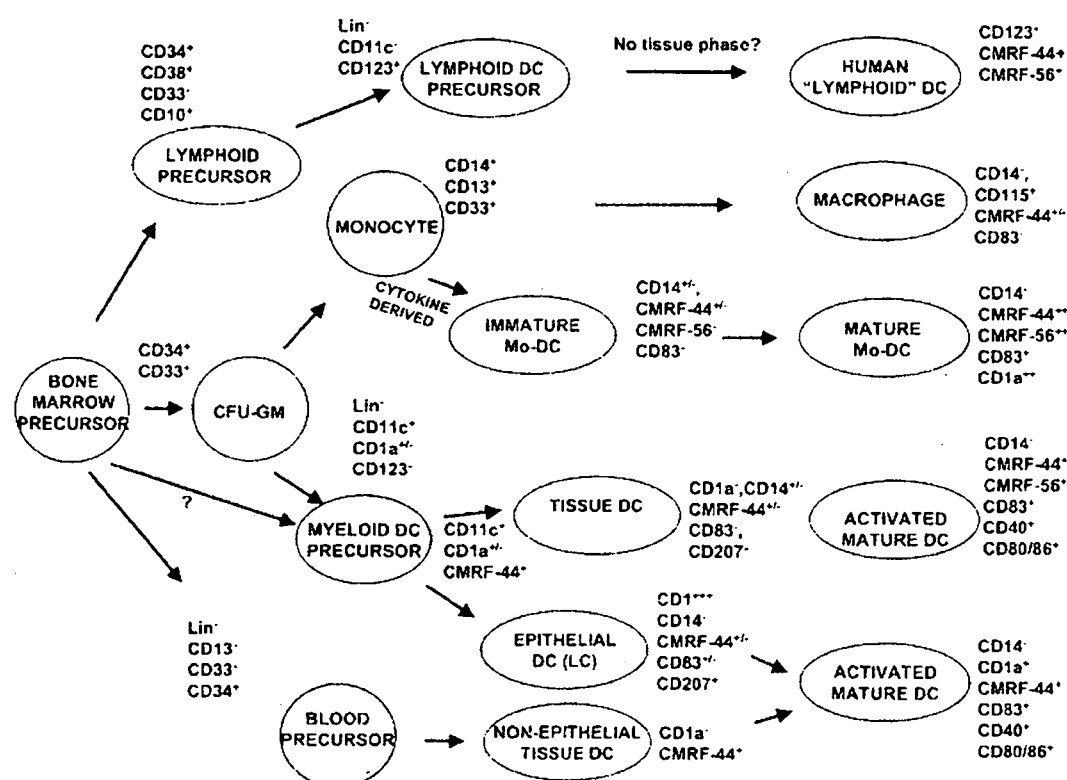


Figure 4-23: The pluripotent haematopoietic stem cell gives rise to CD34⁺ precursors which proliferate and differentiate into DC populations.

The critical functional properties of DC include the following abilities:

(i) to take up, process, and present antigen (Ag). Immature DCs have an unsurpassed machinery to take up antigens by constitutive macropinocytosis, receptor-mediated endocytosis and phagocytosis [123].

After internalization, most exogenous antigens are processed through an endosomal and lysosomal pathway in which proteins are cleaved into peptides and loaded onto MHC class II molecules [124]. Alternatively, exogenous antigens can be released into the cytosol, gaining access to the proteasome - the main nonlysosomal protease - that

generates peptides and transfers them to the endoplasmic reticulum, where they are loaded onto MHC class I molecules [125, 126]. This exogenous MHC class I presentation pathway is also referred to as cross-presentation.

(ii) to migrate selectively through tissues. Therefore mature DCs upregulate the lymph node-directing chemokine receptor CCR7 and acquire migratory capacity toward lymphnode-directing chemokines CCL21 and CCL19 [127, 128].

(iii) to interact with, stimulate, and direct primary T and B lymphocyte responses. DC maturation is triggered by numerous stimuli, including endogenous factors that are released by necrotic cells, proinflammatory cytokines that are secreted by bystander cells, exogenous microbial products that bind to Toll-like receptors (TLRs) (e.g. LPS), pathogen signals or CD40L [129, 130]. In the latter two cases DCs induce INF- γ and cytolytic function in T cells.

The basic surface membrane phenotype identifies DCs as CD45 + leukocytes that express high levels of major histocompatibility complex (MHC) class II molecules in the absence of markers of leukocyte differentiation (lineage negative) including CD3, CD15, CD56, CD19, CD20, and CD14 (\pm CD16).

According to stage of DC differentiation the following subsets can be distinguished:

The 'myeloid' DC originates in the bone marrow and migrates into the blood as an immature population before forming an extensive network of interstitial DC in most non-lymphoid organs except brain, parts of the eye, and testes [131]. The first human '**myeloid**' dendritic cell population, called type 1 (DC1), is CD11c+ CD123^{dim}. The CD11c+ DC induces a strong MLR and produces IL-12. Mature myeloid DC express large amounts of MHC class II and co-stimulatory molecules such as CD40, CD80 (B7-1) and CD86 (B7-2) that are prerequisites for their potent T cell-sensitizing capacity [132, 127]. Tolerance induction mediated by myeloid DC seems to be mainly related to an immature developmental stage.

Immature DC are active in antigen uptake and processing but show only a moderate surface expression of MHC class II molecules and no or low levels of co-stimulatory molecules [133, 134]. Antigen presentation without co-stimulation can lead to T cell anergy [135] and, indeed, such immature DC can be tolerogenic [136, 137].

The possibility that blood monocytes (Mo) as opposed to blood DC traffic to tissues and differentiate into monocyte-derived DC (MoDC) is becoming accepted [138]. This at first sight makes less biological sense as a primary APC, and McLellan et al have proposed that it may reflect a secondary boost pathway for developing an amplified APC population [139]. Subsets of monocytes probably exist and an alternative view is that certain phenotypically defined subsets of blood Mo are destined to differentiate into tissue DC [140]. Monocyte subsets may also contribute directly to the heterogeneity of blood DC preparations as a result of differential cell separation technologies. Heavy reliance on CD14 as a monocyte marker should be a concern to DC biologists as its multiple epitopes, variable expression, and soluble form all have the potential to confound.

The second human 'lymphoid' dendritic cell population, called type 2 (DC2) is CD11c-CD123^{bright}.

In contrast, the CD11c- DC produces large quantities of IFN- γ and stimulates a weaker MLR [109]. These latter cells, also known as **plasmacytoid** DCs probably equate to the natural IFN- α producing cells described somewhat earlier [141]. This DC population may traffic directly to lymph nodes from the blood as CD123+ cells are particularly prominent around high endothelial venules [142]. Indeed it is tempting to speculate that the apparently non-activated DC and/or 'lymphoid' DC are involved in maintaining peripheral tolerance.

1.5.2. Assessment of Dendritic Cells of Healthy Volunteers

A group of healthy volunteers (8 female, 10 men) with a median age of 40 (range, 20 to 62) were analyzed at one time point. I analyzed median populations of 13.46 DC1/ μ l, 8.25 DC2/ μ l, 44.57 basophile/ μ l, a median total DC population of 25.09 DC/ μ l as shown in Figure 4-24 and a median DC1/DC2 ratio of 1.66.

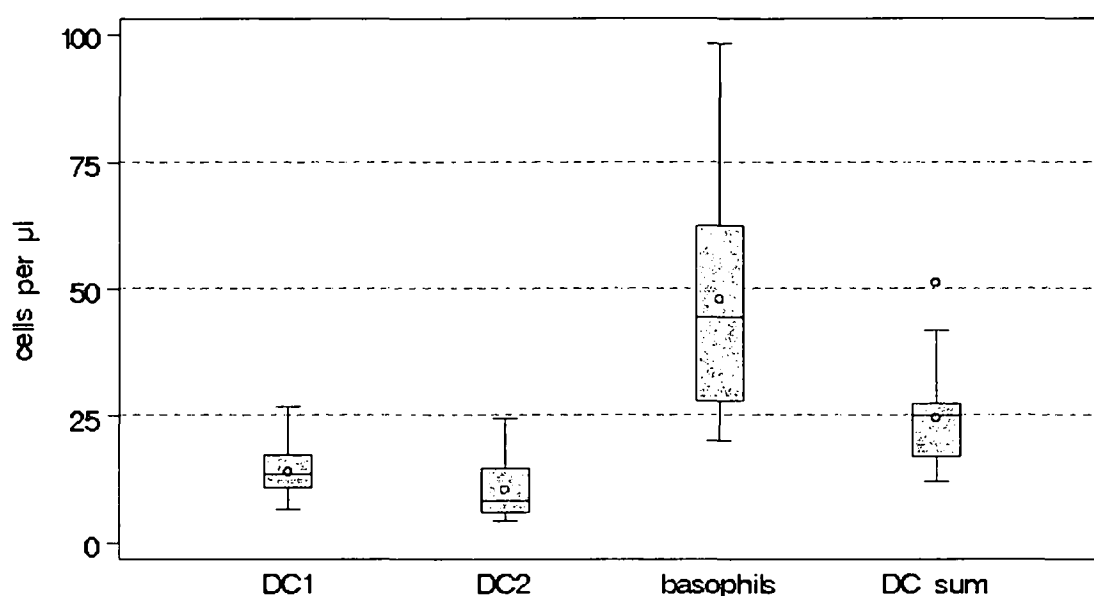


Figure 4-24: Healthy volunteers' dendritic cells and basophils.

Total DC population (DC sum) and its two sub-fractions DC1, DC2 and basophils of the healthy group are shown in box plots. An Outlier is marked as point. Points within the boxes show the mean.

1.5.3. Assessment of Dendritic Cells of Patients after HSCT

We have analyzed dendritic cells of 30 patients serially for 200 days after HSCT. These patients are further divided in 6 categories depending on post-transplanted diagnoses namely 'no problems', 'acute GvHD', 'chronic GvHD', 'Infections', 'TRM' and 'Relapse'. Table 4-1 shows the patients ID and their post-transplanted diagnosis.

We assessed the circulating dendritic cell population DC1 and DC2 of the same patients as described in chapter 1.1.3. Results of DC1 populations are shown in the 6 graphics in Figure 4-25. The DC2 population is shown in Figure 4-26.

Of the same patient group we assessed the total circulating dendritic cell population (DC sum). Results of DC sum are shown in Figure 4-27.

Results

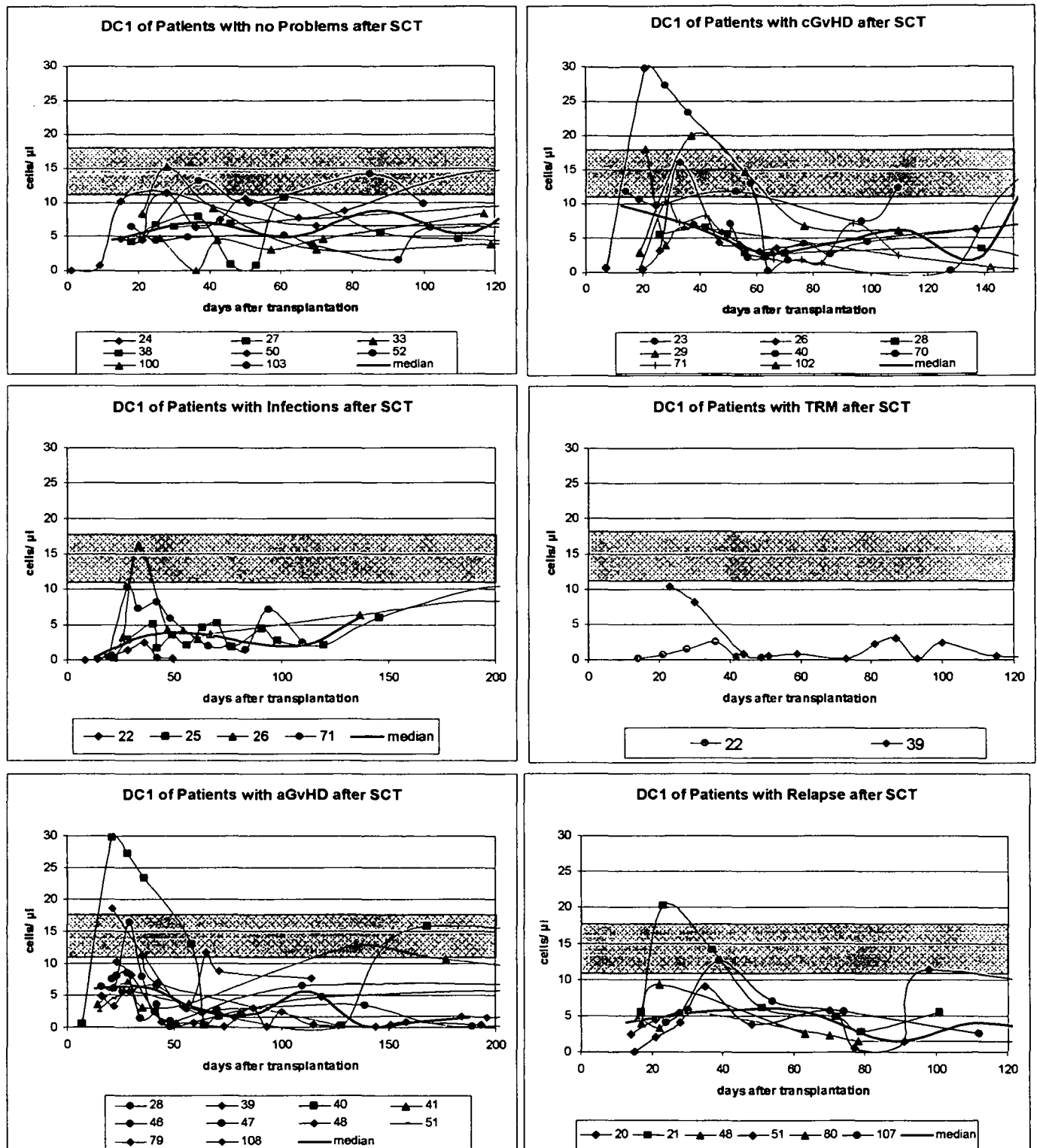


Figure 4-25: Development of DC1 in patients after HSCT

Patients with multiple diagnoses as described in Table 4-1 are plotted several times in the 6 graphics. The black median line is calculated by cumulating all measurements within 25-day-intervals. The median is plotted in the middle of each interval. In case of fewer than 3 values the median is dropped. The pink bar in the graphics is the inter-quartile range of the healthy volunteer group (10.8-17.4) as shown in Figure 4-24.

Results

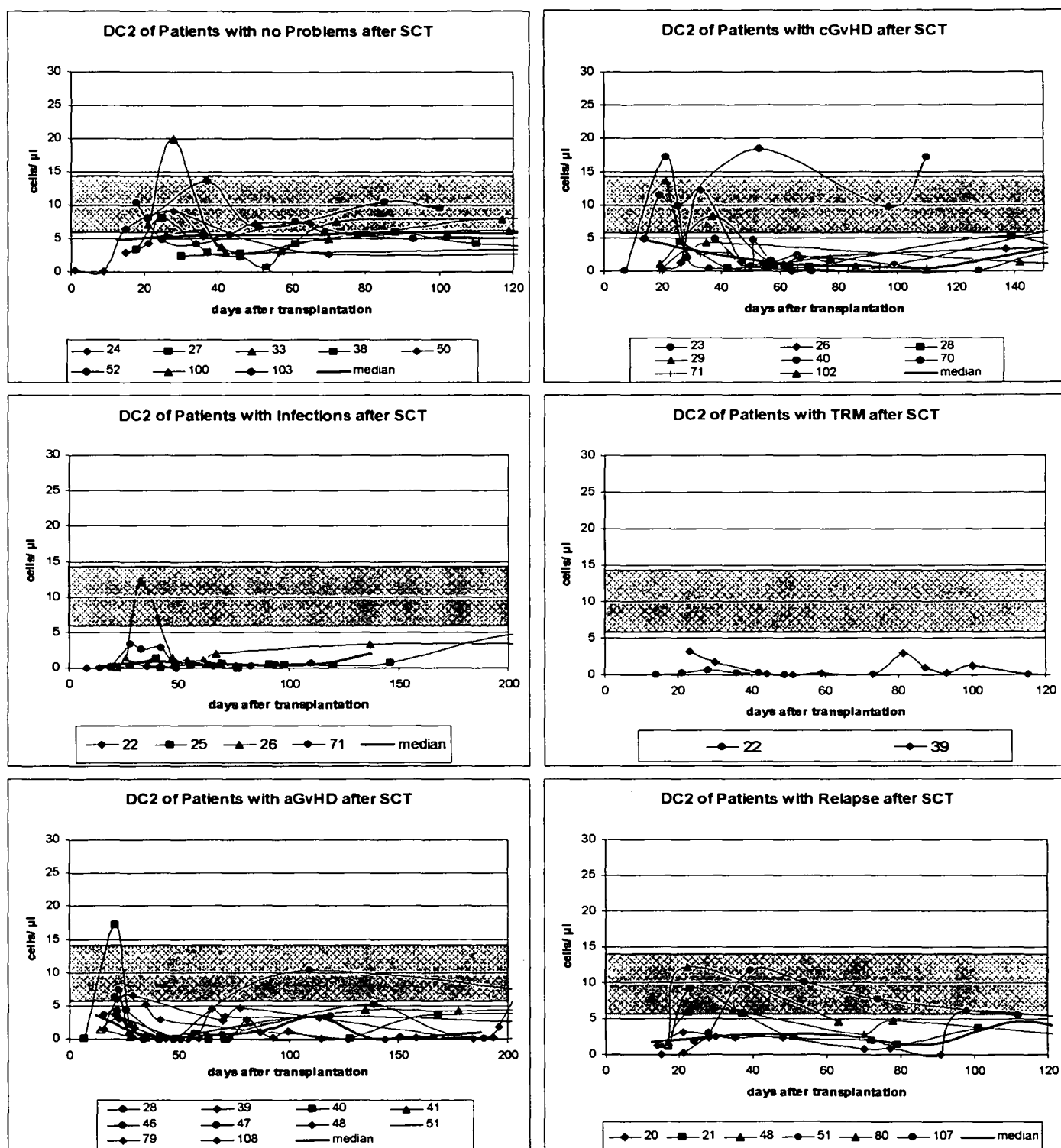


Figure 4-26: Development of DC2 in patients after HSCT

Patients with multiple diagnoses as described in Table 4-1 are plotted several times in the 6 graphics. The black median line is calculated by cumulating all measurements within 25-day-intervals. The median is plotted in the middle of each interval. In case of fewer than 3 values the median is dropped. The pink bar in the graphics is the inter-quartile range of the healthy volunteer group (6.1-14.7) as shown in Figure 4-24.

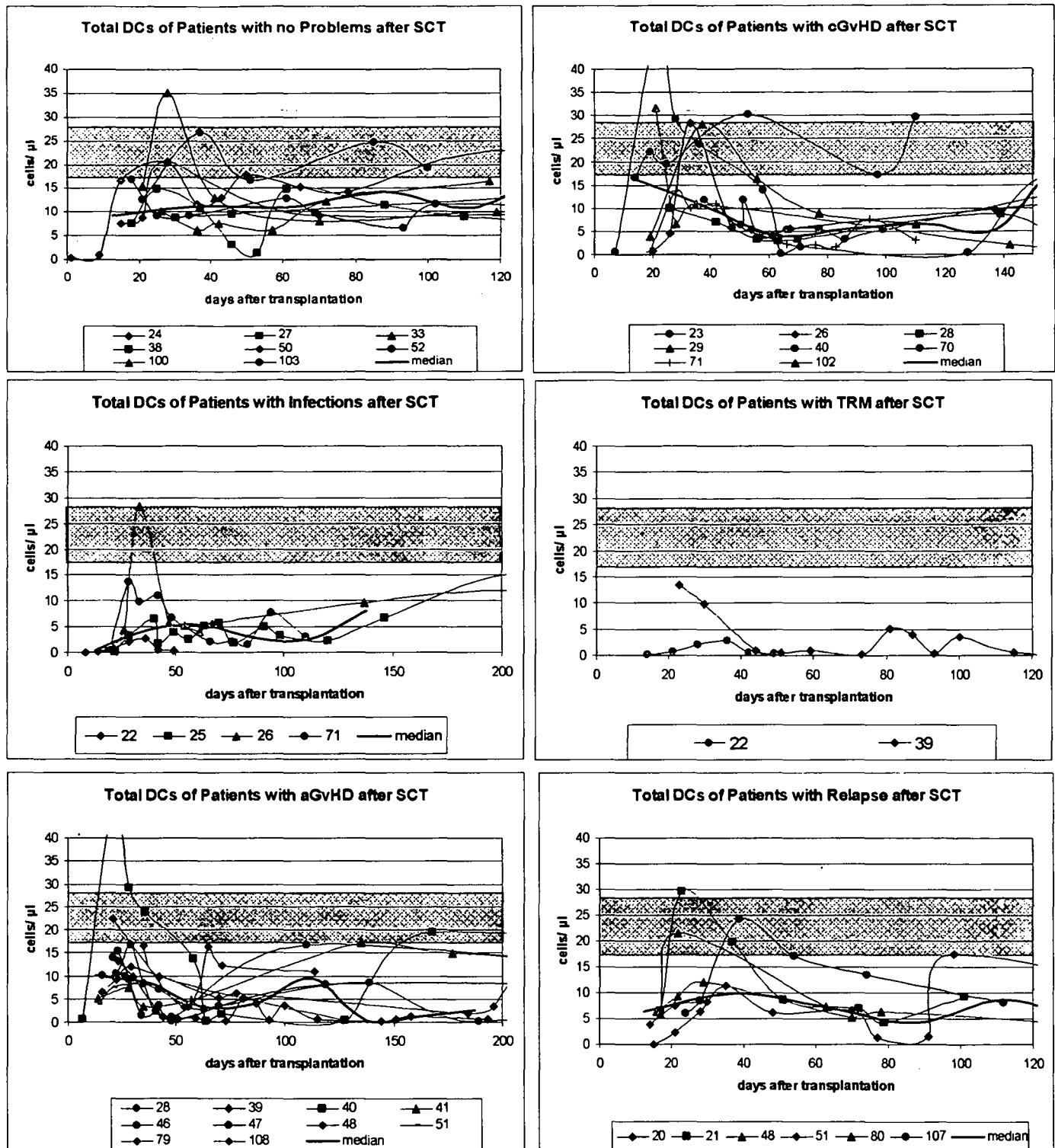


Figure 4-27: Development of total circulating DC in patients after HSCT

Patients with multiple diagnoses as described in Table 4-1 are plotted several times in the 6 graphics. The black median line is calculated by cumulating all measurements within 25-day-intervals. The median is plotted in the middle of each interval. In case of fewer than 3 values the median is dropped. The pink bar in the graphics is the inter-quartile range of the healthy volunteer group (17.0-25.1) as shown in Figure 4-24.

2. Analyses of Patients with chronic Graft-versus-Host Disease

2.1. Overview

Murine and human studies of chronic GvHD have revealed involution of the thymic epithelium, T-lymphocyte depletion, disappearance of Hassall corpuscles, and loss of thymic function [143, 144]. Taken together, these findings suggest that chronic GvHD, which can occur months after allogeneic HSCT, is not simply a continuation of acute GvHD. It may be due to the Th2 immune response of donor CD4⁺ T cells that escaped the negative thymic selection and which then go on to recognize MHC antigens on host APC. Thymus damage is caused by conditioning regimens, acute GvHD, and/or age-related atrophy [145]. These donor CD4⁺ T cells then provide help to host B cells to synthesize auto-antibodies against various host tissue antigens.

2.2. Intracytoplasmatic Cytokine Production of stimulated T cells during ECP-Treatment of Patients with chronic GvHD

In 7 patients with cGvHD we analyzed the cytokine production of CD4⁺ T cells as shown in Figure 4-28 and the CD8⁺ T cells as shown in Figure 4-30. Patients received ECP treatment for various lengths of time and had different manifestations and severities of cGvHD. Since blood samples were not available from all treatment cycles, and treatment duration is ongoing in all patients, no final conclusion can be made.

2.2.1. Assessment of Th1 Cytokines during ECP in cGvHD

We assessed the production of Th1-cytokines IL-2, INF- γ and TNF- α in CD4⁺ and CD8⁺ T cells prior to and after ECP therapy of 7 patients. During the time of analysis, patients 1, 3, 4 and 7 had high percentages of up to 80% of Th1-cytokine producing CD4⁺ and CD8⁺ T cells. Only in patient 3 Th1 cytokines decreased in PB during the course of ECP whereas in patients 1, 4, and 7 high percentages of Th1-cytokine producing cells remained. Patients 2, 5, and 6 had low to moderate levels of Th1-cytokine producing CD4⁺ and CD8⁺ cells in PB prior to and during ECP.

During ECP Th1-cytokines decreased markedly in patients 2, 5 and 6 and remained continuously low whereas in patients 1, 3, 4, and 7 decrease of Th1-cytokines was followed by further increases in other ECP cycles. Especially in patient 7 Th1-cytokines

increased between the third and sixth cycle of ECP as shown in Figure 4-28. Figure 4-29 shows the cumulative Th1-cytokine production of CD4+ T cells demonstrating the decrease of IL-2, IFN- γ and TNF- α producing cells in post-ECP samples compared to PB. CD8+ T cells contained more IFN- γ producing cells than CD4+ cells. The later had higher frequencies of IL-2 producing cells.

2.2.2. Assessment of Th2 Cytokines during ECP in cGvHD

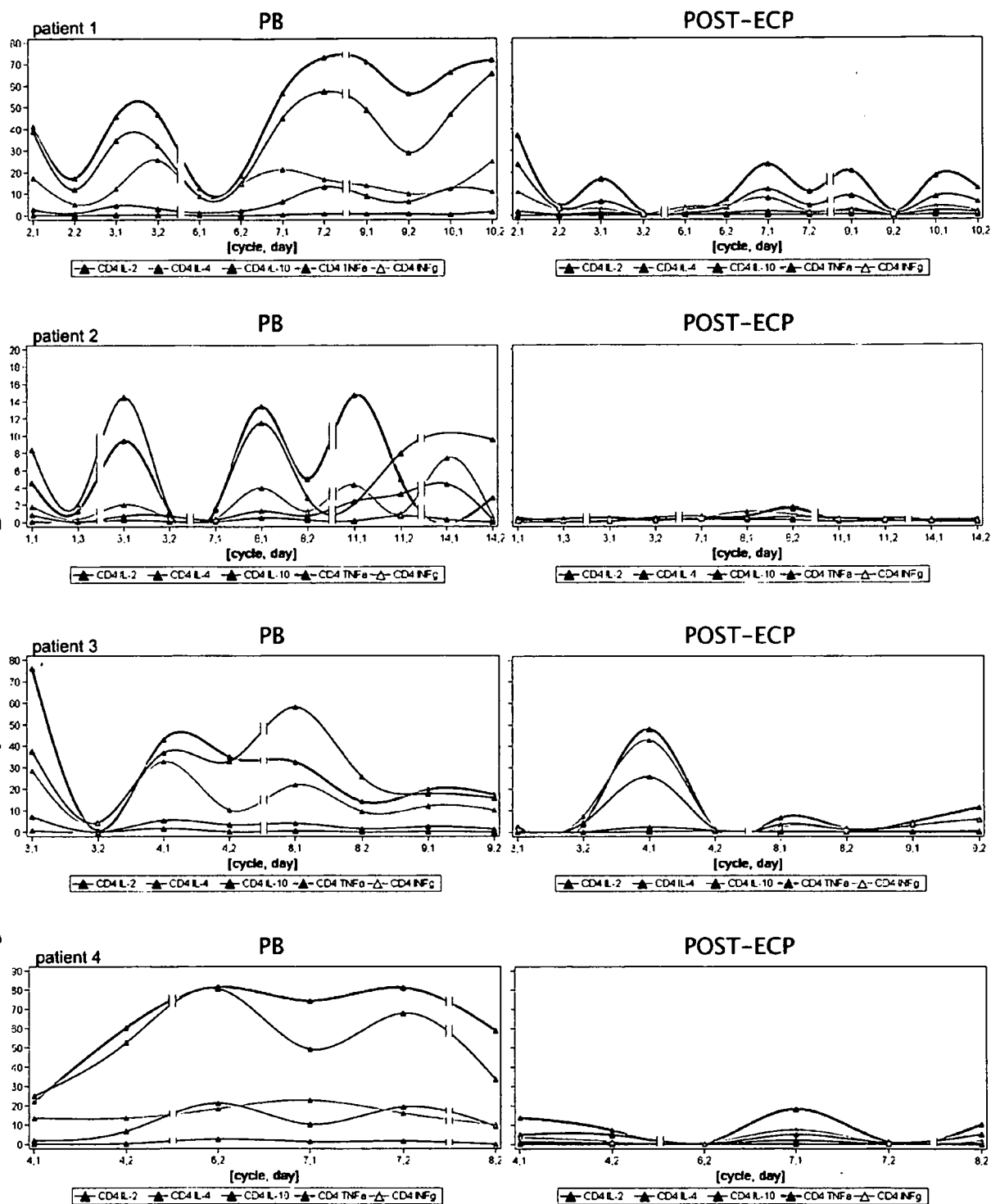
We assessed the production of Th2-cytokines IL-4 and IL-10 in CD4+ and CD8+ T cells prior to and after ECP in 7 patients. In patients 1, 2, and 4 IL-4 producing cells increased in PB during the time of our analysis whereas all other patients had low IL-4 and IL-10 levels during analyses of PB.

After ECP Th2-cytokine producing cells were low in all patients. Figure 4-29 shows the cumulative Th2-cytokine production of CD4+ cells demonstrating almost unchanged levels of IL-4 and IL-10 producing cells in post-ECP samples compared to PB.

No significant difference in Th2-cytokine production between CD4+ and CD8+ T cells was observed.

Results

% cytokine producing CD4+ T cells



Results

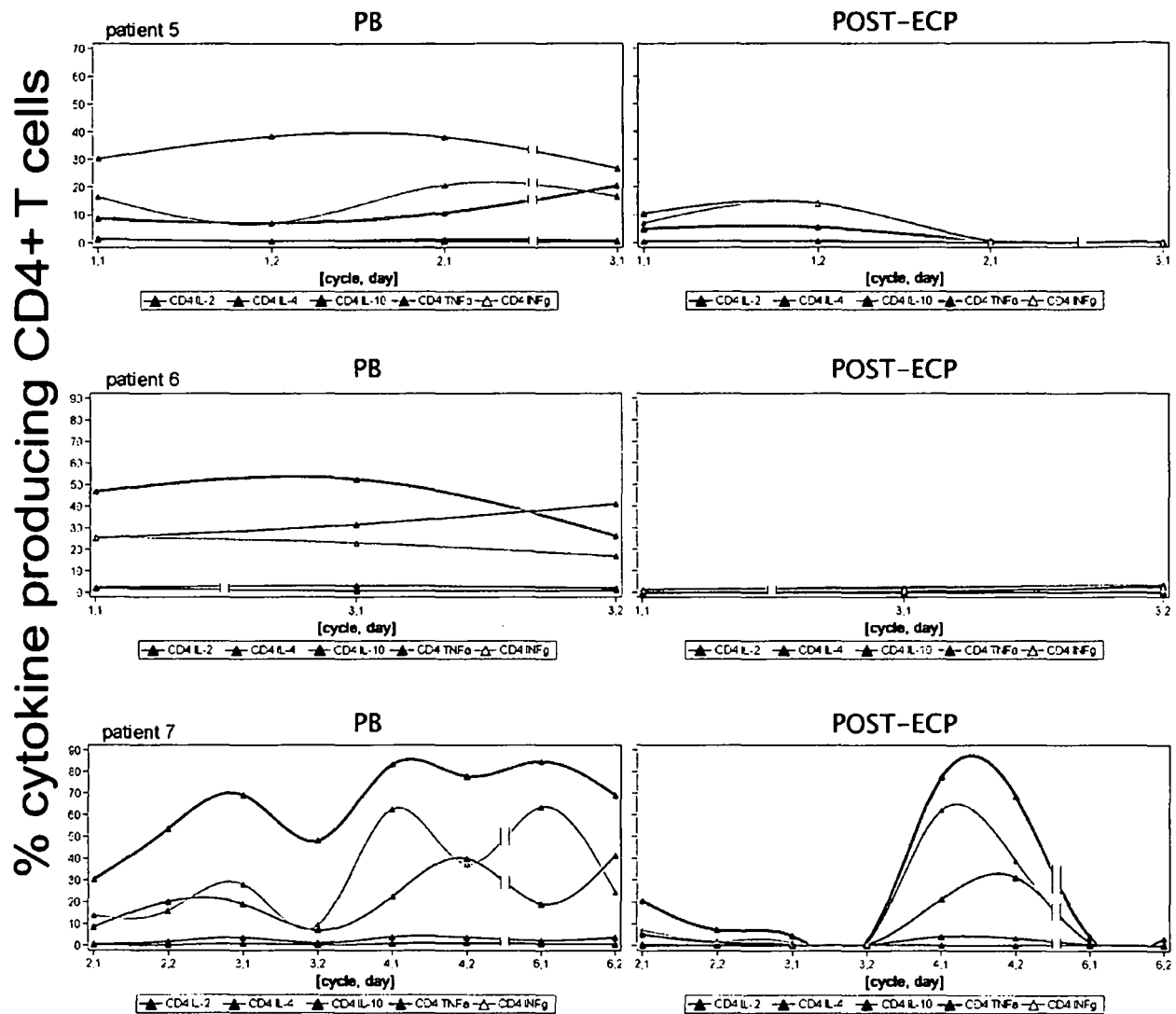


Figure 4-28: Intracytoplasmatic cytokine production of stimulated CD4+ T cells of seven patients during ECP-treatment

On the x-axes the number of ECP cycles given on day 1 and day 2 are shown [cycle, day]. The range of the y-axes differs between each patient. The percentages of cytokine producing CD4+ T cells are combined by spline curves, cycles inaccessible for analysis are shown by broken curves. Each patient's cytokine producing cells are compared by PB (left plot) and Post-ECP (right plot).

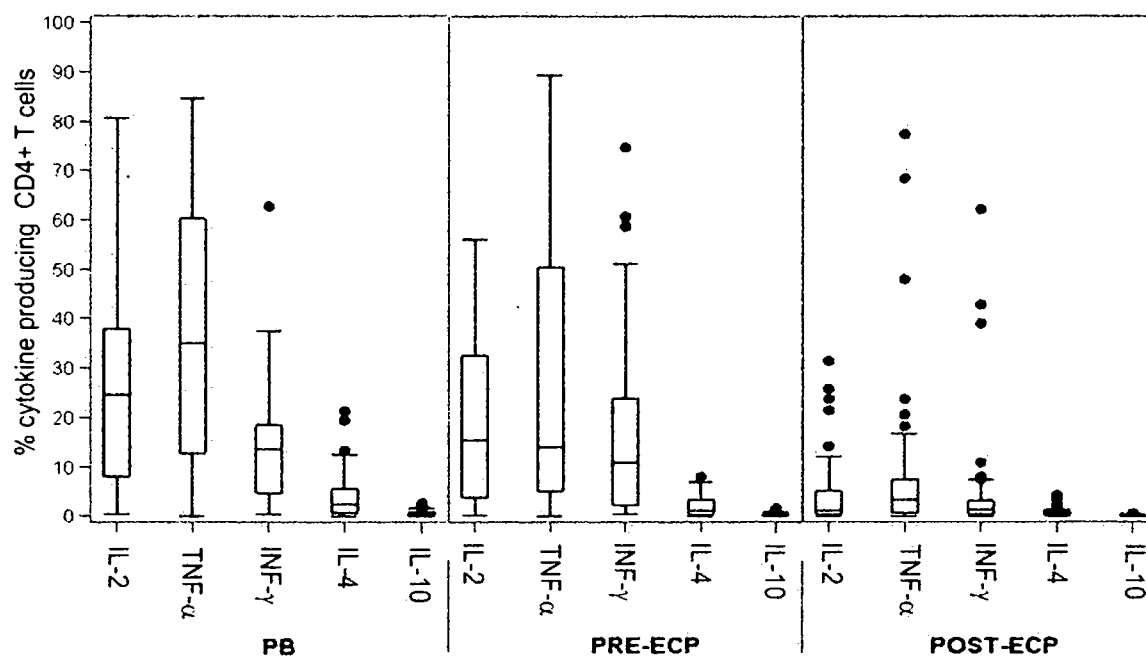
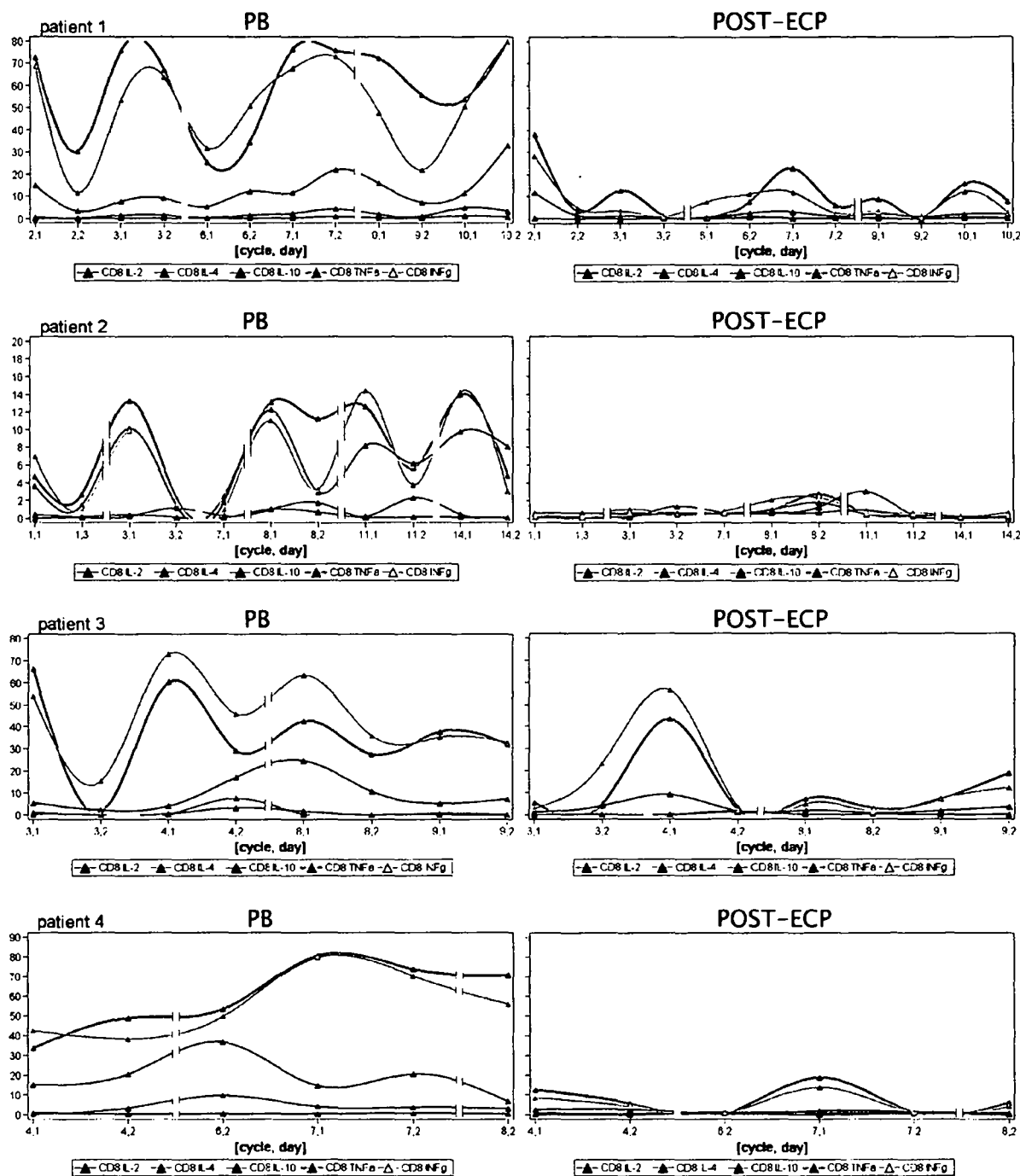


Figure 4-29: Cumulative cytokine production of CD4+ T cells

Cytoplasmatic cytokine producing cells are shown in percent of total CD4 T cells population. For each sample of PB (n=53), Pre-ECP (n=55) and Post-ECP (n= 55) the 5 cytokines (IL-2, TNF-α, INF-γ, IL-4, IL-10) are cumulated in one box. Outliers are signed as points.

Results

% cytokine producing CD8+ T cells



Results

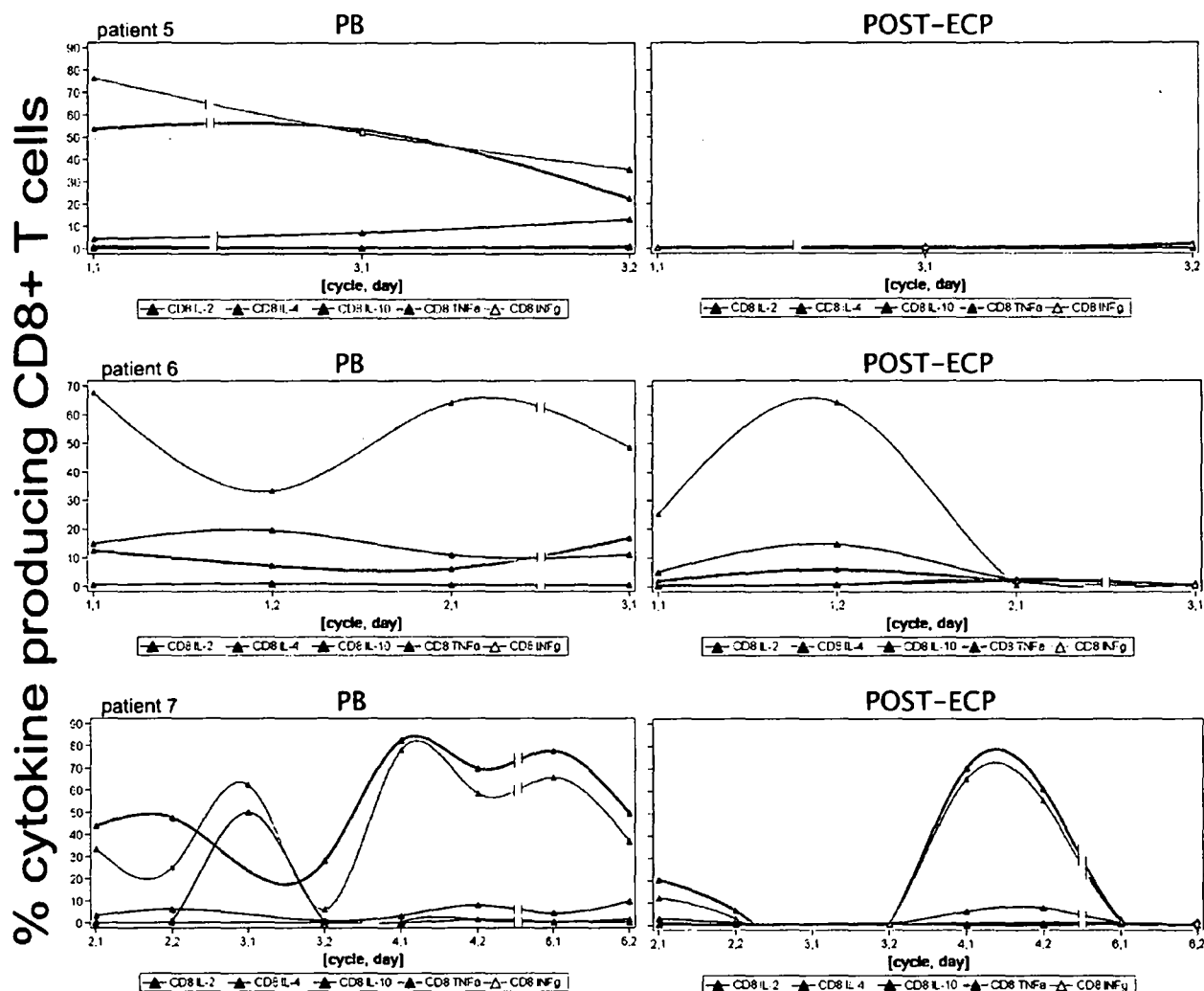


Figure 4-30: Intracytoplasmatic cytokine Production of stimulated CD8+ T cells of seven patients during ECP-Treatment

On the x-axes the number of ECP cycles given on day 1 and day 2 are shown [cycle, day]. The range of the y-axes differs between each patient. The percentages of cytokine producing CD4+ T cells are combined by spline curves, cycles inaccessible for analysis are shown by broken curves. Each patient's cytokine producing cells are compared by PB (left plot) and Post-ECP (right plot).

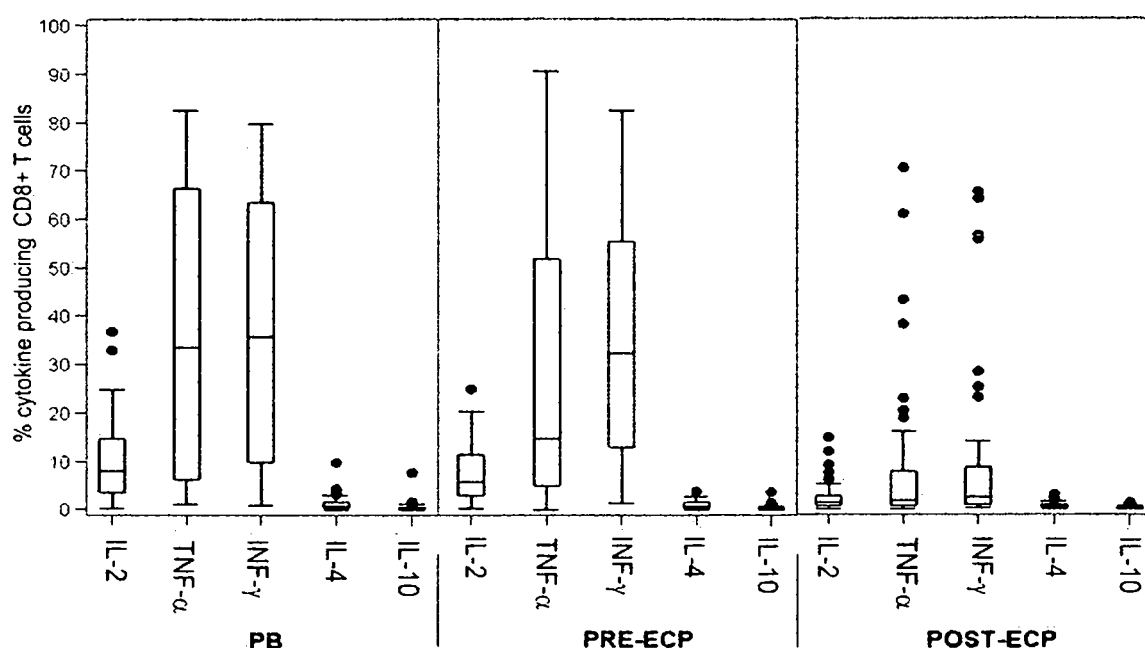


Figure 4-31: Cumulative cytokine production of CD8+ positive T cells

Cytoplasmatic cytokine producing cells are shown in percent of total CD8+ T cells population. For each sample of PB (n=53), Pre-ECP (n=54) and Post-ECP (n= 54) the 5 cytokines (IL-2, TNF-α, INF-γ, IL-4, IL-10) are cumulated in one box. Outliers are signed as points.

2.3. Apoptosis of White Blood Cells after Extracorporeal Photochemotherapy of Patients with chronic Graft-versus-Host Disease

2.3.1. Assessment of Apoptosis in PB of cGvHD Patients

PB samples of 5 patients with cGvHD were analyzed for apoptosis. PB was taken from the first of the 2 consecutive days and CD4+ T cells and CD8+ T cells were analyzed separately.

Figure 4-32 shows the percentage of viable CD4+ and CD8+ T cells in PB, Pre-ECP and Post-ECP blood samples 10 hours and 24 hours after irradiation. The viability of CD4+ T cells in PB and pre-ECP did not significantly change between 10 and 24 hours of

culture whereas in post-ECP samples at 10 and 24 hours only 65% and 25% of CD4+ were vital.

CD8+ T cells nearly have the same rapidly decreasing tendency of 50% vital cells at 10 hours decreasing to 10% at 24 hours. The loss of viability of CD4+ and CD8+ T cells in post-ECP samples at 24 hours was found to be statistically significant compared with pre-ECP samples. The particular p-values are shown within Figure 4-32. Pre-ECP CD8+ T cells have an insignificant increase of vitality of 5% compared to PB at both time points. The same tendency is shown by CD4+ T cells at both time points and is also insignificant.

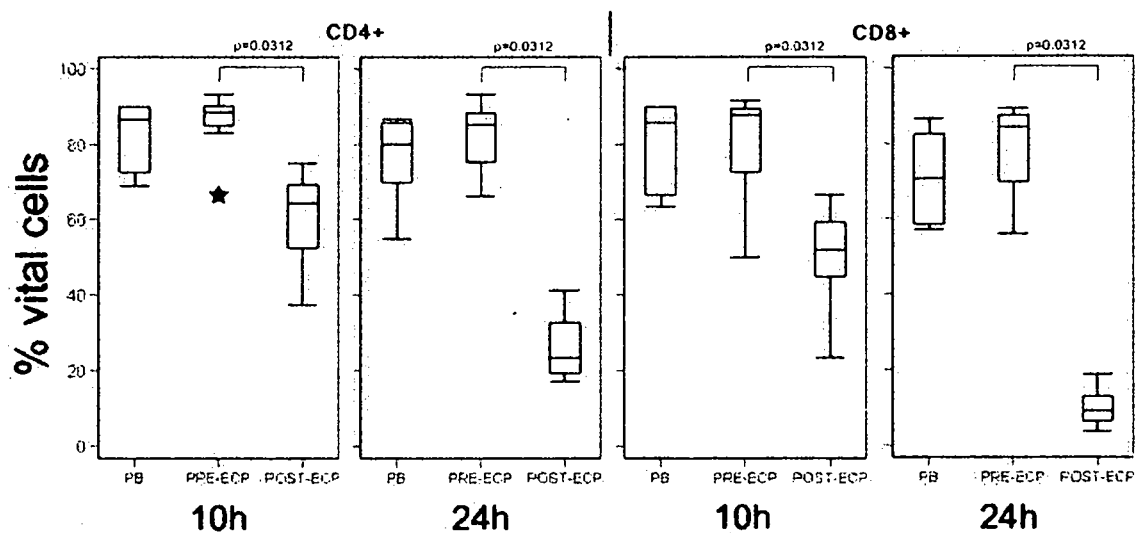


Figure 4-32: Interpolated 10-hour-point and 24-hour-point within apoptosis kinetics of CD4+ and CD8+ T cells of cGvHD patients

The following numbers of analyses were performed: The patient group differed by PB (n=7) and Pre-ECP (n=8) or Post-ECP (n=8), but was kept equal for both subpopulations

2.4. Comparison of Apoptosis of Leukocyte Subsets of Patients with aGvHD and cGvHD during ECP

The have described the effect of ECP on CD4+ and CD8+ T cells in aGvHD (Figure 4-22) and cGvHD (Figure 4-32) previously in this chapter. Patients suffering of aGvHD and cGvHD were treated with the same protocol of ECP. Therefore we have recombined the graphics to demonstrate if there is any difference in the effect of apoptosis caused by ECP

treatment. ECP treatment of patients suffering on aGvHD and cGvHD was found to show no difference in apoptosis in leukocyte subsets.

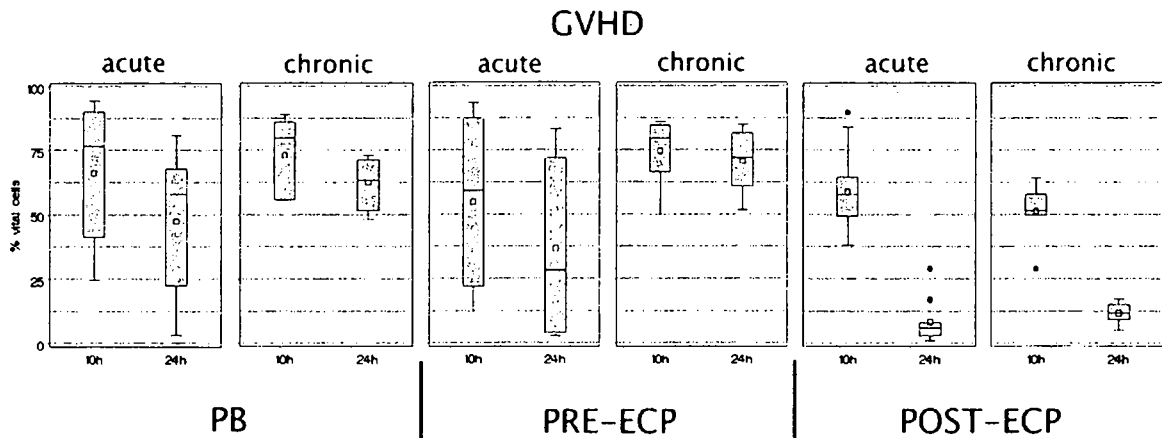


Figure 4-33: Comparison of interpolated 10-hour-point and 24-hour-point within apoptosis kinetics of CD3+ lymphocytes of aGvHD and cGvHD patients

The following numbers of analyses of patients with aGvHD were performed: The patient group differed by PB (n=8), Pre-ECP (n=10) and Post-ECP (n=13), but was kept equal for both subpopulations. The following numbers of analyses of patients with cGvHD were performed: The patient group differed by PB (n=7), Pre-ECP (n=8) and Post-ECP (n=8), but was kept equal for both subpopulations.

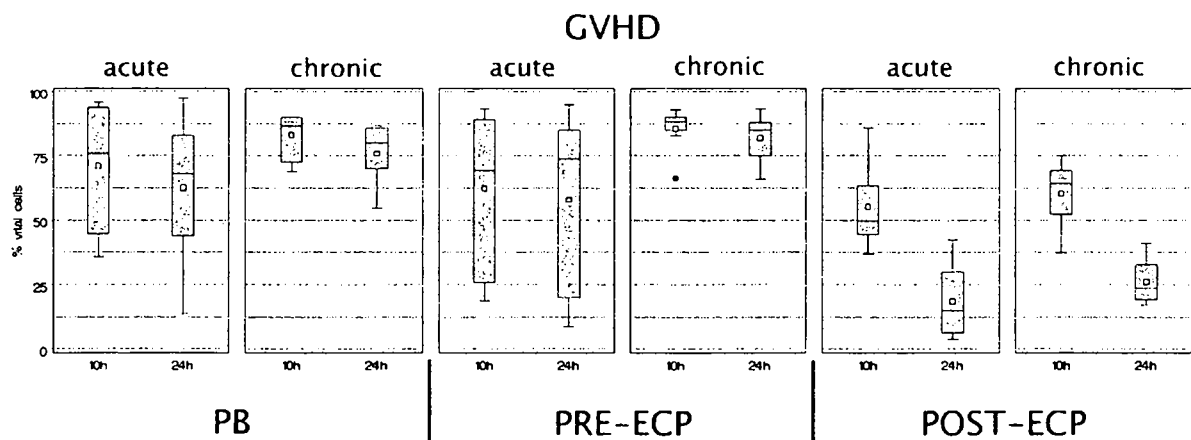


Figure 4-34: Comparison of interpolated 10-hour-point and 24-hour-point within apoptosis kinetics of CD4+ T cells of aGvHD and cGvHD patients

The following numbers of analyses of patients with aGvHD were performed: The patient group differed by PB (n=8), Pre-ECP (n=10) and Post-ECP (n=13), but was kept equal for both subpopulations. The following numbers of analyses of patients with cGvHD were performed: The patient group differed by PB (n=7), Pre-ECP (n=8) and Post-ECP (n=8), but was kept equal for both subpopulations.

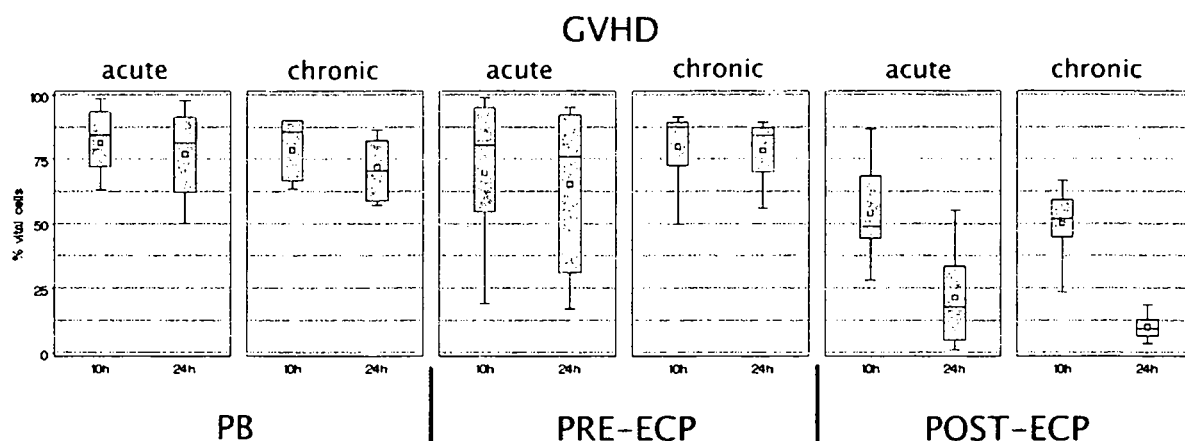


Figure 4-35: Comparison of interpolated 10-hour-point and 24-hour-point within apoptosis kinetics of CD8+ T cells of aGvHD and cGvHD patients

The following numbers of analyses of patients with aGvHD were performed: The patient group differed by PB (n=8), Pre-ECP (n=10) and Post-ECP (n=13), but was kept equal for both subpopulations. The following numbers of analyses of patients with cGvHD were performed: The patient group differed by PB (n=7), Pre-ECP (n=8) and Post-ECP (n=8), but was kept equal for both subpopulations.

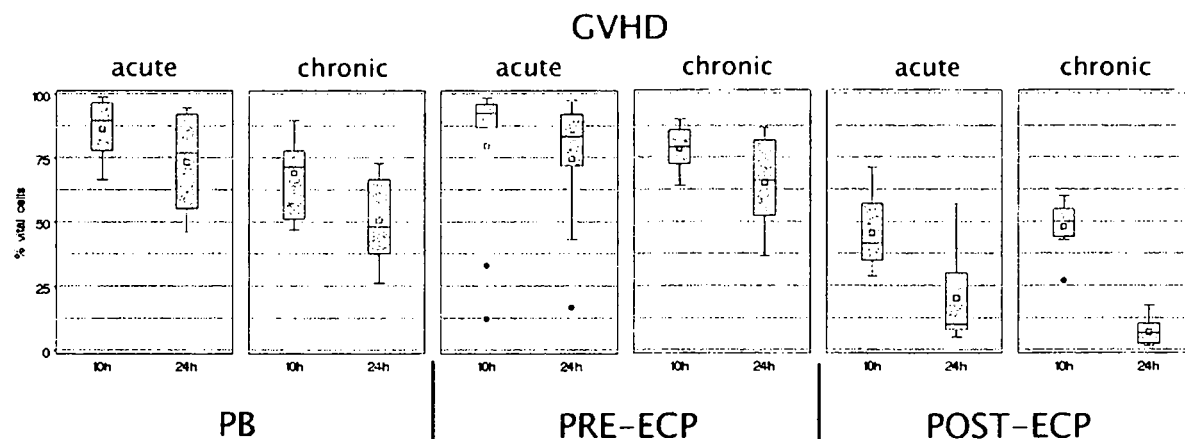


Figure 4-36: Comparison of interpolated 10-hour-point and 24-hour-point within apoptosis kinetics of NK cells of aGvHD and cGvHD patients

The following numbers of analyses of patients with aGvHD were performed: The patient group differed by PB (n=8), Pre-ECP (n=10) and Post-ECP (n=13), but was kept equal for both subpopulations. The following numbers of analyses of patients with cGvHD were performed: The patient group differed by PB (n=7), Pre-ECP (n=8) and Post-ECP (n=8), but was kept equal for both subpopulations.

Chapter 5

Comparison and Conclusions

In this chapter we discuss related literature and finally we give conclusions of the results.

1. ECP and Apoptosis

1.1. General

An important aspect of apoptosis is that cells undergoing this phenomenon are recognized by phagocytes and taken up before the release of intracellular contents, protecting the surrounding tissue from potential tissue damage [146].

The effects of 8-MOP and UVA are complex and the degree of cell damage is random. But it is a clear fact, that in vitro PUVA as well as ECP cause apoptosis in treated cells [40, 41].

About 24 h after MNC phototreatment, apoptosis starts in T-lymphocytes with DNA crosslinking, mitochondrial dysfunction, caspase activation and other cell damages, but monocytes seem to be resistant to apoptosis [42]. Apoptosis has a crucial role in ECP action, but its role may be different in different disorders.

The most characteristic surface change associated with apoptosis is loss of phospholipid asymmetry and exposure of phosphatidylserine [147]. Macrophages and other phagocytes clearly discriminate between apoptotic cells and viable cells. Recognition occurs prior to the lysis of the dying cell, implying an early surface change.

Uptake of apoptotic cells by macrophages is associated with the production of TGF- β and the downregulation of inflammatory cytokines [148, 149]. Phosphatidylserine

presented to mouse peritoneal macrophages down-regulates several macrophage functions, including TNF- α production [150]. Chang and colleagues showed that oxidation of membrane phospholipids during apoptosis results in the development of a recognition ligand for mouse macrophages, as uptake can be inhibited by the mAb's that recognize oxidized forms of choline-containing phospholipids. The antibodies bind to the surface of apoptotic but not viable cells [151], and preliminary evidence suggests that the oxidized epitope appears on the cell surface only after phospholipid asymmetry is compromised [151].

DCs employ the avb5 vitronectin receptor, which appears to be coupled to the cell's phagocytic machinery [152]. The phagocytosis of apoptotic cells can be inhibited stereospecifically by phosphatidylserine and its structural analogues, but not by other anionic phospholipids, suggesting that phosphatidylserine is specifically recognized by a PS receptor (PSR) on phagocytes [153-156]. Fadok hypothesized that the engulfment of microbial organisms that fail to express PS externally does not engage the PS receptor (PSR). In contrast, when apoptotic cells are recognized, they expose PS, thus engaging the PSR, which provides an anti-inflammatory signal [157].

1.2. Comparable Literature

Tambur *et al.* [42] observed cell death only among treated T-lymphocytes independently of monocyte treatment in four allogeneic bone marrow transplant recipients with cGvHD and two patients with cutaneous T-cell lymphoma (CTCL), both before and after the completion of individual (ECP) treatment cycles. In addition, none of the incubation conditions induced monocyte apoptosis, leading us to speculate that monocytes have the capacity to escape ECP-induced apoptosis.

Aringer *et al.* [158] investigated the effects of ECP in 12 systemic sclerosis patients by flow cytometric analyses of fas (CD95) expression and found increased CD4+CD95+ cells 24 h after ECP within PB lymphocytes, taken directly from the photopheresis system.

Di Renzo *et al.* [159] observed in their study that the exposure of PS was also significantly increased on the collected T-lymphocytes before treatment. They tried to explain that the mechanism of separation itself, that is cannulation, peristalsis pumping and centrifugation, affects cell membranes.

Bladon *et al.* [160] determined CD95 expression on CD4+ and CD8+ T lymphocytes and the expression of the costimulation antigens CD80 and CD86 and, on monocytes, at several stages after ECP of nine cutaneous T cell lymphoma (CTCL) patients. They found no increase in CD95 or Fas-L expression on T cells tested immediately following ECP. However, the number of T cells expressing Fas-L significantly increased 24 h post ECP. The expression of the co-stimulatory molecules, (CD80, CD86) and adhesions molecule ICAM-1 (CD54) remained unaltered on monocytes treated by ECP. Although the later apoptosis involves Fas-L expression, the mechanism responsible for early induction of lymphocyte apoptosis remains unclear.

1.3. Conclusions

The apoptosis analyses of ECP treated T-lymphocytes as described in the previous chapter show that up to 90% of reinfused T-lymphocytes became apoptotic within 24 hours. Mechanically collected but untreated T-lymphocytes show the same viability than T-lymphocytes taken freshly from peripheral blood. This result stands in contrast to studies of Di Renzo *et al.* [159].

Several investigations have shown, that ECP treated cells have a negligible inflammatory potential. Scarce information is available concerning the underlying mechanism(s) of cellular photodamage. Canton *et al.* [161] clearly shows that PUVA causes the loss of mitochondrial membrane potential in Jurkat cells which can be antagonized by CsA suggesting the involvement of mitochondrial permeability transition pore.

On the one hand we have a well-established damage of DNA induced by the covalent addition of psoralen upon UVA irradiation [162] on the other hand the present evidence of mitochondrial dysfunction followed by apoptosis in PUVA-treated cells.

However, the link between the DNA damage and mitochondrial alterations leading eventually to cell death is still to verify. There is a discussion about the involvement of p53, a product of the proapoptotic- regulating Trp53 tumor suppressor gene as a necessary factor in the case of permeability transition pore -induced apoptosis [163].

1.4. ECP and Immunomodulation

Based on the prevention of EAE by ECP experience [164] the first hypothesis of the mechanism of action of ECP was the induction of an antiidiotypic response by CD8 suppressors against a single clone, or multiple clones of normal T-cells in autoimmune diseases, graft rejection and GvHD.

In mycosis fungoides, which in most cases is a malignancy of skin homing CD4+ lymphocytes with a Th2 phenotype, a reversal to a Th1 predominance has been described during Photopheresis [165]. This result has been confirmed by an *in vitro* study using T-lymphocytes from one Sezary syndrome patient as well as from healthy volunteers [166]: The number of INF- γ -secreting T-lymphocytes was markedly increased in PUVA-treated PBMC 20 h after treatment, whereas that of Th2 cytokine-producing cells was decreased and interleukin-4 was significantly reduced. This enhanced production of INF- γ , however, was found only until 3 days after PUVA-treatment and was declined by 5 days after treatment [166].

Otherwise, Klosner *et al.* [167] isolated PBL from healthy human volunteers stimulated them for 2 days with anti-CD3, IL-2 and IL-4 and further 3 days with IL-2 and IL-4 before PUVA treatment. PUVA treatment, comparable to ECP, leads to an increase in IL-4-producing Th2 cells and a concomitant decrease of IL-2 and IFN- γ producing Th1 cells.

Rubegni *et al.* [168] suggested that patients whose immune system is less suppressed (fewer drugs) respond better to ECP. Of course nobody can exclude that patients initially on fewer immunosuppressants had less aggressive cGvHD, and responded better only for this reason.

Clinically, Greinix *et al.* [169] reported from 6 patients with aGvHD grade II to III not responding to CsA and prednisolone when referred to ECP. After a median of 14 cycles of ECP, acute GVHD resolved completely in 4 of 6 patients (67%) and partially in another 2 patients. Additionally 15 patients, who developed extensive cGvHD with involvement of skin (n = 15), liver (n = 10), oral mucosa (n = 11), ocular glands (n = 6), and thrombocytopenia (n = 3) 2 to 24 months after BMT were treated with ECP. The cGvHD was unresponsive to conventional therapy in all patients, including steroids although ECP treatment completely resolved cutaneous cGvHD in 12 of 15 (80%)

patients. Contractures of knees and elbows due to scleroderma resolved partially. Oral mucosal ulcerations resolved in all patients. Seven of 10 patients (70%) with liver involvement had complete responses after ECP. After discontinuation of ECP, no severe infections were observed.

Rubegni *et al.* [168] analyzed the main clinical and laboratory parameters related to evolution of the disease in 32 steroid-refractory cGvHD patients, to identify any useful response predictors to ECP. The patients in this study received a total of 1128 cycles of ECP, with only minor side-effects, none of which required interruption of treatment. Their experience seems to confirm that ECP is indeed useful in the treatment of patients with steroid-refractory cGvHD. On this basis they can say that ECP affected the course of the disease positively in 78% (25/32) of their cases.

1.5. Immunological Aspects of aGvHD

There is convincing evidence that T-cells contained in the donor graft or subsequently derived from donor SC react to host antigen-presenting cells (APCs) (alloreactivity), causing target organ damages that are recognised as clinical manifestations of GvHD. The immunobiology of aGvHD is complex. Three sequential phases of cytokine dysregulation are responsible for the manifestations of acute GvHD [63]:

The first phase depends on host conditioning. Donor T-cells are infused into a host that has been profoundly damaged by underlying disease, infections and particularly by the conditioning regimen, all of which result in activation of host cells with secretion of proinflammatory cytokine such as TNF- α and IL-1 and nitric oxide [64]. As a consequence, expression of MHC Ag and adhesion molecules is increased, thus enhancing the recognition of host alloantigens.

The second phase was described by the secretion of predominantly IL-2 and INF- γ of donor CD4 (Th1) and CD8 (Tc1) T cells after interaction with host APCs [65, 66, 170]. These cytokines are pivotal mediators of aGvHD and amplify the immune response by priming monocytes to produce the proinflammatory cytokines IL-1 and TNF- α [67, 68].

Based on the observation that IL-4 and IL-10 gene expression in PBMC was suppressed in patients with severe GvHD compared to those without severe GvHD [69, 170] arised the thesis, that phase 3 of aGvHD is culminating in a cytokine dysregulation in synergy

with T- and natural killer (NK) cell-mediated cytotoxicity, producing the systemic morbidity of GvHD-associated immunosuppression. Finally, the inflammatory response, together with the CTL and NK components, leads to target tissue destruction, via target cell apoptosis, in the transplant host.

Fimiani *et al.* [171] suggested, that keratinocytes of the skin and digestive tract may also play a non-negligible role in the mechanisms of epithelial damage of aGvHD. They may express intercellular adhesion molecules (e.g. ICAM-1) and may produce both TNF- α and IL-1 α in response to various stimuli. These cytokines stimulate endothelial cells to synthesize adhesion molecules, which attract donor T cells and trigger aGvHD manifestations. Expression of intercellular adhesion molecules by keratinocytes presumably enables lymphocytes to enter and attack the epidermis.

Differential activation of donor T-cell subsets has been evoked in the immunopathogenesis of various other autoimmune, infectious, and immunodeficiency diseases [74, 75] and there is thus a significant interest in the potential relevance of the Th1/Th2 paradigm for aGvHD and the positive effects of ECP. There is now considerable evidence that a type 1 \rightarrow type 2 immune deviation after allogeneic transplantation is associated either with decreased acute GvHD or with the development of a “chronic” GvHD syndrome that is characterized by decreased lethality and autoantibody formation [70-73].

1.6. Conclusions

The intracytoplasmatic cytokine production of stimulated CD4⁺ and CD8⁺ T cells described in the previous chapter shows a significant decrease of IL-2, TNF- α and INF- γ in Post-ECP samples compared to PB and Pre-ECP samples in both CD4⁺ as well as CD8⁺ T cells. As described in Figure 4-22, 50% of ECP treated CD4⁺ and CD8⁺ T cells are still vital at the 10-hour-time-point. So at the first thought it seems be clear, that the significant cytokine reduction is caused by the destruction of the T cells. But we have recalculated that all cell stimulations were done within 10 hours after ECP treatment. So at least half of the detected cells will have the potential to produce cytokines if ECP has no influence on the cytokine reduction of T cells.

Macrophages and monocytes are the main sources of TNF- α production. In case of inflammations TNF- α further stimulates T cells to produce TNF- α by themselves,

known as autocrine/paracrine mechanisms. As shown in Figures 4-13 and 4-14 we found an increasing amount of TNF- α production in CD4+ and CD8+ T cells in PB samples over the duration of 4 therapies. So there is convincing evidence, that monocytes and macrophages remain sources of inflammation during ECP treatment of patients with aGvHD.

In contrast to the literature on chronic GvHD the clinically observed benefited effects of ECP treatment on our patients with aGvHD cannot be explained by change in the T helper cell cytokine profile from type 1 to type 2 during ECP. Unfortunately, the numbers of patients not responding to ECP was small so that we were unable to be used for predicting response to ECP.

2. Immunological Aspects of cGvHD

The mechanism of action of ECP in cGvHD is not fully understood. It has been proposed that ECP modulates host effector cells, including CD8+ T- cells, NK cells and circulating APC, leading to an attenuation of host antigen-presenting activity, thereby leading to the development of tolerance [172, 173]. Evidence supporting the role of intact host dendritic cells in GVHD has been derived from studies by Shlomchik *et al.* [174] who demonstrated in a murine GvHD model that the initial targets for CD8+ T cells in GvHD were restricted to proteins expressed by residual host antigen-presenting dendritic cells [174].

2.1. Effects of ECP on cGvHD

Gurgun *et al.* [173] found that the clinical response to ECP in 10 patients with chronic GvHD was associated with normalization of CD4/CD8 ratio, increase in CD3-CD56+ NK cells and decrease in circulating DCs and decrease in T-cell proliferation (autologous and allogeneic) in MLR. A shift from DC1 to DC2 and a shift from predominantly Th1 (IL-2, IFN- γ) to Th2 (IL-4, IL-10) was also observed.

Darvay *et al.* [175] analyzed nine patients with chronic cutaneous GVHD of at least 1-year duration. They demonstrate an increased percentage of cells expressing IL-2 and IFN- γ in both CD4+ and CD8+ T cells but no change in IL-4 expression.

Nakamura *et al.* [7] examined cytokine production of peripheral blood T cells from 19 patients in the chronic phase of allogeneic-HSCT. The percentage of IFN- γ producing CD8+ T cells among CD8+ T cells was significantly higher in patients with or without cGvHD than in normal control subjects. On the other hand, the percentage of IL-4 producing CD8+ T cells among CD8+ T cells was significantly higher in patients with cGvHD (mean 3.3%; range 1.3-8.2%) than in patients without cGvHD (mean 1.2%; range 0.8-1.7%) and normal control subjects (mean 1.1%; range 0.1-1.6%). By contrast, the percentage of IL-4-producing CD4+ T cells was not different among patients with and without cGvHD and normal controls. Nakamura *et al.* [7] suggested that IL-4 producing CD8+ T cells may be an immunological marker of cGvHD.

2.2. Conclusions

Our analyses of CD8+ T cells producing IL-4 was as low as described in the literature, but we found no significant change during ECP therapies. Because of non-existent PR and CR patient group a comparison between response to ECP and IL-4 production was not feasible.

Although results of Gorgun *et al.* [173] and Nakamura *et al.* [7] appear to contradict our study, there are important differences. First, the number of patients receiving immunosuppressive therapy is very low in all studies and the therapy appears to have been varied during the course of the studies. Second, samples were taken prospective and serially at different times, whereas in our own study PB, Pre-ECP and post-ECP samples were taken between the first and second treatments and the week following ECP. Finally, cytokine assessment appears to be different, certainly in terms of the agent used to stimulate cytokine production and possibly in terms of the methodology, although this is difficult to ascertain as no references are provided. Even so, the results of the Gorgun paper [173] support the hypothesis on which our current study was originally based. In conclusion, we have shown no significant change in Th1-cytokine and Th2-cytokine production during ECP therapy, so it seems that these cytokines are probably secondary to the therapeutic effect of ECP rather than providing an explanation of its mode of action. Fimiani *et al.* [171] explained that CD4+ or CD8+ T cells once activated during the phases of aGvHD, home in the skin and may attract other inflammatory cells through production of cytokines. Therefore it is necessary to mention

that the T cells we analyzed in the peripheral blood are only a small part of the complete T cell repertoire and maybe are not representative for the complete immune status of a patient with cGvHD. An alternative would be to additionally monitor the inflammatory potential of effector cells (T cells, Langerhans cells, keratinocytes, DCs) in the skin and digestive tract. The later would involve repeated tissue biopsies and thus, is neither methodically nor ethically justified in transplantations.

3. Development of White Blood Cells after SCT

The ultimate goal of successful allogeneic transplantation is the complete eradication of tumor cells and reconstitution of an immune system that is able to prevent opportunistic infection and reduce TRM without the development of life-threatening severe GvHD. It has been suggested that the content of the cellular components in the graft may influence the transplant outcomes, the most consistent of which is the CD34+ cell dose [176]. But also post-transplantation influences, possible infections and kinds of therapies have a great influence on the reconstruction.

3.1. Development of Leukocytes Subsets after SCT

3.1.1. Development of NK cells after SCT

NK cells are cytotoxic lymphocytes that play an important role in host immune responses to viruses, parasites, intracellular bacteria, and tumor cells and in the development of GvHD and graft rejection after allogeneic SCT. Kim *et al.* [177] reported that a high dose of NK cells may play an important role in improving transplant outcomes, in terms of reducing non-relapse mortality and infectious events together with CD34+ cells.

NK cells are also believed to play a positive role in a successful transplantation in terms of protection from GvHD and graft. Yamasaki *et al.* [178] reported that the CD56+ NK cells in G-CSF mobilized PBSC allografts from HLA-matched sibling donors may play a major role in preventing the development of acute GvHD.

Comparing the NK cell development in Figure 4-5 shows a rapid and later on continuous increase of NK cells in patients with no problems after SCT, it reaches the range upon the healthy group. Patients in the other categories having post-transplanted complications have lower or fluctuating NK cells. Our data are not significant, but seem to be consistent with current theories regarding the prevention of complications.

3.1.2. Development of Leukocytes and T-Lymphocytes

The immunological interesting subpopulations of T-lymphocytes are the CD4+ and CD8+ T cells. In the current literature these two populations are very often set in proportion leading to a non-dimensional unit the CD4 to CD8 ratio.

Scholl *et al.* [179] analyzed 24 patients (median age 49) who received conventional conditioning regimen. Patients' engraftment (1000 leukocytes/ μ l) took place at median day 15, whereas they observed leukocytes engraftment at median day 11 after dose-reduced preparative regimen (27 patients). The observed mean CD4/CD8 ratios after conventional and dose-reduced conditioning were significantly different: 1.29 vs. 0.35.

Tauchmanova *et al.* [180] found a significant lower CD4/CD8 ratio both in 24 auto-SCT (mean: 0.95) and 36 allo-SCT (mean 0.7) patients compared with normal individuals (normal range: 1.1–2.4). A majority of allo-SCT patients with cGvHD showed a CD4/CD8 ratio (mean: 0.59) significantly lower than patients without cGvHD (mean: 0.97).

We have described the median CD4/CD8 ratio of patients during ECP therapy that were not altered during therapy in patients with CR. One patient with PR was within the range of CR. At the moment there is no comparable literature describing a CD4/CD8 ratio during ECP therapy.

Although our leukocyte subset monitoring has no significance there are a lot of interesting pattern comparing patients with 'no problems' and the other categories. Concerning CD4/CD8 ratio, we have found higher values after SCT until day 50 in aGvHD and cGvHD patients compared to patients with no problems after SCT. The comparison of the values in Figure 4-6 with the literature above shows controversial ratios. So far, our monitoring is still in progress to gain statistical relevant patients numbers in all 6 categories.

Monocytes belong to the fastest cell population reconstructed after SCT. Little is known so far about effects of immunosuppressive therapy with CsA on cell lineages other than T cells. A moderate inhibition of DC functions was demonstrated following CsA treatment of DCs isolated from human PB or derived from monocytes [181, 13]. There is convincing evidence that monocytes are forerunner of tolerogenic dendritic cells [43].

3.2. Development of Dendritic Cells after SCT

The recovery of DC1 and DC2 cells after grafting is very rapid. As soon as 14 days after SCT both cell types circulate in measurable numbers in the PB and can be detected in the BM of graft recipients. According to recent chimerism studies, the major proportion of DCs is donor derived [182] and, at this early time point, may represent a mixture of cells transferred with the graft and those developing from the newly engrafted hematopoietic progenitors.

The process of recovery of bone marrow function is tightly regulated and involves complex cell-cell interactions in the enriched cytokine milieu within the environment provided by BM stroma.

Chklovskaya *et al.* [183] demonstrated that flt3 ligand (FL), present in highly elevated concentrations in a vast majority of patients during the first 14 days after SCT, correlates with early recovery of the DC lineage of both lymphoid and myeloid origin. FL treatment increases numbers of CD11c⁺ DC1 about 4 times more efficiently than those of CD11c⁻ DC2. Interestingly, during the period of DC regeneration after SCT, the DC1 subset prevails to the same extent over DC2, suggesting that the preferential expansion of DC1 lineage is a response to high endogenous FL levels. This prevalence of DC1 occurs despite a simultaneous increase of G-CSF, the cytokine that selectively mobilizes the DC2 subset into blood [184-186]. It is also possible that FL, which rises only transiently during the period of aplasia, is not available after stem cell engraftment long enough for the DC2 subset to develop.

3.2.1. Comparable Literature

Dodero *et al.* [187] analysed the reconstitution kinetics of circulating DC1 and DC2 of 14 patients with a median age of 57 years. The value of DC1 and DC2 remained depressed for the entire follow-up period: median values of DC1/ μ L and DC2/ μ L were 1.75 and 1.9 at day 60 (median normal values were 15/ μ L and 11 / μ L for DC1 and DC2, respectively) and 3.9 and 3.8 at day 180, respectively.

In contrast to the data of Dodero *et al.* we have found higher DC subsets as shown in Figure 4-25, 4-26 and 4-27. We have found higher (> 5 DC/ μ l) DC1 and DC2 in patients with no problems after SCT compared with patients with infections and GVHD until day 120 after SCT. Interestingly, the latter group reach the 5 DC/ μ l level but decrease at day 50 to zero.

Reddy *et al.* [188] observed fifty patients with hematologic disorders undergoing allogeneic SCT and postulated that reconstitution of absolute numbers of circulating DCs after allogeneic hematopoietic SCT is an independent predictor of post-transplantation survival, relapse, and aGvHD. Their results indicated that higher numbers of DCs reconstituted after transplantation may reduce relapse.

Additional mechanisms for a protective impact of DCs against relapse and aGvHD could be extrapolated from the study by Sato *et al.* [189], which suggests the role of immune regulatory cells.

A recent study by Fagnoni *et al.* [190] in which 43 children were followed immediately after SCT showed that initially DC counts were somewhat higher in those children who later on developed aGVHD than in uncomplicated cases. Progression of aGvHD or use of Corticosteroids in their study was associated especially with decreasing plasmacytoid DC (DC2) values.

Evidence that DCs are involved in the pathophysiology of GvHD is based on murine models in which the lack of host DC activity prevented aGVHD development [174].

Mixed chimerism and persistence of host DCs appear to be associated with aGvHD [191, 192]. DC chimerism was not performed in our patients who underwent myeloablative transplantation. Although DC chimerism was not analyzed in our study, it is possible that most of our patients had full donor DC chimerism, as suggested by Auffermann-Gretzinger *et al.* [182] in which patients, after myeloablative and

nonmyeloablative SCT, had donor-derived DCs by day 14. Chimerism analysis is difficult to perform because of the rarity (1%) of DCs [193] and the requirement to propagate DCs in culture before analysis [191]. Therefore, measuring DC1 and DC2 counts, as in our study, may be a simple and reproducible method to predict clinical outcomes of relapse, aGVHD, and survival after PBSCT and myeloablative transplantation. Determining whether posttransplantation DC counts are clinically relevant after nonmyeloablative transplantation requires additional studies with larger numbers of patients.

3.3. Conclusions

We have started to monitor the development of new build blood cells in all patients after SCT. The presentation of the current data (till September 2005) gives only a small insight in the project planned in the future. Therefore we have not collected enough patients in all 6 categories to make statistical analyses yet. The determination of the six categories no problems, infections, aGvHD, cGvHD, TRM and relapse was never done in the literature before. With this new aspects we are convinced to find new pattern in the cells' development after SCT to forecast severe post-transplanted complications.

Abbreviations

7-AAD	7-Amino-Actinomycin D
8-MOP	8-methoxypsoralen
ADC	Analog to Digital Converter
ADP	adenosine diphosphate
Ag	antigen
aGvHD	acute graft-versus-host-disease
APC	allophycocyanin
APC	Antigen-presenting cells
AxV	Annexin V
BfA	Brefeldin A
BM	Bone Marrow
BMT	bone marrow transplantation
BP	bandpass
CB	cord blood
CBT	cord blood transplantation
CD	Cluster of differentiation
cGvHD	chronic graft-versus-host-disease
CNS	central nervous system
CR	complete response
CsA	cyclosporine A
CTCL	cutaneous T cell lymphoma
CTL	cytotoxic T-lymphocyte
Cy5	cyanin dye 5
Cy7	cyanin 7
DAG	diacylglycerol

DC	dendritic cells
DNA	deoxyribonucleic acid
EAE	experimental allergic encephalomyelitis
ECP	extracorporeal photochemotherapy
ELISPOT	Enzyme Linked ImmunoSorbent SPOT-Assay
FCS	flow cytometer standard
FITC	fluorescein-5-isothiocyanate
FK506	tacrolimus
flt3	fms-like tyrosine kinase
FL	fms-like tyrosine kinase ligand
FSC	forward scatter
G-CSF	granulocyte colony-stimulating factor
GM-CSF	granulocyte-macrophage colony stimulating factor
GvHD	graft-versus-host-disease
GvL	graft versus leukaemia
HLA	human leukocyte antigen
HSCT	haematopoietic stem cell transplantation
ICAM	intracellular adhesion molecule 1
ICC	intracytoplasmatic cytokine
IDC	interdigitating DC
Ig	immunoglobulin
IL	interleukin
INF	interferon
IRC	interstitial reticulum cell
ITAM	immunoreceptor tyrosine-based activation motif
KIRs	killer cell immunoglobulin-like receptors
LC	Langerhans cell
LP	longpass
LPS	lipopolysaccharide
mAb	monoclonal antibody
MHC	major histocompatibility complex

Abbreviations

MLR	mixed lymphocyte reaction
MMF	Mycophenolate mofetil
MNC	Mononuclear cells
MoDC	monocyte-derived DC
MPA	mycophenolic acid
MTX	methotrexate
NAFT	nuclear transcription factor of activated T cells
NCAM	neuronal cell adhesion molecule
NCRs	natural cytotoxicity receptors
NK	natural killer
NR	no response
PARP	polyADP-ribose polymerase
PBL	peripheral blood lymphocytes
PBMC	peripheral blood mononuclear cells
PBPC	peripheral blood progenitor cells
PBS	phosphate buffered saline
PBSCT	peripheral blood stem cell transplantation
PC	phosphatidylcholine
PCR	polymerase chain reaction
PE	phycoerythrin
PE	phosphatidylethanolamine
PerCP	Peridinin-chlorophyll-protein
PKC	protein kinase C
PLC	phospholipase C
PMT	photomultiplier tube
PS	phosphatidylserine
PSR	phosphatidylserine receptor
PUVA	Psoralen and UVA
RIC	reduced intensity conditioning
RNA	ribonucleic acid
ROS	reactive oxygen species

Abbreviations

SC	Stem cell
SP	shortpass
SSC	side scatter
TBI	total body irradiation
Tc1	T cytotoxic cell type 1
TCR	T-cell receptor complex
TdT	terminal deoxynucleotidyl transferase
Th1	T helper cell type 1
Th2	T helper cell type 2
TLR	Toll-like receptor
TNF	tumor necrosis factor
TRM	transplant-related mortality
UVA	ultraviolet a rays

Appendix A

Cell Separation Protocol

- Obtain Heparin-anticoagulated blood and leave at room temperature on mixer.
- Dilute blood with an equal volume of PBS-H (maximum dilution 2:1 buffer: blood).
- Inject 7 ml Bicol (1.077 g/ml; BioChrom) underneath the blood in a 30-ml-Sterilin conical tube or 10 ml underneath a 50-ml-Falcon conical tube by using an automatic pipette.
- Centrifuge tubes at 550 x g without brake for 20 min at 20 °C.
- Prepare 10 ml PBS pH 7.4 in 30-ml Sterilin tubes.
- Pipette the WBC band into the prepared tubes and mix by pipetting up and down with a 3.5 transfer pipette.
- Centrifuge tubes at 450 x g for 10 min at 20 °C.
- Decant the supernatant and resuspend cells by pipetting with a 1-ml tip in 10 ml PBS pH 7.4.
- Centrifuge tubes at 450 x g for 10 min at 20 °C.
- Discard liquid and resuspend in 2 ml cultivation medium by pipetting with a blue 1-ml tip.

Appendix B

Intracytoplasmatic Cytokine Staining Protocol

In Figure Appendix B- 1 the big time bar summarizes all working steps. The small time bar shows the appropriate working temperature.

Cell Stimulation and Cultivation

- Take 200 µl from each sample and measure WBC concentration by CELL-DYN 3500R.
- Dilute remaining cells with culture medium up to 3×10^6 cells / ml in a 50-ml-Falcon flask equipped with membrane skew.
- Add 10 µl/ml brefeldin A solution, stock B (concentration in culture is 10 µg/ml).
- Add 10 µl/ml PMA solution, stock B (concentration in culture is 10 ng/ml).
- Add 12.5 µl/ml Ionomycin solution, stock B (concentration in culture is 1.25 µg/ml).
- Cultivate flasks for 4 hours at 37 °C, 95% water- and 5% CO₂- saturated atmosphere.

Cell Harvest and Fixation

- Put flasks on ice for 5 min.
- Discard medium in a 30-ml Sterilin tube, loose cells with a sterile scraper and wash flask with cold PBS pH 7.4, at least three times.
- Wash cells in 20 ml and then in 10 ml cold PBS pH 7.4 at 450 x g for 7 min at 4°C.
- Gently discard liquid and resuspend cells by pipetting with a blue 1-ml tip in 1 ml PBS pH 7.4.
- Take an aliquot of maximum 0.8×10^6 cells into one 1.2-ml-Micronics tube, fill up to 1 ml with PBS pH 7.4 and centrifugate at 300 x g for 5 min at 4°C.

- Gently discard supernatant via a multi-channel suction unit.
- Add 25µl of blocking solution, mix gently and incubate for 10 min at 4°C in the dark.
- Add 20 µl of surface antibody cocktail and incubate for 20 min at 4°C in the dark.
- Add 100µl of fixation solution into each tube, mix immediately after addition and incubate for 15 min at room temperature in the dark.
- Add 900µl of PBS pH 7.4 to each tube and centrifugate at 300 x g for 5 min.
- Gently discard supernatant via a multi-channel suction unit.

Cell Permeabilization and Cell Staining

- Add 70 µl of permeabilization solution and resuspend cells gently by vortexing.
- Incubate for 5 min at room temperature in the dark.
- Add 14 µl of cytokine antibody cocktail, mix gently and incubate for 15 min at room temperature in the dark.
- Add 900 µl PBS pH 7.4 and centrifugate at 300 x g for 5 min.
- Gently discard supernatant via a multi-channel suction unit.
- Resuspend cells in 300 µl PBS pH 7.4 and keep on ice till flow cytometric measurement.

Surface staining

All antibodies are prepared with PBS buffer, pH 7.4. The FITC-conjugated antibody (INF-γ) is combined with one of the listed PE-conjugated antibodies (IL-2, IL-4, IL-10, TNF-α) as shown in Table Appendix C- 1. Proper working concentrations, manufactures and clone specificity of all mouse antibodies are summarized in Table Appendix B- 2.

	FL1	FL2	FL3	FL4
Panel 1	IgG ₁ -FITC	IgG _{2a} -PE	CD8-PE-Cy7 or CD8-PerCp	CD4-APC
Panel 2	INF- γ -FITC	IL-4-PE	CD8-PE-Cy7 or CD8-PerCp	CD4-APC
Panel 3	INF- γ -FITC	IL-4-PE	CD8-PE-Cy7 or CD8-PerCp	CD4-APC
Panel 4	INF- γ -FITC	IL-10-PE	CD8-PE-Cy7 or CD8-PerCp	CD4-APC
Panel 5	INF- γ -FITC	TNF- α -PE	CD8-PE-Cy7 or CD8-PerCp	CD4-APC

Table Appendix B-1: Applied Fluorescence Conjugated Antibodies of Intracytoplasmatic Cytokine Analyses

Cocktail	Clone	Antibody-fluorochrome conjugate	IgG class	Company	Dilution in cocktail
Surface antibody	SK3	mouse ah CD4-APC	1	BD Bioscience	1: 50
	SK1	mouse ah CD8-PerCp	1	BD Bioscience	1:30
	SFCI21Thy 2D3	mouse ah CD8-PC7	1	Beckman coulter	1:100
Cytokine antibody	MQ1-17H12	rat ah IL-2-PE	2a	Pharmingen	1:100
	MP4-25D2	rat ah IL-4-PE	1	Pharmingen	1:100
	JES3-9D7	rat ah IL-10-PE	1	Pharmingen	1:100
	MAb11	mouse ah TNF- α -PE	1	Pharmingen	1:100
	B27	mouse ah INF- γ -FITC	1	Pharmingen	1:800
Isotype control	MOPC-21	mouse IgG ₁ -FITC	1	Pharmingen	1:100
	G115-178	mouse IgG _{2a} -PE	2a	Pharmingen	1:250

Table Appendix B-2: Applied Antibody Specificity and Working Concentrations of Intracytoplasmatic Cytokine Analyses

Reagents

PBS-H

Add 5000 I.E. Heparin (Baxter) to 500ml PBS pH 7.4 under sterile conditions.

Culture medium

Ultra Culture-Medium, serum free (BioWhittaker)

Gentamycinsulphate (Sigma G-3632): 170 mg/l

L-glutamine (Sigma G-5763): 2mM

2-Mercapto-ethanol (Merck #12006): 50mM (3.5µl/l)

Fixation solution

5.5 Vol % Formaldehyd diluted in PBS pH 7.4.

Otherwise IntraPep™ Fixation Reagent is commercially available from Immunotech, France.

Permeabilization buffer

10 g Saponin (Aldrich S-130-2) and 23.8 g Hepes are solubilized in 100 ml PBS pH 7.4 and sterile filtrated. The stock solution is stored at 4 °C.

For usage the buffer is freshly prepared as a 0.5% Saponin solution with PBS pH 7.4.

Otherwise IntraPep™ Permeabilization Reagent is commercially available from Immunotech, France.

Blocking solution

Add 4 ml of sterile PBS pH 7.4 to 1 ml of mouse IgG₁ (1 mg/ml; MOPC-21, Sigma) and add 50 mg of 0.22-µm-filtrated BSA (Sigma). Aliquote the solution into 500µl units and keep at 4°C in the dark.

Brefeldin A stock solution

5 mg brefeldin A (Sigma; B-7651) is diluted in 500 µl ethanol (>98 Vol%), aliquoted and stored at -20 °C.

Before usage as stock solution, thawed aliquot is diluted 1:10 with culture medium.

PMA stock solution (stock B)

Stock A: 1 mg Phorbol 12-myristate 13-acetate (Sigma P-8139) is solubilized in 1 ml ethanol (> 98Vol%) and further diluted in 9 ml culture medium. (stock A: 100µg/ml)

Stock B: stock A is further diluted 1:100 with culture medium and stored at -80 °C (stock B: 1µg/ml). Before usage aliquots are stored at -20 °C to aim shorter thawing duration.

Ionomycin stock solution

1 mg ionomycin (Sigma, I-0634) is solubilized in 1.34 ml sterile, pyrogenfree and endotoxinfree DMSO (Cryo-Sure-DMSO; WAK-CHEMIE MEDICAL GMBH) and further diluted 1:10 with culture medium and stored at -20 °C.

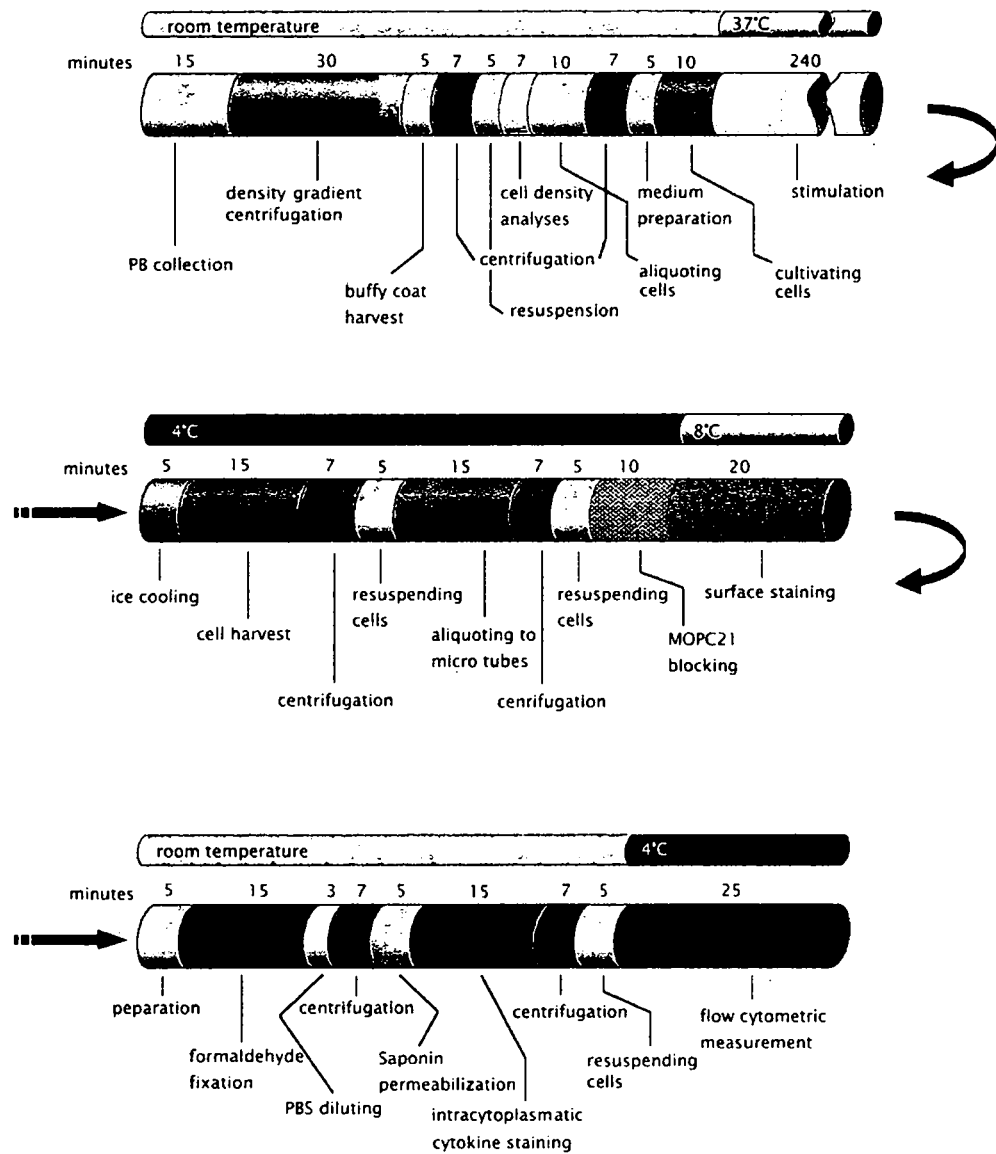


Figure Appendix B-1: Time bars of working steps of Intracytoplasmic cytokine Analysis.

Appendix C

Staining protocol of Whole Blood Cell Subpopulations

- Obtain Heparin-anticoagulated blood and leave at room temperature on mixer.
- Pipette 85 μ l of well-mixed undiluted blood into the bottom of each 1.2ml-Micronic tube. Avoid blood residue on the walls of the tube.
- Add a certain amount of antibody reagent into each tube (see Table Appendix C- 2).
- Vortex thoroughly for 5 seconds and incubate for 15 minutes at room temperature in the dark.
- Add 150 μ l of room temperature 1X FACS Lysing Solution to each tube. Immediately vortex thoroughly and add further 900 μ l 1X FACS Lysing Solution with a 5-ml-Combitip in each tube. The jet of water from the multipipette replaces further vortexing.
- Incubate for 10 minutes at room temperature in the dark. Avoid prolonged exposure of the cells to lytic reagents, which can cause white cell destruction.
- Immediately after incubation, spin down with 300 x g for 5 minutes at room temperature.
- Aspirate the supernatant, leaving approximately 20 μ l of residual fluid in the tubes to avoid disturbing the pellets.
- Add 150 μ l PBS pH 7.4 to each tube. Immediately vortex thoroughly and add further 900 μ l PBS pH7.4 with a 5-ml-Combitip in each tube. The jet of water performed with a multipipette displaces further vortexing.
- Centrifugate tubes at 300 x g for 5 minutes at room temperature.

- Aspirate the supernatant, leaving approximately 50µl of residual fluid in the tube to avoid disturbing the pellet.
- Add 0.5 ml of 1% paraformaldehyde to each tube. Vortex thoroughly at low speed for 5 seconds.
- The cells are now ready to be analyzed on the flow cytometer. The prepared tubes are stored on ice in the dark until flow cytometric analysis can be performed.
- Analyze the fixed cells thoroughly before putting them through the flow cytometer to reduce cell aggregation.
- Flow Cytometry Data Acquisition
- Instrument Settings were taken from the current FACS Comp protocol (updated every 7 days) to adjust the PMT voltages and fluorescence compensation and to check the sensitivity of the instrument.
- Acquire prepared samples on the FACSCalibur. For data acquisition use CellQuest Pro™ software with threshold on FSC to exclude debris.
- FSC and SSC amplifier are adjusted manually to view all cell populations in the dot plot.

The analyses of 5 different 4-color samples are adapted to the questioned population and a special analysis program was generated. Table Appendix C- 1 shows all applied fluorescence conjugated antibodies of all 6 panels and the 4 fluorescence channels. Proper working concentrations, manufactures and clone specificity of all mouse antibodies are summarized in Table Appendix C- 2.

	FL1	FL2	FL3	FL4
Panel 1	Lin 1-FITC	IgG ₂ -PE	HLA-DR-PerCp	IgG ₁ -APC
Panel 2	Lin 1-FITC	CD123-PE	HLA-DR-PerCp	CD11c-APC
Panel 3	CD45-FITC	CD14-PE	CD3-PerCp	IgG ₁ -APC
Panel 4	CD45-FITC	CD14-PE	CD3-PerCp	CD56-APC
Panel 5	CD4	CD8	-	CD3-APC

Table Appendix C-1: Applied Fluorescence Conjugated Antibodies of Whole Blood Analyses

panel	Clone	antibody-fluorochrome conjugate	IgG class	company	dilution in sample
1, 2		Linage 1 cocktail (lin 1):		BD Bioscience	1: 13
	SK7	ah CD3-FITC	1		
	MφP9	ah CD14-FITC	2b		
	3G8	ah CD16-FITC	1		
	SJ25C1	ah CD19-FITC	1		
	L27	ah CD20-FITC	1		
	NCAM.16.2	ah CD56-FITC	2b		
1, 2	L423	ah HLA-DR-PerCp	2a	BD Bioscience	1:22.3
1, 2	MOPC-21	mouse IgG-PE	1	BD Bioscience	1:43.5
1, 2, 3	X40	mouse IgG-APC	1	BD Bioscience	1:29.3
2	9F5	ah CD123 -PE	1	BD Pharmingen	1:43.5
2	B-ly6	ah CD11c-APC	1	BD Pharmingen	1:29.3
3		Simultest™ LeukoGate:		BD Bioscience	1:13
	2D1	ah CD45-FITC	1		
	MφP9	ah CD14-PE	2b		
3	SK7	ah CD3-PerCp	1	BD Bioscience	1:22.3
4	B159	ah CD56-APC	1	BD Pharmingen	1:29.3
4, 5, 6	SK3	ah CD3-APC	1	BD Pharmingen	1:29.3
4, 5		Simultest™:		BD Bioscience	1:13
	SK3	ah CD4-FITC	1		
	SK1	ah CD8-PE	1		

Table Appendix C-2: Applied Antibody Specificity and Working Concentrations of Whole Blood Analyses

Reagents

PBS-H

Add 5000 I.E. Heparin (Baxter) to 500ml PBS pH 7.4 under sterile conditions.

Fixation solution

10X FACS Lysing Solution (BD Bioscience) is diluted 1:10 with bi-distillated water to receive 1X FACS Lysing Solution. The solution is stored in glass at room temperature for maximum 2 weeks.

Blocking solution

Add 4 ml of sterile PBS pH 7.4 to 1 ml of mouse IgG₁ (1 mg/ml; MOPC-21, Sigma) and add 50 mg of 0.22- μ m-filtrated BSA (Sigma). Aliquote the solution into 500 μ l units and keep at 4°C in the dark.

Appendix D

4-Color Analyses of Intracytoplasmatic Cytokines

Plot Characteristics

Dot Plot: A dot plot provides a 2-parameter data display. Each dot in a dot plot represents one or more cells. Gated cell populations can be multi-colored and also highlighted.

Density Plot: A density plot simulates a three-dimensional display of cells. It is similar to a dot plot except it uses colors to show the number of events. The color shows the cells at each x and y position on the plot. The data used by density plots have a resolution of only 128x128 channels. The data from adjacent channels are added to condense higher resolution data into 128 channels. The density levels used for analyses are 50%, 25%, 12%, 6%, 3% and 1% of the peak height. This method shows more detail in the lower regions, while still showing high peaks.

In Figure Appendix D- 1, 7 plots describe the set of region for the discrimination of the CD4-positive and CD8-positive lymphocyte subpopulations and their intracytoplasmatic cytokines IL-2, IL-4, IL-10, INF- γ and TNF- α . As mentioned in the staining protocol anti-INF- γ -FITC is combined with the four PE labeled antibodies anti-IL-2-PE, anti-IL-4-PE, anti-IL-10-PE and anti-TNF- α -PE.

The following protocol is used:

- Load the negative control data file as shown in Figure Appendix D- 1.
- Discriminate lymphocytes: As shown in Figure Appendix D- 1 region R1 in density plot 1 is created and the location of the leukocytes is checked in dot plot 2.

- Discriminate subpopulations of lymphocytes: As shown in Figure Appendix D- 1 in density plot 4 region R1 is created on CD4+CD8- cells, region R4 is created on CD4-CD8- cells and region R5 is created on CD4-CD8+ cells. In the Gate Statistics Table in Figure Appendix D- 1 the populations are summarized.
- Discriminate cytokines of the subpopulations by quadrants: Based on the density plot 4 each region was transferred in another dot plot. CD4+CD8- T cells are shown in dot plot 5, CD4+CD8- T cells in dot plot 6 and CD4-CD8- T cells in dot plot 7. Each dot plot contains 4 quadrants and the centre is set to keep the main population in the lower left (LL) quadrant as shown in Figure Appendix D- 1. To make the results comparable, the quadrant location was kept equal in all 3 dot plots 4-7.
- Take the record button in the batch window to export results to the spreadsheet file.
- Load the sample data file as shown in Figure Appendix D- 2. The latter settings are kept for the sample file.
- Take a look at the right compensation in Figure Appendix D- 2 dot plot 2. Green colored CD4+CD8- T cell population with high PE-signals is clearly divided from red colored CD4-CD8+ T cell population.
- Take a look at the quadrant setting in dot Figure Appendix D- 2 plot 4-7: The location of cells with high cytokine fluorescence should stand in right angle to negative cells.
- Press the record button of the batch to add results to the spreadsheet file.
- Load appropriate other three files with PE-labeled anti-IL-4, anti-IL-10 and anti-TNF- α antibody conjugates.

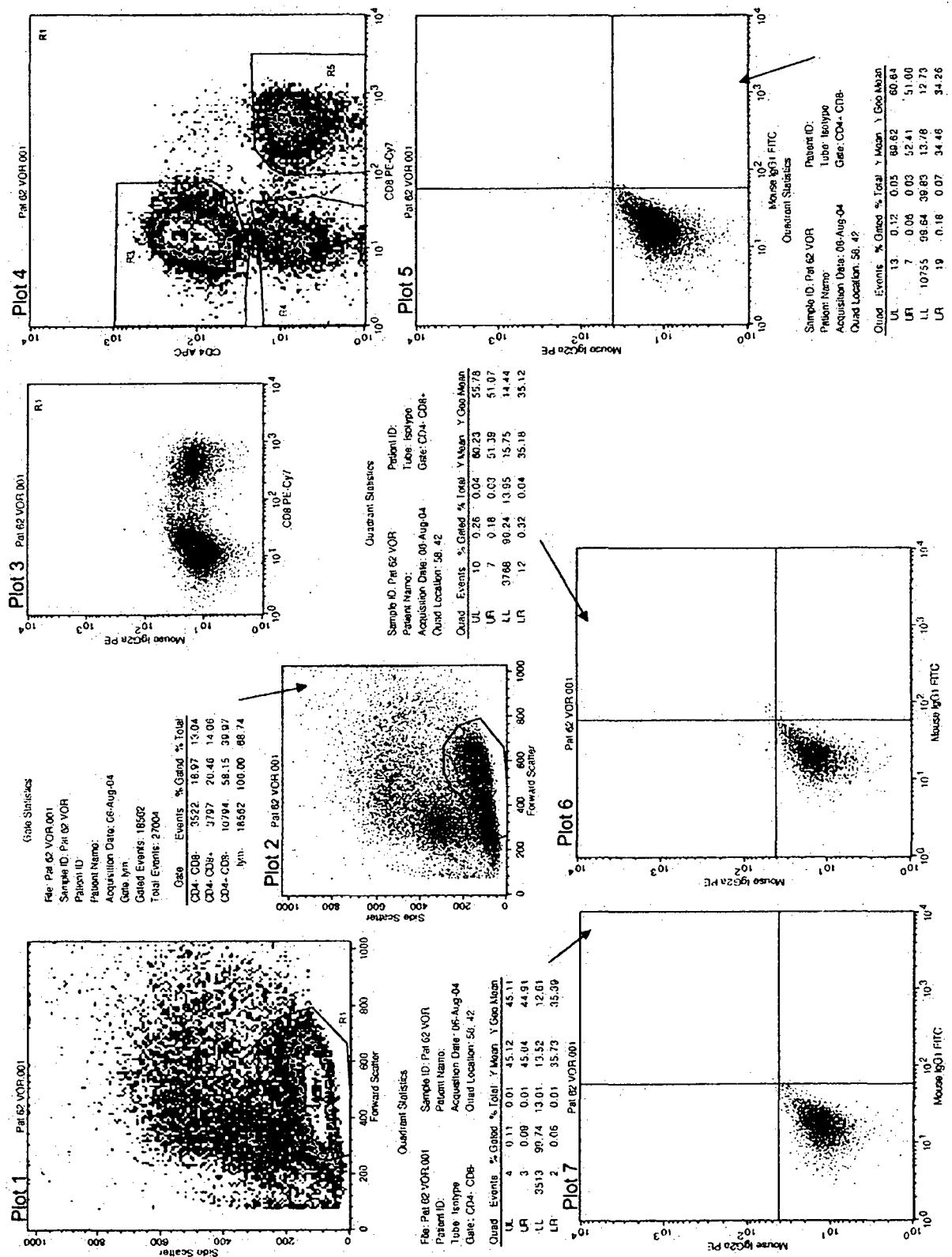


Figure Appendix D-1: Spreadsheet of graphics output of a negative control sample of cytoplasmatic cytokine analysis.

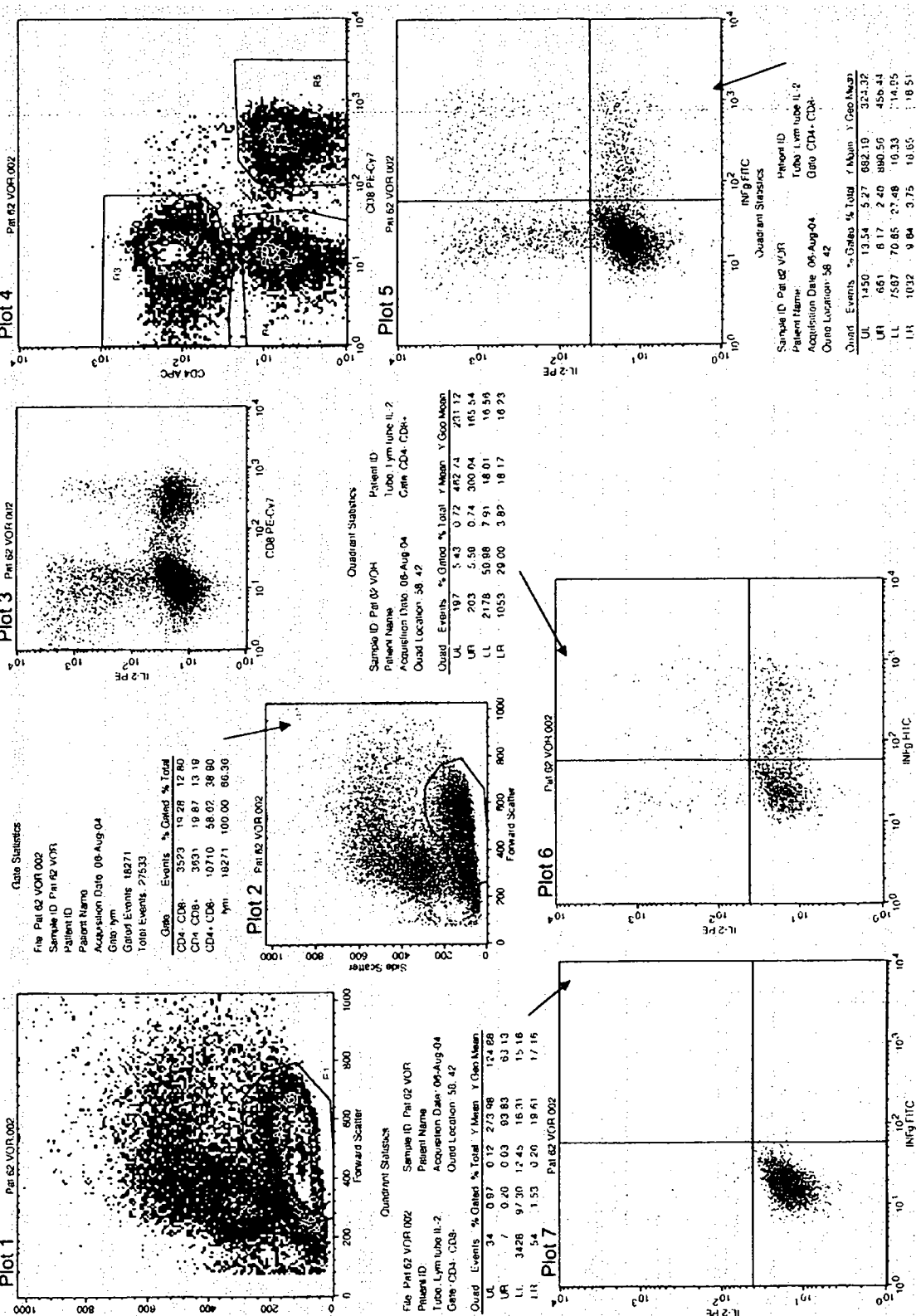


Figure Appendix D-2: Spreadsheet of graphics output of a positive sample of cytoplasmatic cytokine analyses.

Spreadsheet Output

Based on the combination of the composed regions, the gate lists of each population (CD4+CD8- T cells, CD4+CD8- T cells and CD4-CD8- T cells) is shown in Table Appendix D- 1 and includes the description of label names, gate definitions and the colors of the cells.

The Gate Statistics, and the three Quadrant Statistics of CD4+CD8-, CD4+CD8- and CD4-CD8- T cells are included in Figure Appendix D- 2 and shows the data output sequence into an ASCII file.





	Multi			Label	Definition
	Hilite	color	Color		
◆	<input type="checkbox"/>	<input type="checkbox"/>		CD4- CD8-	R1*r4
◆	<input type="checkbox"/>	<input checked="" type="checkbox"/>		CD4- CD8+	R1*r2
◆	<input type="checkbox"/>	<input checked="" type="checkbox"/>		CD4+ CD8	r1*r3
◆	<input type="checkbox"/>	<input type="checkbox"/>		lym	r1

Table Appendix D-1: Gate list of Intracytoplasmatic analyses

Cell Quest Pro™ is not able to rearrange the matrix to receive a sorted output with one character in one column. Therefore the output file is imported and converted by SAS Enterprise Guide 2.0 as described in chapter 3 issue 7.7.5.

Appendix E

4-Color-Analyses Protocol of CD4+ and CD8+ T Cells Apoptosis

In Figure Appendix E- 1 and Figure Appendix E- 2, 5 plots describe the set of attractors for the discrimination of T helper cells (CD4+) and cytotoxic T cells (CD8+) and further discrimination in vital, early and late apoptosis. The Hierarchy Legend at the bottom of Figure Appendix E- 2 describes the color and composition of all attractors used for the analysis. The following protocol is used:

- Load the negative control data file as shown in Figure Appendix E- 1.
- Discriminate the lymphocyte gate: As shown in Figure Appendix E- 1 plot 3 [negK] the fixed violet attractor excludes larger cell population and a fixed grey attractor excludes debris. The position of the attractors are fixed and set as black hole attractor.
- Adjust CD4- and CD8- attractors to isotype fluorescence: In Figure Appendix E- 1 plot 1 the fixed green attractor (CD4 in sample) is positioned on the right border of the negative population. The same is done with the red attractor (CD8 in sample) as shown in plot 2.
- Choose 'Classify Data' from the Attractors menu to write data to the spreadsheet. Unload negative control data file.
- Load sample file and keep the former attractor settings.
- Adjust left and right apoptosis attractors: As shown in Figure Appendix E- 2. plot 5 both cell population (CD4 and CD8) are subdivided in a left and right part by 4 fixed sub-attractors: CD4+ cells are divided in left turquoise attractor (CD4_L) and right olive attractor (CD4_R). CD8+ T cells are divided in left light orange attractor

(CD8_L) and right dark brown attractor (CD8_R).

The borders of the right attractors are arranged together with the apoptotic population in FSC/SSC in plot 3 and are kept during one kinetic.

- Adjust lower left (LL) attractors: As shown in Figure Appendix E- 2 in plot 5, the left attractor of both cell population (CD4 and CD8) CD4+ is further divided in a AxV-Cy5 high and low fluorescence population: AxV-Cy5 low binding CD4+ cells are enclosed in dark blue fixed subattractor (CD4LL) and AxV-Cy5 low binding CD8+ cells are enclosed in fixed dark orange subattractor (CD8LL).
- Adjust upper right (UR) attractors: As shown in Figure Appendix E- 2 in plot 5, the right attractor of both cell population (CD4 and CD8) CD4+ is further divided in a 7-AAD high and low fluorescence population: 7-AAD low binding CD4+ T cells are enclosed in a fixed violet subattractor (CD4LL) and 7-AAD low binding CD8+ T cells are enclosed in a fixed beige subattractor (CD8LL).
- Exclude CD4+CD8+ T cells: In Figure Appendix E- 2 in plot 4 a large and a small fixed black hole attractor exclude unspecific cells outside the main cloud populations as well as CD4+CD8+ T cells.
- Choose 'Classify Data' from the Attractors menu to export data to the spreadsheet file.

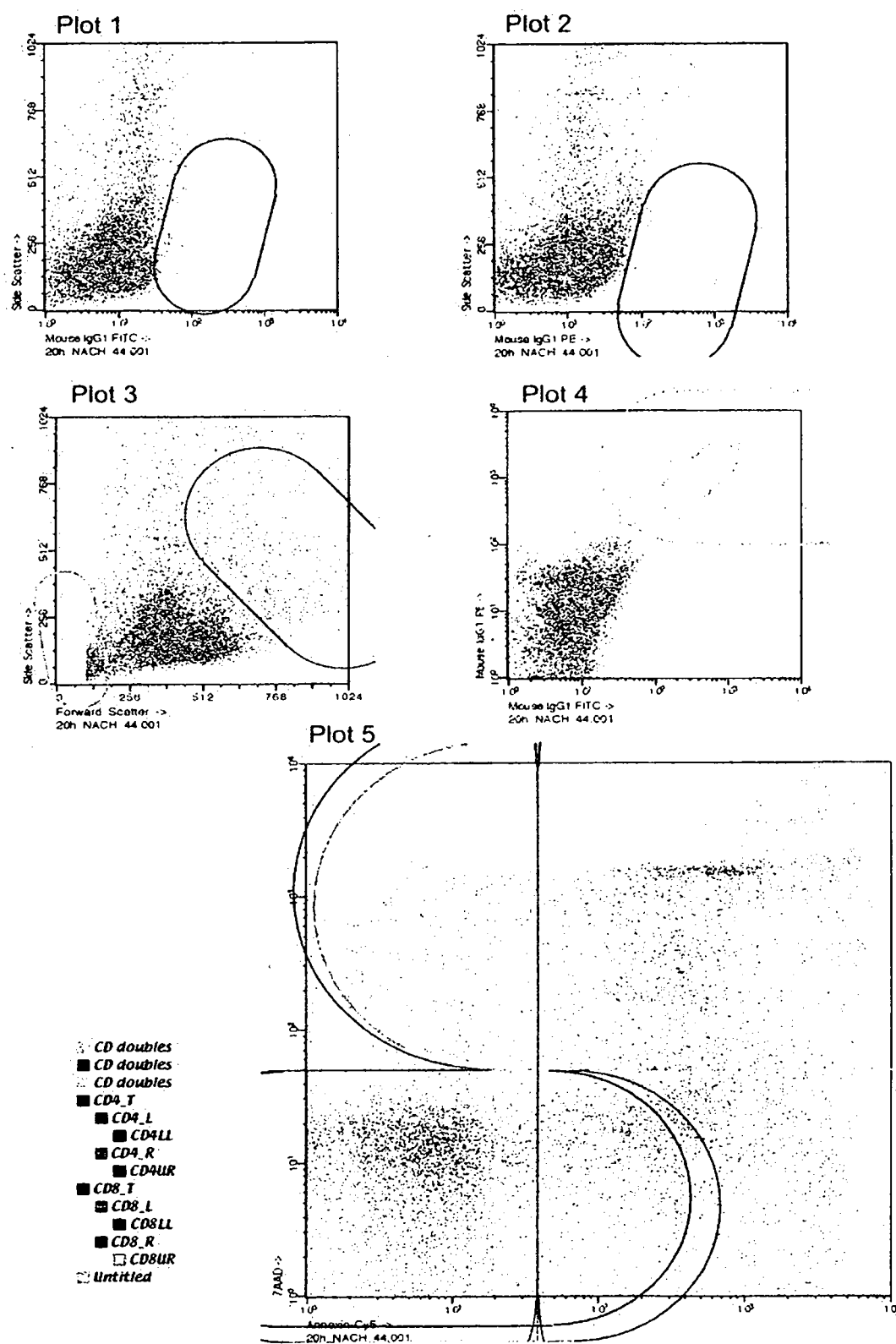


Figure Appendix E-1: Spreadsheet of graphics output of a negative control analyzing early and late apoptotic CD4⁺ T cells and CD8⁺ cytotoxic T cells.

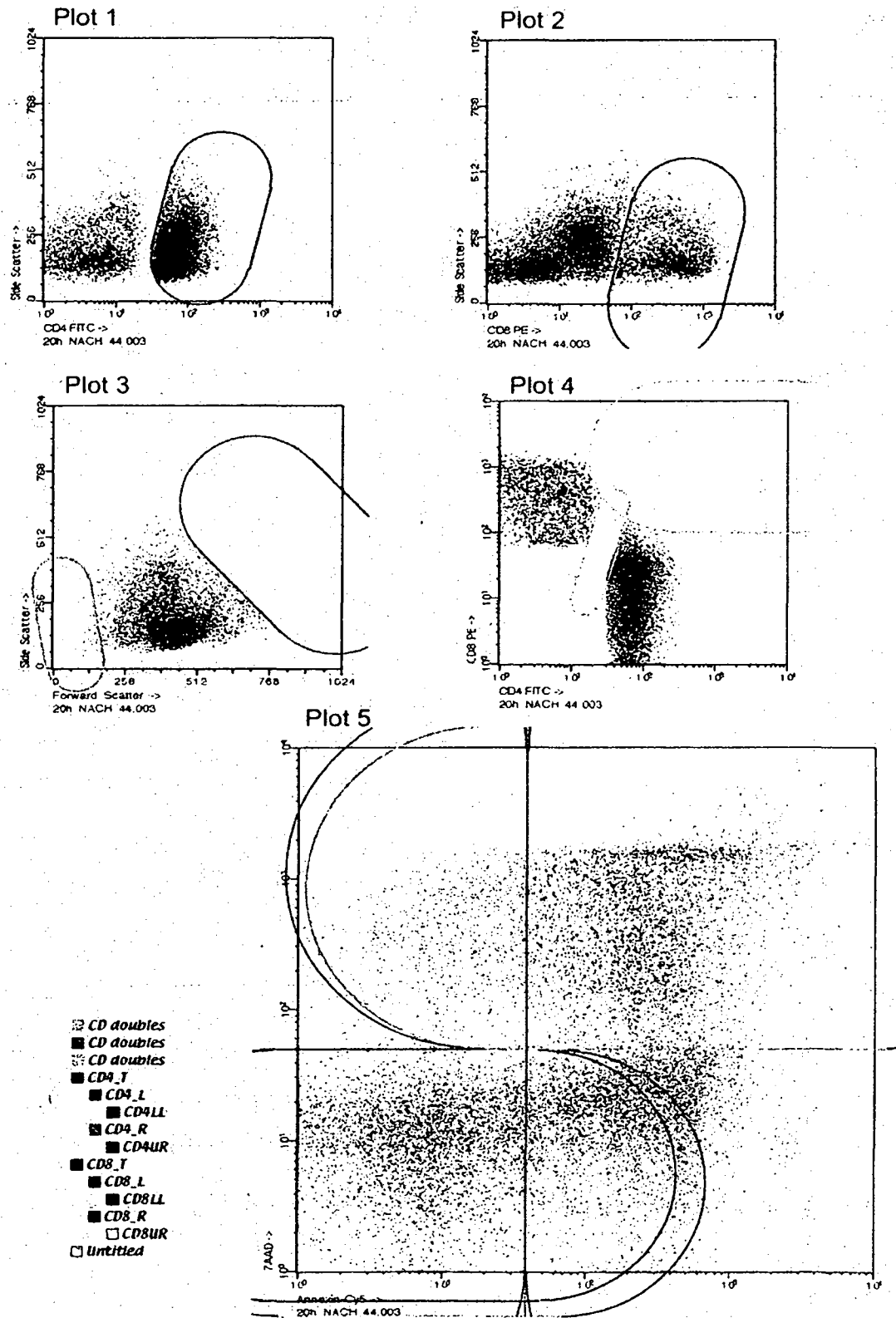


Figure Appendix E-2: Spreadsheet of graphics output of a sample analyzing early and late apoptotic CD4+ T cells and CD8+ cytotoxic T cells.

Spreadsheet Output

Based on composed attractors' hierarchy, the cell population sizes, percent of top-level population and fluorescence statistics (Mean, SD, CV) are written in an output file. The benefit of the file output is that each character in the printable matrix are automatically rearranged and set in one column in the stored data file.

The stored data file needs only few changes to be read into a SAS file. The protocol is described in chapter 3 issue 7.7.5.

Appendix F

4-Color-Analyses Protocol of NK cells Apoptosis

In Figure Appendix F- 1 and Figure Appendix F- 2, 5 plots describe the set of attractors for the discrimination of T cells (CD3+) and NK cells (CD3-CD56+) and further discrimination in vital, early and late apoptosis. The Hierarchy Legend at the bottom of Figure Appendix F- 2 describes the color and composition of all attractors used for the analysis. The following protocol is used:

- Load the negative control data file as shown in Figure Appendix F- 1.
- Discriminate the lymphocyte gate: As shown in Figure Appendix F- 1 plot 3 [negK] the fixed violet attractor excludes larger cell population and a fixed grey attractor excludes debris. The position of the attractors are fixed and set as black hole attractor.
- Adjust CD3- and CD56- attractors to Isotype fluorescence: In Figure Appendix F- 1 plot 1 the fixed green attractor (CD4 in sample) is positioned on the right border of the negative population. The same is done with the red Attractor (CD8 in sample) as shown in plot 2.
- Choose 'Classify Data' from the Attractors menu to write data to the spreadsheet. Unload negative control data file.
- Load sample file and keep the former attractor settings.
- Adjust left and right apoptosis attractors: As shown in Figure Appendix F- 2 in plot 5, both cell population (CD3 and CD56) are subdivided in a left and right part by 4 fixed sub-attractors: CD3+ cells are divided in left turquoise attractor (CD3__L) and right olive attractor (CD3__R). CD8+ T cells are divided in left light orange attractor (CD56_L) and right dark brown attractor (CD56_R). The borders of the

right attractors are arranged together with the apoptotic population in FSC/SSC in plot 3 and are kept during one kinetic.

- Adjust lower left (LL) attractors: As shown in Figure Appendix F- 2 in plot 5, the left attractor of both cell population (CD3 and CD56) CD3+ is further divided in a AxV-Cy5 high and low fluorescence population: AxV-Cy5 low binding CD3+ cells are enclosed in dark blue fixed subattractor (CD3_LL) and AxV-Cy5 low binding CD56+ cells are enclosed in fixed dark orange subattractor (CD56LL).
- Adjust upper right (UR) attractors: As shown in Figure Appendix F- 2 in plot 5, the right attractor of both cell population (CD4 and CD8) CD4+ is further divided in a 7-AAD high and low fluorescence population: 7-AAD low binding CD4+ cells are enclosed in a fixed violet subattractor (CD3_UR) and 7-AAD low binding CD8+ cells are enclosed in a fixed beige subattractor (CD56UR).
- Exclude CD3+CD56+ T cells: In Figure Appendix F- 2 plot 4 a large and a small fixed black hole attractor exclude unspecific cells outside the main cloud populations as well as CD3+CD56+ cells.
- Choose Classify Data from the Attractors menu to export data to the spreadsheet file.

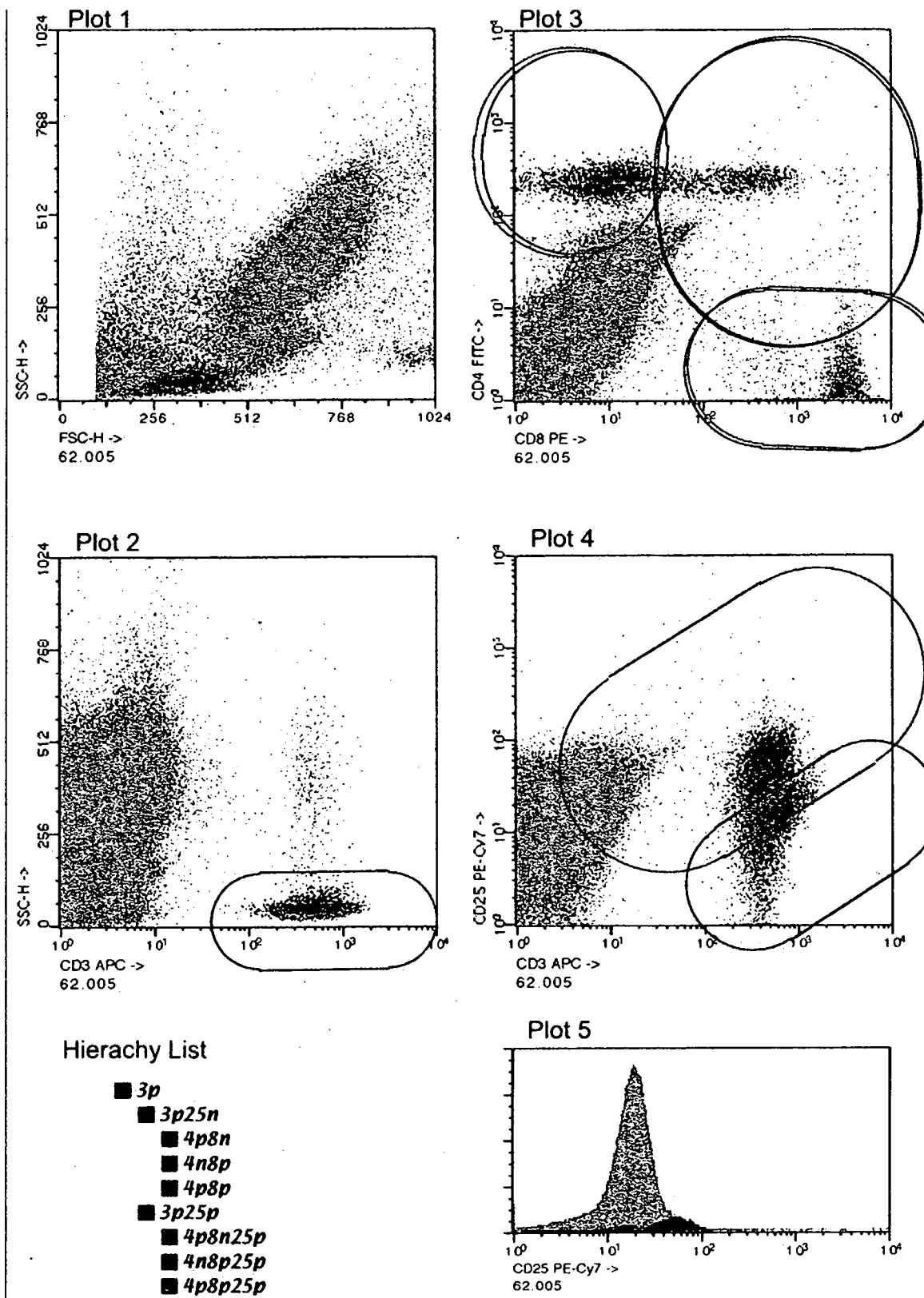


Figure Appendix F-1: Spreadsheet graphics output of a sample analyzing early and late apoptotic CD3+ T cells and CD3-CD56+ NK cells.

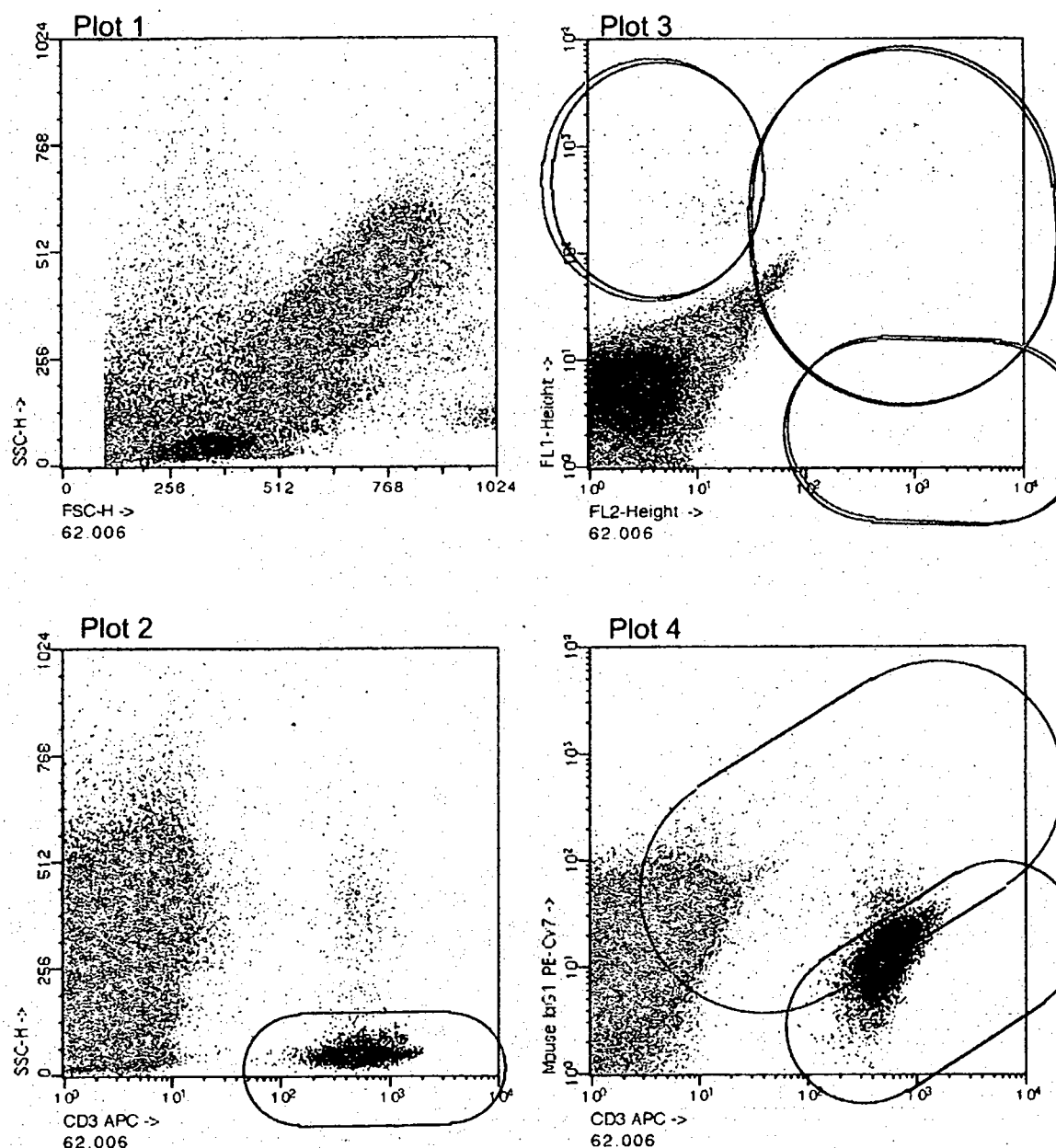


Figure Appendix F-2: Spreadsheet graphics output of a negative control analyzing early and late apoptotic CD3⁺ T cells and CD3-CD56⁺ NK cells.

Spreadsheet Output

Based on composed attractors' hierarchy, the cell population sizes, percent of top-level population and fluorescence statistics (Mean, SD, CV) are written in an output file. The benefit of the file output is that each character in the printable matrix are automatically rearranged and set in one column in the stored data file. The stored data file needs only few changes to be read into a SAS file. The protocol is described in chapter 3 issue 7.7.5.

Appendix G

4-Color-Analyses of Dendritic Cells

Plot Characteristics

Dot Plot: A dot plot provides a 2-parameter data display. Each dot in a dot plot represents one or more cells. Gated cell populations can be multi-colored and also highlighted. Highlighting cells is used by small populations (e.g. CD123, CD11c), showing four times bigger dots for better locating a rare population or to differentiate between a mixed population within a region. Highlighting does not add events nor does it affect statistics.

Density Plot

A density plot simulates a three-dimensional display of cells. It is similar to a dot plot except it uses colors to show the number of events. The color shows the cells at each x and y position on the plot. The data used by density plots have a resolution of only 128x128 channels. The data from adjacent channels are added to condense higher resolution data into 128 channels. The density levels used for analyses are 50%, 25%, 12%, 6%, 3% and 1% of the peak height. This method shows more detail in the lower regions, while still showing high peaks.

Histogram: A histogram plot is a graphical means of presenting a single parameter of data. The horizontal axis of the graph represents the signal intensity of the parameter and the vertical axis represents the number of cells.

In Figure Appendix G- 1, 11 plots describe the set of region for the discrimination of dendritic cells (DC1, DC2) and basophils. The following protocol is used:

Discriminate cells from debris: Region R1 in plot 1 is created and the location of the debris is checked in Plot 11. Some patients have a high population of non-lytic erythrocytes which can be excluded by R1. The lineage cocktail 1 is approximately comparable with a CD45 marker. As shown in Figure Appendix G- 2 the density plot CD3-PerCp against CD45-FITC has nearly the same shape of cell populations in region R1.

- Discriminate lineage negative cells by creating region R2 in Figure Appendix G- 1 in plot 1.
- Discriminate DC2 (R4) and basophils (R3) in plot 5. In plot 4 the cell density is helpful to centre the population. The location of basophils is shown in plot 11.
- Discriminate DC1 (R5) in plot 8. The cell density in plot 7 is helpful to centre the DC1-population. To discriminate HLR-DR positive cells from unspecific CD11c staining, the negative control panel 1 is loaded as shown by the 2 comparable plots in Figure Appendix G- 3.
- Check double discrimination of DC1 and DC2 population: The location of DC2 (red dots) and DC1 (orange dots) is shown in plot 4. DCs with both markers (CD123 and CD11c) are shown in plot 6.
- Exclude unspecific cells with larger SSC: As shown in plot 9 the region R6 is adjusted on DC1 and DC2. Additionally in plot 3 the location of basophils and DCs are colored in contrast to the background.

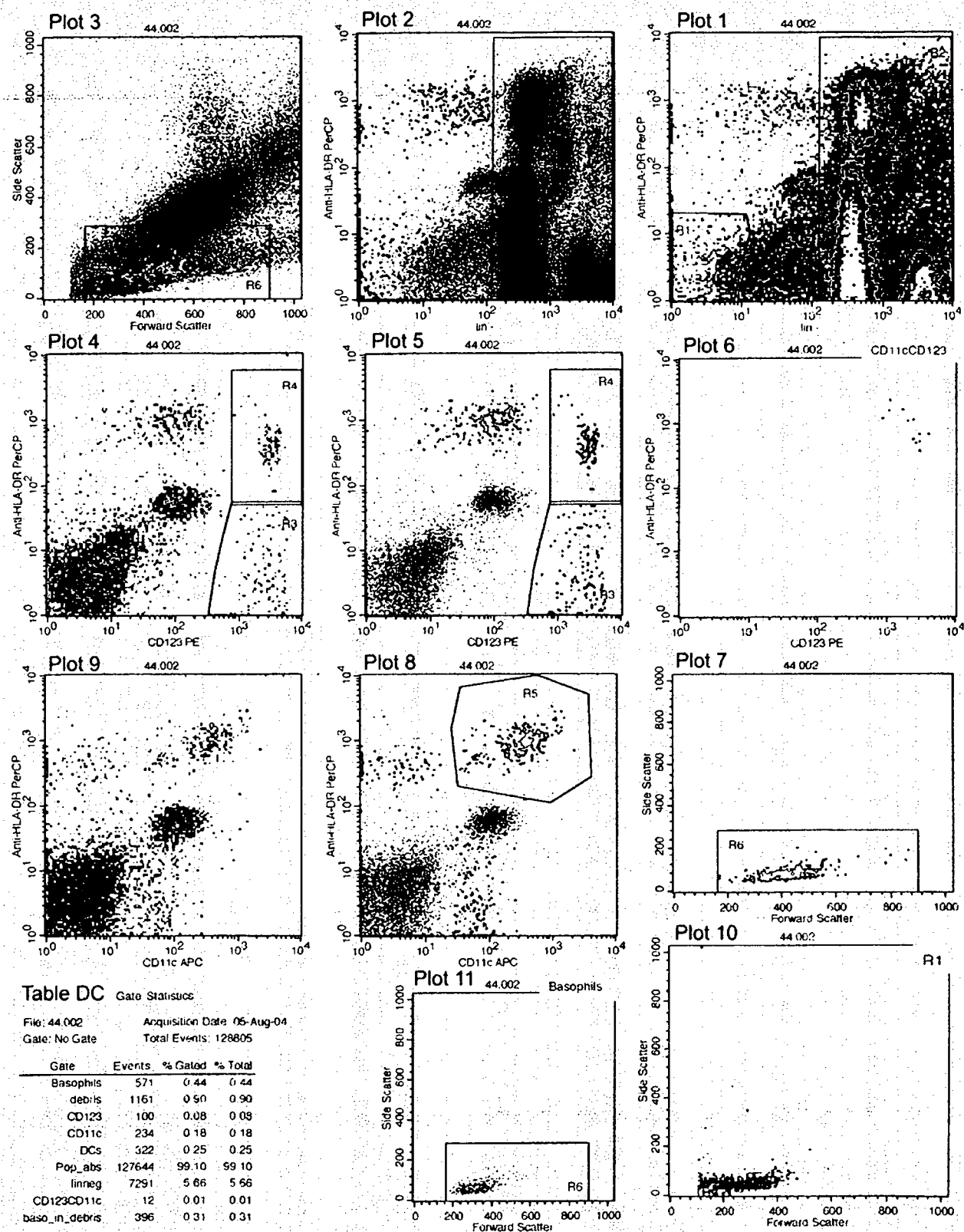


Figure Appendix G-1: Spreadsheet graphics output of dendritic cell analyses.

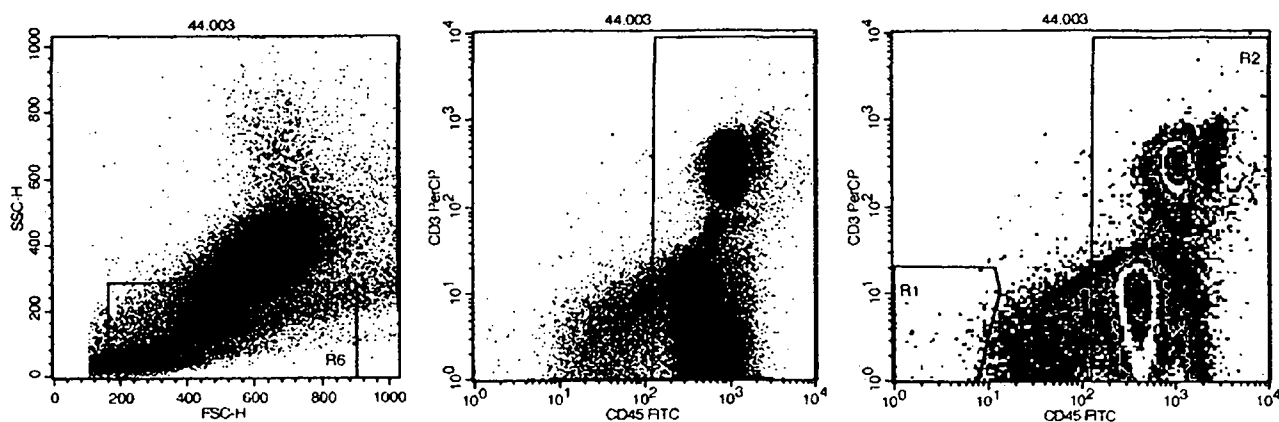


Figure Appendix G-2: Discrimination of debris in panel 3 (CD3 versus CD45)

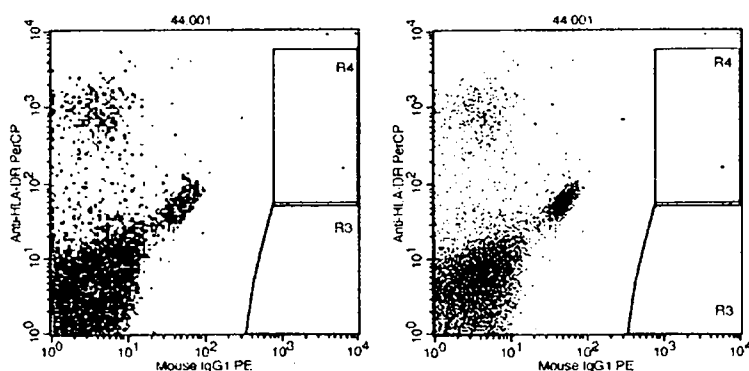


Figure Appendix G-3: Density and dot plot of negative control discriminating the gate of CD11c.

Spreadsheet Output

Based on the combination of the composed regions, the gate list shown in Table Appendix G- 1 includes the description of label names, gate definitions, highlighted populations and the colors of the cells.

The Gate Statistics Table (Table DC), included in Figure Appendix G- 1, shows the data as is exported into an ASCII file.

Cell Quest Pro™ is not able to rearrange the matrix to receive a sorted output with one character in one column. Therefore the output file is imported and converted by SAS Enterprise Guide 2.0 as described in chapter 3 issue 7.7.5.










	Multi	Hi lite	color	Color	Label	Definition
◆	<input type="checkbox"/>	<input checked="" type="checkbox"/>			debris	R1
◆	<input checked="" type="checkbox"/>	<input checked="" type="checkbox"/>			CD123	-R2*r4*r6
◆	<input checked="" type="checkbox"/>	<input checked="" type="checkbox"/>			CD11c	-R2*r5*r6
◆	<input checked="" type="checkbox"/>	<input checked="" type="checkbox"/>			Basophils	-R2*R3*r6
◆	<input type="checkbox"/>	<input type="checkbox"/>			DCs	-R2*-r1*(r4 or R5)*r6
◆	<input type="checkbox"/>	<input type="checkbox"/>			Pop_abs	-R1
◆	<input type="checkbox"/>	<input type="checkbox"/>			linneg	-r2*-r1
◆	<input type="checkbox"/>	<input type="checkbox"/>			CD123CD11c	-R2*-r1*(r4*R5)*r6
◆	<input type="checkbox"/>	<input type="checkbox"/>			baso_in_debris	r1*r3*-r2

Table Appendix G-1: Gate List of Dendritic Cell Analyses

Appendix H

4-Color-Leukocyte Differentiation Analysis

In Figure Appendix H- 1, 7 plots describe the set of attractors for the discrimination of leukocytes, and further subpopulations. The Hierarchy Legend at the top of Figure Appendix H- 1 describes the composition of all attractors used for the analysis.

The following protocol is used:

- Load the negative control data file.
- Discriminate the leukocytes as top-level population. As shown in Figure Appendix H- 2 plot 2 the blue attractor encloses the target cell population. The position of the attractor is dissociated from their data centre of mass by a vector to exclude debris with higher FL1-fluorescence.
- Discriminate monocytes: A subattractor within the leukocyte attractor discriminates the red colored monocytes. The attractor is set automatically on the centre of the population as shown in Figure Appendix H- 2 plot 2.
- Discriminate CD3 positive lymphocytes: Within the blue colored CD45 population a grey attractor is created on low isotype in FL4 as shown in Figure Appendix H- 2 plot 5
- Define cytotoxic cells attractor: In Figure Appendix H- 2 plot 5 a light blue fixed attractor is created on the CD3+IgG-APC+ cells in the right upper sector of the plot.
- Define NK attractor: Also in Figure Appendix H- 2 plot 5 a dark brown fixed attractor is set on the IgG-APC+ cells in the left upper sector of the plot. The attractor cuts off CD56 positive cells from the background.

- In Figure Appendix H- 1 plot 1 NK cells, cytotoxic cells and CD3+ lymphocytes with higher SSC are also excluded by further subattractors: On the grey CD3+ attractor a new fixed green subattractor is created, on dark brown NK attractor a new light brown subattractor and on light blue cytotoxic attractor a new pink subattractor. The advantage of separately set subattractors is that excluded cells by the latter subattractors keep their color and are shown in Figure Appendix H- 1 plot 1 for quality control.
- Choose 'Classify Data' from the attractors menu to export data to the spreadsheet file automatically. Unload negative control data file.
- Load sample file. The latter settings are kept for the sample file analyses automatically.
- Choose Classify Data from the Attractors menu: Cells are automatically classified to several attractors constituted with the negative control. In Figure Appendix H- 2 plot 4 and plot 5 the determination of NK, cytotoxic and CD3+ T cells of a sample is shown. Data export to spreadsheet data file is done automatically by classifying.

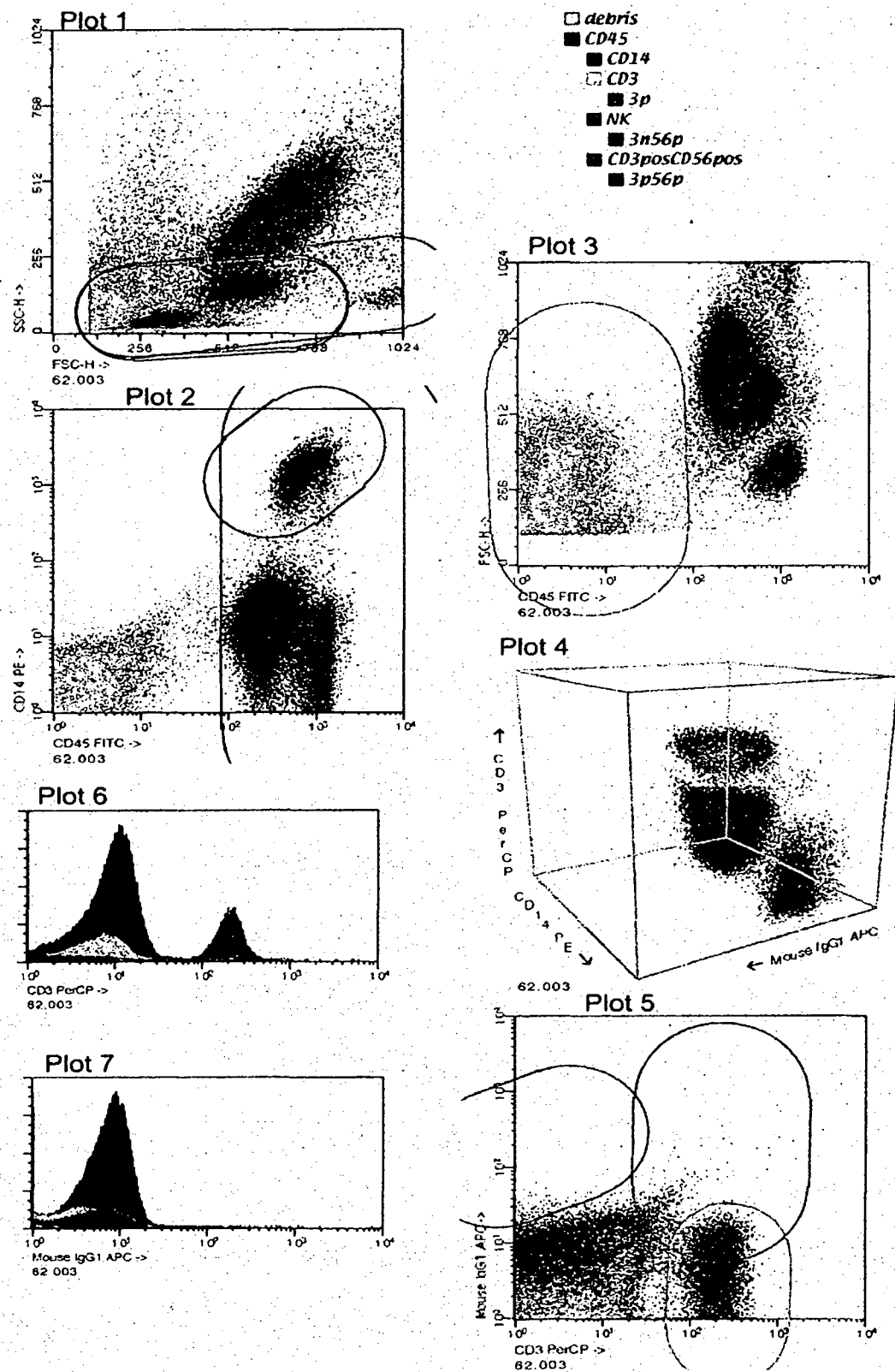


Figure Appendix H-1: Spreadsheet graphics output of a sample of the leukocyte differentiation analysis.

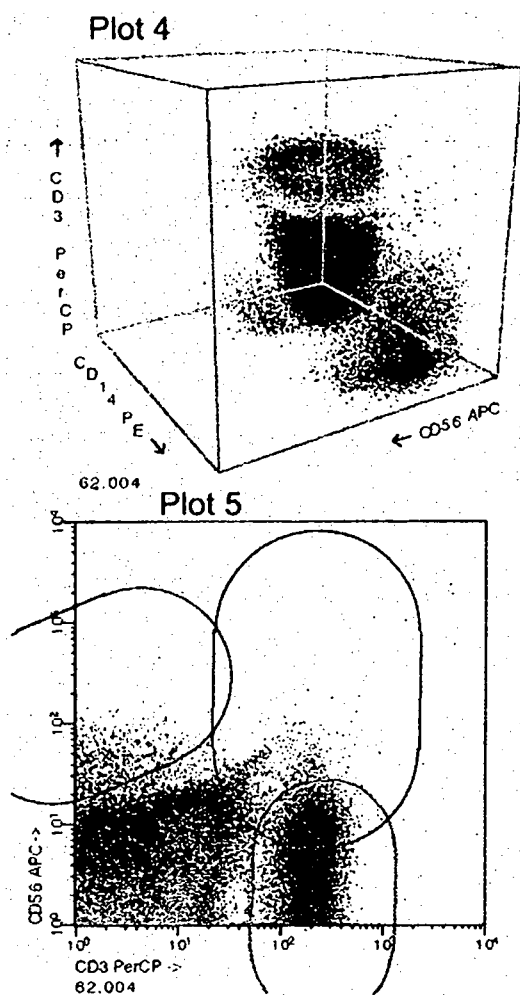


Figure Appendix H-2: Part of the spreadsheet output of a negative control of the leukocyte differentiation analysis..

Appendix I

T Cell Differentiation Analyses

Plots Characteristics

Characteristics are the same as described in 1.4.2.2.

4-Color-Analyses Protocol

In Figure Appendix I- 1, 5 plots describe the set of attractors for the discrimination of T cells (CD3+), and further subpopulations. The Hierarchy Legend at the bottom of Figure O.3 describes the composition of all attractors used for the analysis. The following protocol is used:

- Load sample data file.
- Discriminate the CD3 positive T cells as top-level population. As shown in Figure Appendix I- 3 plot 2 the red attractor encloses the target cell population. The position of the attractor is dissociated from their data centre of mass by a vector to exclude cells with higher SSC.
- Discriminate CD3+CD4+, CD3+CD8+ and CD3+CD4+CD8+ T cells:
Choose 'Classify Data' from the Attractors menu to export data to the spreadsheet file. As shown in Figure Appendix I- 3 in plot 3 the orange fixed attractor encloses the CD4 positive cells and the green fixed attractor encloses the CD8 positive cells. The blue attractor, the latter in the hierarchy, can overlap the 2 previous described attractors in plot 3.
- Choose 'Classify Data' from the Attractors menu to export data to the spreadsheet file. In Figure Appendix I- 3 plot 4 all four characterized populations are shown in a cube for quality control.

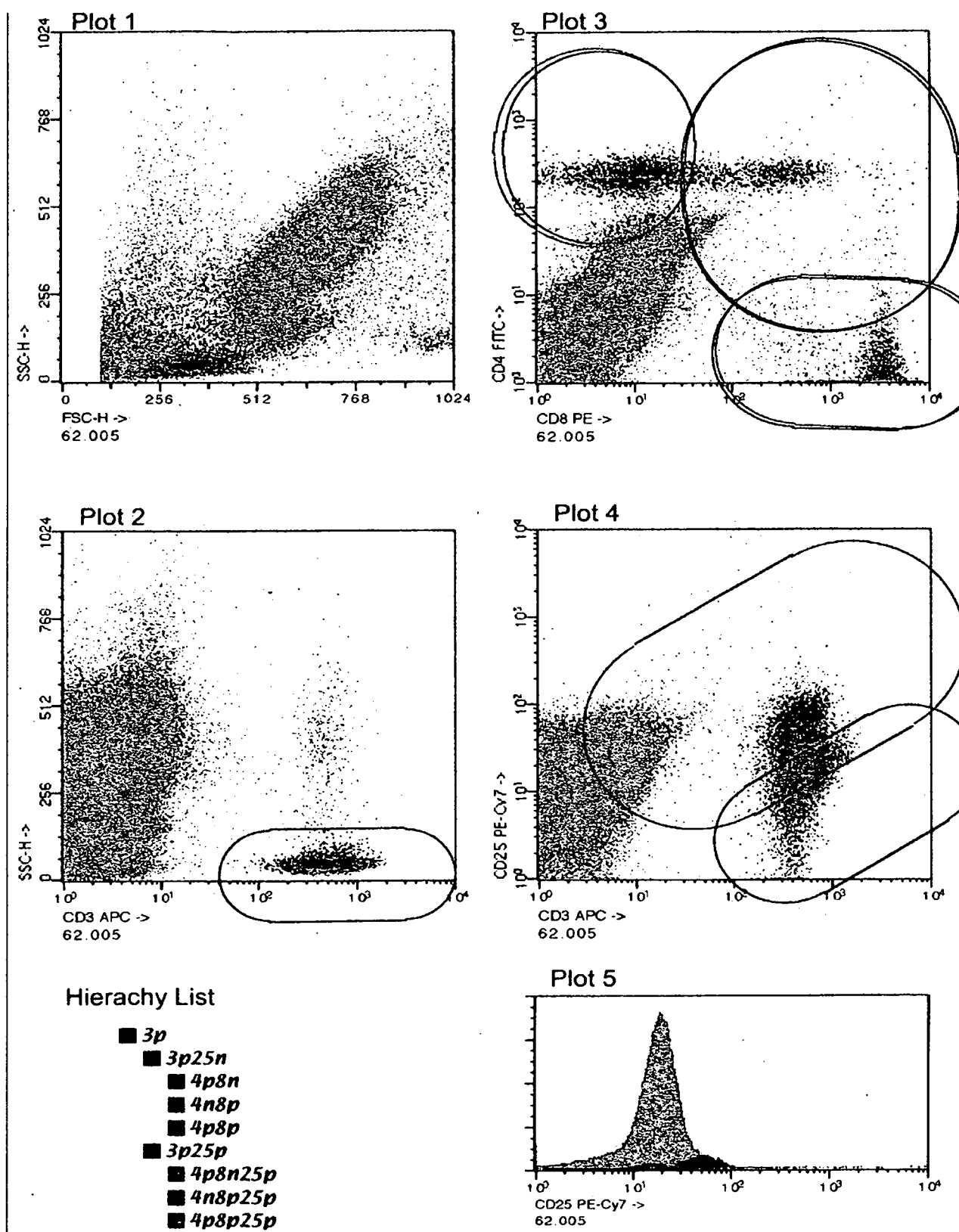


Figure Appendix I-8-1: Spreadsheet graphics of a sample analyzing CD4+ and CD8+ T cells.

Spreadsheet Output

Based on composed attractors' hierarchy, the cell population sizes, percent of top-level population and fluorescence statistics (Mean, SD, CV) are written in an output file. The benefit of the file output is that each character in the printable matrix are automatically rearranged and set in one column in the stored data file.

Based on composed attractors' hierarchy, the cell population sizes, percent of top-level population and fluorescence statistics (Mean, SD, CV) are written in a output file. The benefit of the file output is that each character in the printable matrix (see Table Appendix I- 1) are automatically rearranged and set in one column in the stored data file. The gate statistics table 1, included in Table Appendix I- 1, shows the matrix of the Spreadsheet output an ASCII file. The stored data file is ready to be read into a SAS file.

```

* * * * *
Method      : bcpanel5_3.0
File        : 32.005
Sample ID   : 32
Acquired    : 26-Jul-04
* * * * *

Cluster Membership      3p      7940
% of Total Classified   100,00
Parameter              Mean      SD      CV
FSC-H (Lin)[]          376,73    60,10   15,95
SSC-H (Lin)[]          63,74    18,03   28,28
CD4 FITC (Log)[]       85,19    132,78  155,85
CD8 PE (Log)[]         2455,47  2074,89  84,50
CD3 APC (Log)[]        292,11    140,95  48,25

Cluster Membership      4p8n    1874
% of 3p[]              23,60
Parameter              Mean      SD      CV
FSC-H (Lin)[]          373,66    68,09   18,22
SSC-H (Lin)[]          54,31    18,08   33,29
CD4 FITC (Log)[]       274,02    68,61   25,04
CD8 PE (Log)[]          8,57     5,75    67,11
CD3 APC (Log)[]        250,19    93,85   37,51

Cluster Membership      4p8p    534
% of 3p[]              6,73
Parameter              Mean      SD      CV
FSC-H (Lin)[]          394,38    98,38   24,95
SSC-H (Lin)[]          69,50    25,81   37,14
CD4 FITC (Log)[]       284,89    93,65   32,87
CD8 PE (Log)[]         373,96    545,92  145,98
CD3 APC (Log)[]        257,63    86,35   33,52

Cluster Membership      4n8p    5136
% of 3p[]              64,69
Parameter              Mean      SD      CV
FSC-H (Lin)[]          376,41    51,54   13,69
SSC-H (Lin)[]          66,29    15,97   24,09
CD4 FITC (Log)[]       1,54     1,73    112,43
CD8 PE (Log)[]         3753,02  1358,45  36,20
CD3 APC (Log)[]        289,47    125,21  43,26

```

Table Appendix I-1: Spreadsheet data file output of a sample analyzing CD4+ and CD8+ T cells.

References

1. Thomas, E., *A history of bone marrow transplantation*, in *Hematopoietic Cell Transplantation*, K.F. Blume, S.J. Appelbaum, F.R., Editor. 2004, Blackwell Publishing Oxford, Malden, Victoria. p. 4-8.
2. Ho, A.Y., et al., *Reduced-intensity allogeneic hematopoietic stem cell transplantation for myelodysplastic syndrome and acute myeloid leukemia with multilineage dysplasia using fludarabine, busulphan, and alemtuzumab (FBC) conditioning*. *Blood*, 2004. **104**(6): p. 1616-23.
3. Vela-Ojeda, J., et al., *Allogeneic peripheral blood stem cell transplantation using reduced intensity versus myeloablative conditioning regimens for the treatment of leukemia*. *Stem Cells Dev*, 2004. **13**(5): p. 571-9.
4. Valcarcel, D., et al., *Conventional versus reduced-intensity conditioning regimen for allogeneic stem cell transplantation in patients with hematological malignancies*. *Eur J Haematol*, 2005. **74**(2): p. 144-51.
5. Billingham, R.E., *The biology of graft-versus-host reactions*. Harvey Lect, 1966. **62**: p. 21-78.
6. Thomas, E., et al., *Bone-marrow transplantation (first of two parts)*. *N Engl J Med*, 1975. **292**(16): p. 832-43.
7. Nakamura, K., et al., *IL-4-producing CD8(+) T cells may be an immunological hallmark of chronic GVHD*. *Bone Marrow Transplant*, 2005. **36**(7): p. 639-47.
8. Borel, J.F., et al., *Biological effects of cyclosporin A: a new antilymphocytic agent*. *Agents Actions*, 1976. **6**(4): p. 468-75.
9. Borel, J.F., et al., *Effects of the new anti-lymphocytic peptide cyclosporin A in animals*. *Immunology*, 1977. **32**(6): p. 1017-25.
10. Liu, J., et al., *Calcineurin is a common target of cyclophilin-cyclosporin A and FKBP-FK506 complexes*. *Cell*, 1991. **66**(4): p. 807-15.
11. Shi, Y.F., B.M. Sahai, and D.R. Green, *Cyclosporin A inhibits activation-induced cell death in T-cell hybridomas and thymocytes*. *Nature*, 1989. **339**(6226): p. 625-6.
12. Nikolic, B., et al., *A novel application of cyclosporine A in nonmyeloablative pretransplant host conditioning for allogeneic BMT*. *Blood*, 2000. **96**(3): p. 1166-72.
13. Tajima, K., et al., *Immunomodulatory effects of cyclosporin A on human peripheral blood dendritic cell subsets*. *Immunology*, 2003. **108**(3): p. 321-8.
14. Evans, R.M., *The steroid and thyroid hormone receptor superfamily*. *Science*, 1988. **240**(4854): p. 889-95.
15. Piemonti, L., et al., *Glucocorticoids affect human dendritic cell differentiation and maturation*. *J Immunol*, 1999. **162**(11): p. 6473-81.

References

16. Bamberger, C.M., H.M. Schulte, and G.P. Chrousos, *Molecular determinants of glucocorticoid receptor function and tissue sensitivity to glucocorticoids*. *Endocr Rev*, 1996. **17**(3): p. 245-61.
17. Pratt, W.B. and D.O. Toft, *Steroid receptor interactions with heat shock protein and immunophilin chaperones*. *Endocr Rev*, 1997. **18**(3): p. 306-60.
18. Yang-Yen, H.F., et al., *Transcriptional interference between c-Jun and the glucocorticoid receptor: mutual inhibition of DNA binding due to direct protein-protein interaction*. *Cell*, 1990. **62**(6): p. 1205-15.
19. Ray, A. and K.E. Prefontaine, *Physical association and functional antagonism between the p65 subunit of transcription factor NF-kappa B and the glucocorticoid receptor*. *Proc Natl Acad Sci U S A*, 1994. **91**(2): p. 752-6.
20. Heck, S., et al., *I kappaB alpha-independent downregulation of NF-kappaB activity by glucocorticoid receptor*. *Embo J*, 1997. **16**(15): p. 4698-707.
21. Kino, T., et al., *FK-506, a novel immunosuppressant isolated from a Streptomyces. I. Fermentation, isolation, and physico-chemical and biological characteristics*. *J Antibiot (Tokyo)*, 1987. **40**(9): p. 1249-55.
22. Shibasaki, F., et al., *Role of kinases and the phosphatase calcineurin in the nuclear shuttling of transcription factor NF-AT4*. *Nature*, 1996. **382**(6589): p. 370-3.
23. Woltman, A.M., et al., *Rapamycin induces apoptosis in monocyte- and CD34-derived dendritic cells but not in monocytes and macrophages*. *Blood*, 2001. **98**(1): p. 174-80.
24. Monti, P., et al., *Rapamycin impairs antigen uptake of human dendritic cells*. *Transplantation*, 2003. **75**(1): p. 137-45.
25. Hackstein, H., et al., *Rapamycin inhibits macropinocytosis and mannose receptor-mediated endocytosis by bone marrow-derived dendritic cells*. *Blood*, 2002. **100**(3): p. 1084-7.
26. Allison, A.C., et al., *In vitro immunosuppressive effects of mycophenolic acid and an ester pro-drug, RS-61443*. *Transplant Proc*, 1991. **23**(2 Suppl 2): p. 10-4.
27. Allison, A.C. and E.M. Eugui, *Purine metabolism and immunosuppressive effects of mycophenolate mofetil (MMF)*. *Clin Transplant*, 1996. **10**(1 Pt 2): p. 77-84.
28. Basara, N., et al., *Mycophenolate mofetil for the treatment of acute and chronic GVHD in bone marrow transplant patients*. *Bone Marrow Transplant*, 1998. **22**(1): p. 61-5.
29. Bornhauser, M., et al., *Dose-reduced conditioning for allogeneic blood stem cell transplantation: durable engraftment without antithymocyte globulin*. *Bone Marrow Transplant*, 2000. **26**(2): p. 119-25.
30. Edelson, R., et al., *Treatment of cutaneous T-cell lymphoma by extracorporeal photochemotherapy. Preliminary results*. *N Engl J Med*, 1987. **316**(6): p. 297-303.
31. Suchin, K.R., et al., *Extracorporeal photochemotherapy does not suppress T- or B-cell responses to novel or recall antigens*. *J Am Acad Dermatol*, 1999. **41**(6): p. 980-6.
32. Musajo, L., et al., *Photosensitizing Furocoumarins: Interaction With Dna And Photo-Inactivation Of Dna Containing Viruses*. *Experientia*, 1965. **21**: p. 22-4.
33. Song, P.S. and K.J. Tapley, Jr., *Photochemistry and photobiology of psoralens*. *Photochem Photobiol*, 1979. **29**(6): p. 1177-97.

34. Gasparro, F.P., A. Felli, and I.M. Schmitt, *Psoralen photobiology: the relationship between DNA damage, chromatin structure, transcription, and immunogenic effects*. Recent Results Cancer Res, 1997. **143**: p. 101-27.
35. Gasparro, F.P., et al., *Molecular aspects of extracorporeal photochemotherapy*. Yale J Biol Med, 1989. **62**(6): p. 579-93.
36. Joshi, P.C. and M.A. Pathak, *Photophysical and photobiological properties of 3-carbethoxypsoralen*. Indian J Biochem Biophys, 1995. **32**(2): p. 63-73.
37. Bevilacqua, R., et al., *Drug protein interaction: displacement of albumin bound 8-methoxypsoralen by drugs*. Farmaco [Sci], 1981. **36**(7): p. 598-605.
38. Yoo, E.K., et al., *Apoptosis induction of ultraviolet light A and photochemotherapy in cutaneous T-cell Lymphoma: relevance to mechanism of therapeutic action*. J Invest Dermatol, 1996. **107**(2): p. 235-42.
39. Berger, C.L., et al., *Transimmunization, a novel approach for tumor immunotherapy*. Transfus Apheresis Sci, 2002. **26**(3): p. 205-16.
40. Marks, D.I. and R.M. Fox, *Mechanisms of photochemotherapy-induced apoptotic cell death in lymphoid cells*. Biochem Cell Biol, 1991. **69**(10-11): p. 754-60.
41. Enomoto, D.N., et al., *Extracorporeal photochemotherapy (photopheresis) induces apoptosis in lymphocytes: a possible mechanism of action of PUVA therapy*. Photochem Photobiol, 1997. **65**(1): p. 177-80.
42. Tambur, A.R., et al., *Extracorporeal photopheresis induces lymphocyte but not monocyte apoptosis*. Transplant Proc, 2000. **32**(4): p. 747-8.
43. Lamioni, A., et al., *The immunological effects of extracorporeal photopheresis unraveled: induction of tolerogenic dendritic cells in vitro and regulatory T cells in vivo*. Transplantation, 2005. **79**(7): p. 846-50.
44. Andersson, U., et al., *Simultaneous production of interleukin 2, interleukin 4 and interferon-gamma by activated human blood lymphocytes*. Eur J Immunol, 1990. **20**(7): p. 1591-6.
45. Sander, B., et al., *Differential regulation of lymphokine production in mitogen-stimulated murine spleen cells*. Eur J Immunol, 1991. **21**(8): p. 1887-92.
46. Jung, T., et al., *Detection of intracellular cytokines by flow cytometry*. J Immunol Methods, 1993. **159**(1-2): p. 197-207.
47. Misumi, Y., et al., *Novel blockade by brefeldin A of intracellular transport of secretory proteins in cultured rat hepatocytes*. J Biol Chem, 1986. **261**(24): p. 11398-403.
48. Truneh, A., et al., *Early steps of lymphocyte activation bypassed by synergy between calcium ionophores and phorbol ester*. Nature, 1985. **313**(6000): p. 318-20.
49. Weiss, A. and D.R. Littman, *Signal transduction by lymphocyte antigen receptors*. Cell, 1994. **76**(2): p. 263-74.
50. Monroe, J.G. and J.C. Cambier, *B cell activation. I. Anti-immunoglobulin-induced receptor cross-linking results in a decrease in the plasma membrane potential of murine B lymphocytes*. J Exp Med, 1983. **157**(6): p. 2073-86.
51. Craston, R., et al., *Temporal dynamics of CD69 expression on lymphoid cells*. J Immunol Methods, 1997. **209**(1): p. 37-45.
52. Jacob, M.C., et al., *CD45RA expression by CD4 T lymphocytes in tumors invaded by B-cell non-Hodgkin's lymphoma (NHL) or Hodgkin's disease (HD)*. Am J Hematol, 1992. **39**(1): p. 45-51.

References

53. Devaux, P.F., *Static and dynamic lipid asymmetry in cell membranes*. Biochemistry, 1991. **30**(5): p. 1163-73.
54. Williamson, P. and R.A. Schlegel, *Back and forth: the regulation and function of transbilayer phospholipid movement in eukaryotic cells*. Mol Membr Biol, 1994. **11**(4): p. 199-216.
55. Verhoven, B., R.A. Schlegel, and P. Williamson, *Mechanisms of phosphatidylserine exposure, a phagocyte recognition signal, on apoptotic T lymphocytes*. J Exp Med, 1995. **182**(5): p. 1597-601.
56. Frasch, S.C., et al., *Regulation of phospholipid scramblase activity during apoptosis and cell activation by protein kinase Cdelta*. J Biol Chem, 2000. **275**(30): p. 23065-73.
57. Vermes, I., et al., *A novel assay for apoptosis. Flow cytometric detection of phosphatidylserine expression on early apoptotic cells using fluorescein labelled Annexin V*. J Immunol Methods, 1995. **184**(1): p. 39-51.
58. Andree, H.A., et al., *Binding of vascular anticoagulant alpha (VAC alpha) to planar phospholipid bilayers*. J Biol Chem, 1990. **265**(9): p. 4923-8.
59. Gill, J.E., et al., *7-Amino-actinomycin D as a cytochemical probe. I. Spectral properties*. J Histochem Cytochem, 1975. **23**(11): p. 793-9.
60. Zelenin, A.V., et al., *7-Amino-actinomycin D as a specific fluorophore for DNA content analysis by laser flow cytometry*. Cytometry, 1984. **5**(4): p. 348-54.
61. Schmid, I., et al., *Dead cell discrimination with 7-amino-actinomycin D in combination with dual color immunofluorescence in single laser flow cytometry*. Cytometry, 1992. **13**(2): p. 204-8.
62. Lecoecur, H., et al., *Strategies for phenotyping apoptotic peripheral human lymphocytes comparing ISNT, annexin-V and 7-AAD cytofluorometric staining methods*. J Immunol Methods, 1997. **209**(2): p. 111-23.
63. Ferrara, J.L., *The cytokine modulation of acute graft-versus-host disease*. Bone Marrow Transplant, 1998. **21 Suppl 3**: p. S13-5.
64. Krenger, W., et al., *Interferon-gamma suppresses T-cell proliferation to mitogen via the nitric oxide pathway during experimental acute graft-versus-host disease*. Blood, 1996. **88**(3): p. 1113-21.
65. Mosmann, T.R., et al., *Two types of murine helper T cell clone. I. Definition according to profiles of lymphokine activities and secreted proteins*. J Immunol, 1986. **136**(7): p. 2348-57.
66. Seder, R.A. and G.G. Le Gros, *The functional role of CD8+ T helper type 2 cells*. J Exp Med, 1995. **181**(1): p. 5-7.
67. Ferrara, J.L. and H.J. Deeg, *Graft-versus-host disease*. N Engl J Med, 1991. **324**(10): p. 667-74.
68. Nestel, F.P., et al., *Macrophage priming and lipopolysaccharide-triggered release of tumor necrosis factor alpha during graft-versus-host disease*. J Exp Med, 1992. **175**(2): p. 405-13.
69. Tanaka, J., et al., *The important balance between cytokines derived from type 1 and type 2 helper T cells in the control of graft-versus-host disease*. Bone Marrow Transplant, 1997. **19**(6): p. 571-6.
70. Allen, R.D., T.A. Staley, and C.L. Sidman, *Differential cytokine expression in acute and chronic murine graft-versus-host-disease*. Eur J Immunol, 1993. **23**(2): p. 333-7.

References

71. Via, C.S. and F.D. Finkelman, *Critical role of interleukin-2 in the development of acute graft-versus-host disease*. Int Immunol, 1993. **5**(6): p. 565-72.
72. Krenger, W. and J.L. Ferrara, *Graft-versus-host disease and the Th1/Th2 paradigm*. Immunol Res, 1996. **15**(1): p. 50-73.
73. Ferrara, J.L. and W. Krenger, *Graft-versus-host disease: the influence of type 1 and type 2 T cell cytokines*. Transfus Med Rev, 1998. **12**(1): p. 1-17.
74. Heinzl, F.P., et al., *Reciprocal expression of interferon gamma or interleukin 4 during the resolution or progression of murine leishmaniasis. Evidence for expansion of distinct helper T cell subsets*. J Exp Med, 1989. **169**(1): p. 59-72.
75. Romagnani, P., et al., *Th1/Th2 cells, their associated molecules and role in pathophysiology*. Eur Cytokine Netw, 2000. **11**(3): p. 510-1.
76. Ono, S., H. Ohno, and T. Saito, *Rapid turnover of the CD3 zeta chain independent of the TCR-CD3 complex in normal T cells*. Immunity, 1995. **2**(6): p. 639-44.
77. Biassoni, R., et al., *CD3-negative lymphokine-activated cytotoxic cells express the CD3 epsilon gene*. J Immunol, 1988. **140**(5): p. 1685-9.
78. Reth, M., *Antigen receptor tail clue*. Nature, 1989. **338**(6214): p. 383-4.
79. Dietrich, J., et al., *CD3 gamma contains a phosphoserine-dependent di-leucine motif involved in down-regulation of the T cell receptor*. Embo J, 1994. **13**(9): p. 2156-66.
80. Robertson, M.J. and J. Ritz, *Biology and clinical relevance of human natural killer cells*. Blood, 1990. **76**(12): p. 2421-38.
81. Lanier, L.L., *Activating and inhibitory NK cell receptors*. Adv Exp Med Biol, 1998. **452**: p. 13-8.
82. Lopez-Botet, M. and T. Bellon, *Natural killer cell activation and inhibition by receptors for MHC class I*. Curr Opin Immunol, 1999. **11**(3): p. 301-7.
83. Moretta, A., et al., *Activating receptors and coreceptors involved in human natural killer cell-mediated cytotoxicity*. Annu Rev Immunol, 2001. **19**: p. 197-223.
84. Ruggeri, L., et al., *Role of natural killer cell alloreactivity in HLA-mismatched hematopoietic stem cell transplantation*. Blood, 1999. **94**(1): p. 333-9.
85. Ritz, J., et al., *Characterization of functional surface structures on human natural killer cells*. Adv Immunol, 1988. **42**: p. 181-211.
86. Cooper, M.A., T.A. Fehniger, and M.A. Caligiuri, *The biology of human natural killer-cell subsets*. Trends Immunol, 2001. **22**(11): p. 633-40.
87. Cooper, M.A., et al., *Human natural killer cells: a unique innate immunoregulatory role for the CD56(bright) subset*. Blood, 2001. **97**(10): p. 3146-51.
88. Perussia, B., et al., *Human natural killer cells analyzed by B73.1, a monoclonal antibody blocking Fc receptor functions. II. Studies of B73.1 antibody-antigen interaction on the lymphocyte membrane*. J Immunol, 1983. **130**(5): p. 2142-8.
89. Borrego, F., et al., *Structure and function of major histocompatibility complex (MHC) class I specific receptors expressed on human natural killer (NK) cells*. Mol Immunol, 2002. **38**(9): p. 637-60.
90. Farag, S.S., et al., *Natural killer cell receptors: new biology and insights into the graft-versus-leukemia effect*. Blood, 2002. **100**(6): p. 1935-47.
91. Vilches, C. and P. Parham, *KIR: diverse, rapidly evolving receptors of innate and adaptive immunity*. Annu Rev Immunol, 2002. **20**: p. 217-51.
92. Nagler, A., et al., *Comparative studies of human FcR3-positive and negative natural killer cells*. J Immunol, 1989. **143**(10): p. 3183-91.

93. Ulevitch, R.J. and P.S. Tobias, *Receptor-dependent mechanisms of cell stimulation by bacterial endotoxin*. Annu Rev Immunol, 1995. **13**: p. 437-57.
94. Smith, P.D., et al., *Isolation and purification of CD14-negative mucosal macrophages from normal human small intestine*. J Immunol Methods, 1997. **202**(1): p. 1-11.
95. Smith, P.D., et al., *Intestinal macrophages lack CD14 and CD89 and consequently are down-regulated for LPS- and IgA-mediated activities*. J Immunol, 2001. **167**(5): p. 2651-6.
96. Grimm, M.C., et al., *Evidence for a CD14+ population of monocytes in inflammatory bowel disease mucosa--implications for pathogenesis*. Clin Exp Immunol, 1995. **100**(2): p. 291-7.
97. Rogler, G., et al., *Isolation and phenotypic characterization of colonic macrophages*. Clin Exp Immunol, 1998. **112**(2): p. 205-15.
98. Dornblüth O, P.W., *Pschyrembel Klinisches Wörterbuch*. 260. ed. 2004, Berlin: de Gruyter.
99. Doyle, C. and J.L. Strominger, *Interaction between CD4 and class II MHC molecules mediates cell adhesion*. Nature, 1987. **330**(6145): p. 256-9.
100. Cammarota, G., et al., *Identification of a CD4 binding site on the beta 2 domain of HLA-DR molecules*. Nature, 1992. **356**(6372): p. 799-801.
101. König, R., L.Y. Huang, and R.N. Germain, *MHC class II interaction with CD4 mediated by a region analogous to the MHC class I binding site for CD8*. Nature, 1992. **356**(6372): p. 796-8.
102. Newell, M.K., et al., *Death of mature T cells by separate ligation of CD4 and the T-cell receptor for antigen*. Nature, 1990. **347**(6290): p. 286-9.
103. Mazerolles, F., C. Auffray, and A. Fischer, *Down regulation of T-cell adhesion by CD4*. Hum Immunol, 1991. **31**(1): p. 40-6.
104. Salter, R.D., et al., *A binding site for the T-cell co-receptor CD8 on the alpha 3 domain of HLA-A2*. Nature, 1990. **345**(6270): p. 41-6.
105. Veillette, A., et al., *Signal transduction through the CD4 receptor involves the activation of the internal membrane tyrosine-protein kinase p56lck*. Nature, 1989. **338**(6212): p. 257-9.
106. Ravichandran, K.S. and S.J. Burakoff, *Evidence for differential intracellular signaling via CD4 and CD8 molecules*. J Exp Med, 1994. **179**(2): p. 727-32.
107. Fung-Leung, W.P., et al., *CD8 is needed for development of cytotoxic T cells but not helper T cells*. Cell, 1991. **65**(3): p. 443-9.
108. Nakayama, K., et al., *Requirement for CD8 beta chain in positive selection of CD8-lineage T cells*. Science, 1994. **263**(5150): p. 1131-3.
109. Rissoan, M.C., et al., *Reciprocal control of T helper cell and dendritic cell differentiation*. Science, 1999. **283**(5405): p. 1183-6.
110. Kroemer, G., et al., *The biochemistry of programmed cell death*. Faseb J, 1995. **9**(13): p. 1277-87.
111. Majno, G. and I. Joris, *Apoptosis, oncosis, and necrosis. An overview of cell death*. Am J Pathol, 1995. **146**(1): p. 3-15.
112. Darzynkiewicz, Z., et al., *Cytometry in cell necrobiology: analysis of apoptosis and accidental cell death (necrosis)*. Cytometry, 1997. **27**(1): p. 1-20.
113. Ghadimi, M.P., et al., *Identification of interaction partners of the cytosolic polyproline region of CD95 ligand (CD178)*. FEBS Lett, 2002. **519**(1-3): p. 50-8.

114. Finkel, E., *The mitochondrion: is it central to apoptosis?* Science, 2001. **292**(5517): p. 624-6.
115. Villa, P., S.H. Kaufmann, and W.C. Earnshaw, *Caspases and caspase inhibitors*. Trends Biochem Sci, 1997. **22**(10): p. 388-93.
116. Nicholson, D.W., *Caspase structure, proteolytic substrates, and function during apoptotic cell death*. Cell Death Differ, 1999. **6**(11): p. 1028-42.
117. Gottlieb, R.A., et al., *Apoptosis induced in Jurkat cells by several agents is preceded by intracellular acidification*. Proc Natl Acad Sci U S A, 1996. **93**(2): p. 654-8.
118. Gottlieb, E., et al., *Mitochondrial membrane potential regulates matrix configuration and cytochrome c release during apoptosis*. Cell Death Differ, 2003. **10**(6): p. 709-17.
119. van Engeland, M., et al., *Annexin V-affinity assay: a review on an apoptosis detection system based on phosphatidylserine exposure*. Cytometry, 1998. **31**(1): p. 1-9.
120. Wiley, J.S., et al., *Partial agonists and antagonists reveal a second permeability state of human lymphocyte P2Z/P2X7 channel*. Am J Physiol, 1998. **275**(5 Pt 1): p. C1224-31.
121. Bortner, C.D., N.B. Oldenburg, and J.A. Cidlowski, *The role of DNA fragmentation in apoptosis*. Trends Cell Biol, 1995. **5**(1): p. 21-6.
122. Lincz, L.F., *Deciphering the apoptotic pathway: all roads lead to death*. Immunol Cell Biol, 1998. **76**(1): p. 1-19.
123. Banchereau, J., et al., *Immunobiology of dendritic cells*. Annu Rev Immunol, 2000. **18**: p. 767-811.
124. Lennon-Dumenil, A.M., et al., *A closer look at proteolysis and MHC-class-II-restricted antigen presentation*. Curr Opin Immunol, 2002. **14**(1): p. 15-21.
125. Gromme, M. and J. Neefjes, *Antigen degradation or presentation by MHC class I molecules via classical and non-classical pathways*. Mol Immunol, 2002. **39**(3-4): p. 181-202.
126. Delamarre, L., H. Holcombe, and I. Mellman, *Presentation of exogenous antigens on major histocompatibility complex (MHC) class I and MHC class II molecules is differentially regulated during dendritic cell maturation*. J Exp Med, 2003. **198**(1): p. 111-22.
127. Banchereau, J. and R.M. Steinman, *Dendritic cells and the control of immunity*. Nature, 1998. **392**(6673): p. 245-52.
128. Stuhler, G., et al., *Immune regulatory loops determine productive interactions within human T lymphocyte-dendritic cell clusters*. Proc Natl Acad Sci U S A, 1999. **96**(4): p. 1532-5.
129. Cella, M., et al., *Ligation of CD40 on dendritic cells triggers production of high levels of interleukin-12 and enhances T cell stimulatory capacity: T-T help via APC activation*. J Exp Med, 1996. **184**(2): p. 747-52.
130. Luft, T., et al., *IFN-alpha enhances CD40 ligand-mediated activation of immature monocyte-derived dendritic cells*. Int Immunol, 2002. **14**(4): p. 367-80.
131. Hart, D.N., *Dendritic cells: unique leukocyte populations which control the primary immune response*. Blood, 1997. **90**(9): p. 3245-87.
132. Cella, M., F. Sallusto, and A. Lanzavecchia, *Origin, maturation and antigen presenting function of dendritic cells*. Curr Opin Immunol, 1997. **9**(1): p. 10-6.

133. Sallusto, F., et al., *Dendritic cells use macropinocytosis and the mannose receptor to concentrate macromolecules in the major histocompatibility complex class II compartment: downregulation by cytokines and bacterial products*. J Exp Med, 1995. **182**(2): p. 389-400.
134. Lutz, M.B., et al., *An advanced culture method for generating large quantities of highly pure dendritic cells from mouse bone marrow*. J Immunol Methods, 1999. **223**(1): p. 77-92.
135. Schwartz, R.H., *Models of T cell anergy: is there a common molecular mechanism?* J Exp Med, 1996. **184**(1): p. 1-8.
136. Adorini, L., *Intervention in autoimmunity: the potential of vitamin D receptor agonists*. Cell Immunol, 2005. **233**(2): p. 115-24.
137. Xia, C.Q., et al., *Dexamethasone induces IL-10-producing monocyte-derived dendritic cells with durable immaturity*. Scand J Immunol, 2005. **62**(1): p. 45-54.
138. Randolph, G.J., et al., *Differentiation of phagocytic monocytes into lymph node dendritic cells in vivo*. Immunity, 1999. **11**(6): p. 753-61.
139. Vuckovic, S., et al., *Generation of CMRF-44+ monocyte-derived dendritic cells: insights into phenotype and function*. Exp Hematol, 1998. **26**(13): p. 1255-64.
140. Crawford, K., et al., *Circulating CD2+ monocytes are dendritic cells*. J Immunol, 1999. **163**(11): p. 5920-8.
141. Feldman, S.B., et al., *Viral induction of low frequency interferon-alpha producing cells*. Virology, 1994. **204**(1): p. 1-7.
142. Cella, M., et al., *Plasmacytoid monocytes migrate to inflamed lymph nodes and produce large amounts of type I interferon*. Nat Med, 1999. **5**(8): p. 919-23.
143. Seddik, M., T.A. Seemayer, and W.S. Lapp, *T cell functional defect associated with thymid epithelial cell injury induced by a graft-versus-host reaction*. Transplantation, 1980. **29**(1): p. 61-6.
144. Atkinson, K., et al., *Low serum thymic hormone levels in patients with chronic graft-versus-host disease*. Blood, 1982. **59**(5): p. 1073-7.
145. Weinberg, K., et al., *Factors affecting thymic function after allogeneic hematopoietic stem cell transplantation*. Blood, 2001. **97**(5): p. 1458-66.
146. Cohen, J.J., et al., *Apoptosis and programmed cell death in immunity*. Annu Rev Immunol, 1992. **10**: p. 267-93.
147. Fadok, V.A., et al., *The role of phosphatidylserine in recognition of apoptotic cells by phagocytes*. Cell Death Differ, 1998. **5**(7): p. 551-62.
148. Fadok, V.A., et al., *Macrophages that have ingested apoptotic cells in vitro inhibit proinflammatory cytokine production through autocrine/paracrine mechanisms involving TGF-beta, PGE2, and PAF*. J Clin Invest, 1998. **101**(4): p. 890-8.
149. McDonald, P.P., et al., *Transcriptional and translational regulation of inflammatory mediator production by endogenous TGF-beta in macrophages that have ingested apoptotic cells*. J Immunol, 1999. **163**(11): p. 6164-72.
150. Aramaki, Y., et al., *Negatively charged liposomes inhibit tyrosine phosphorylation of 41-kDa protein in murine macrophages stimulated with LPS*. Biochem Biophys Res Commun, 1997. **231**(3): p. 827-30.
151. Chang, M.K., et al., *Monoclonal antibodies against oxidized low-density lipoprotein bind to apoptotic cells and inhibit their phagocytosis by elicited macrophages: evidence that oxidation-specific epitopes mediate macrophage recognition*. Proc Natl Acad Sci U S A, 1999. **96**(11): p. 6353-8.

References

152. Albert, M.L., J.I. Kim, and R.B. Birge, *alphavbeta5 integrin recruits the CrkII-Dock180-rac1 complex for phagocytosis of apoptotic cells*. Nat Cell Biol, 2000. **2**(12): p. 899-905.
153. Fadok, V.A., et al., *Exposure of phosphatidylserine on the surface of apoptotic lymphocytes triggers specific recognition and removal by macrophages*. J Immunol, 1992. **148**(7): p. 2207-16.
154. Pradhan, D., et al., *Multiple systems for recognition of apoptotic lymphocytes by macrophages*. Mol Biol Cell, 1997. **8**(5): p. 767-78.
155. Fadok, V.A., et al., *CD36 is required for phagocytosis of apoptotic cells by human macrophages that use either a phosphatidylserine receptor or the vitronectin receptor (alpha v beta 3)*. J Immunol, 1998. **161**(11): p. 6250-7.
156. Fadok, V.A., et al., *A receptor for phosphatidylserine-specific clearance of apoptotic cells*. Nature, 2000. **405**(6782): p. 85-90.
157. Fadok, V.A., D.L. Bratton, and P.M. Henson, *Phagocyte receptors for apoptotic cells: recognition, uptake, and consequences*. J Clin Invest, 2001. **108**(7): p. 957-62.
158. Aringer, M., et al., *Photopheresis treatment enhances CD95 (fas) expression in circulating lymphocytes of patients with systemic sclerosis and induces apoptosis*. Br J Rheumatol, 1997. **36**(12): p. 1276-82.
159. Di Renzo, M., et al., *ECP-treated lymphocytes of chronic graft-versus-host disease patients undergo apoptosis which involves both the Fas/FasL system and the Bcl-2 protein family*. Arch Dermatol Res, 2003. **295**(5): p. 175-82.
160. Bladon, J. and P.C. Taylor, *Treatment of cutaneous T cell lymphoma with extracorporeal photopheresis induces Fas-ligand expression on treated T cells, but does not suppress the expression of co-stimulatory molecules on monocytes*. J Photochem Photobiol B, 2003. **69**(2): p. 129-38.
161. Canton, M., et al., *PUVA-induced apoptosis involves mitochondrial dysfunction caused by the opening of the permeability transition pore*. FEBS Lett, 2002. **522**(1-3): p. 168-72.
162. Vedaldi, D., et al., *Photochemical, photophysical and photobiological properties of some methylallopсоралens which are potential agents for photochemotherapy*. Biochim Biophys Acta, 1987. **925**(2): p. 101-8.
163. Chipuk, J.E., et al., *PUMA couples the nuclear and cytoplasmic proapoptotic function of p53*. Science, 2005. **309**(5741): p. 1732-5.
164. Gasparro, F.P., C.L. Berger, and R.L. Edelson, *Effect of monochromatic UVA light and 8-methoxypsoralen on human lymphocyte response to mitogen*. Photodermatol, 1984. **1**(1): p. 10-7.
165. Di Renzo, M., et al., *Extracorporeal photochemotherapy restores Th1/Th2 imbalance in patients with early stage cutaneous T-cell lymphoma*. Immunology, 1997. **92**(1): p. 99-103.
166. Tokura, Y., et al., *Treatment of T lymphocytes with 8-methoxypsoralen plus ultraviolet A induces transient but biologically active Th1-skewing cytokine production*. J Invest Dermatol, 1999. **113**(2): p. 202-8.
167. Klosner, G., et al., *Treatment of peripheral blood mononuclear cells with 8-methoxypsoralen plus ultraviolet A radiation induces a shift in cytokine expression from a Th1 to a Th2 response*. J Invest Dermatol, 2001. **116**(3): p. 459-62.

References

168. Rubegni, P., et al., *Role of extracorporeal photochemotherapy in patients with refractory chronic graft-versus-host disease*. Br J Haematol, 2005. **130**(2): p. 271-5.
169. Greinix, H.T., et al., *Successful use of extracorporeal photochemotherapy in the treatment of severe acute and chronic graft-versus-host disease*. Blood, 1998. **92**(9): p. 3098-104.
170. Ju, X.P., et al., *Cytokine expression during acute graft-versus-host disease after allogeneic peripheral stem cell transplantation*. Bone Marrow Transplant, 2005. **35**(12): p. 1179-86.
171. Fimiani, M., M. Di Renzo, and P. Rubegni, *Mechanism of action of extracorporeal photochemotherapy in chronic graft-versus-host disease*. Br J Dermatol, 2004. **150**(6): p. 1055-60.
172. Alcindor, T., et al., *Immunomodulatory effects of extracorporeal photochemotherapy in patients with extensive chronic graft-versus-host disease*. Blood, 2001. **98**(5): p. 1622-5.
173. Gorgun, G., K.B. Miller, and F.M. Foss, *Immunologic mechanisms of extracorporeal photochemotherapy in chronic graft-versus-host disease*. Blood, 2002. **100**(3): p. 941-7.
174. Shlomchik, W.D., et al., *Prevention of graft versus host disease by inactivation of host antigen-presenting cells*. Science, 1999. **285**(5426): p. 412-5.
175. Darvay, A., N. Salooja, and R. Russell-Jones, *The effect of extracorporeal photopheresis on intracellular cytokine expression in chronic cutaneous graft-versus-host disease*. J Eur Acad Dermatol Venereol, 2004. **18**(3): p. 279-84.
176. Zaucha, J.M., et al., *CD34 cell dose in granulocyte colony-stimulating factor-mobilized peripheral blood mononuclear cell grafts affects engraftment kinetics and development of extensive chronic graft-versus-host disease after human leukocyte antigen-identical sibling transplantation*. Blood, 2001. **98**(12): p. 3221-7.
177. Kim, D.H., et al., *Transplantation with higher dose of natural killer cells associated with better outcomes in terms of non-relapse mortality and infectious events after allogeneic peripheral blood stem cell transplantation from HLA-matched sibling donors*. Eur J Haematol, 2005. **75**(4): p. 299-308.
178. Yamasaki, S., et al., *Influence of transplanted dose of CD56+ cells on development of graft-versus-host disease in patients receiving G-CSF-mobilized peripheral blood progenitor cells from HLA-identical sibling donors*. Bone Marrow Transplant, 2003. **32**(5): p. 505-10.
179. Scholl, S., et al., *Impact of early NK cell recovery on development of GvHD and CMV reactivation in dose-reduced regimen prior to allogeneic PBSCT*. Bone Marrow Transplant, 2005. **35**(2): p. 183-90.
180. Tauchmanova, L., et al., *High serum leptin in patients with chronic graft-versus-host disease after hematopoietic stem cell transplantation*. Transplantation, 2004. **78**(9): p. 1376-83.
181. Szabo, G., C. Gavala, and P. Mandrekar, *Tacrolimus and cyclosporine A inhibit allostimulatory capacity and cytokine production of human myeloid dendritic cells*. J Investig Med, 2001. **49**(5): p. 442-9.
182. Auffermann-Gretzinger, S., et al., *Rapid establishment of dendritic cell chimerism in allogeneic hematopoietic cell transplant recipients*. Blood, 2002. **99**(4): p. 1442-8.

References

183. Chklovskaya, E., et al., *Reconstitution of dendritic and natural killer-cell subsets after allogeneic stem cell transplantation: effects of endogenous flt3 ligand*. Blood, 2004. **103**(10): p. 3860-8.
184. Arpinati, M., et al., *Granulocyte-colony stimulating factor mobilizes T helper 2-inducing dendritic cells*. Blood, 2000. **95**(8): p. 2484-90.
185. Pulendran, B., et al., *Flt3-ligand and granulocyte colony-stimulating factor mobilize distinct human dendritic cell subsets in vivo*. J Immunol, 2000. **165**(1): p. 566-72.
186. Klanginsirikul, P. and N.H. Russell, *Peripheral blood stem cell harvests from G-CSF-stimulated donors contain a skewed Th2 CD4 phenotype and a predominance of type 2 dendritic cells*. Exp Hematol, 2002. **30**(5): p. 495-501.
187. Doderio, A., et al., *Reduced-intensity conditioning containing low-dose alemtuzumab before allogeneic peripheral blood stem cell transplantation: graft-versus-host disease is decreased but T-cell reconstitution is delayed*. Exp Hematol, 2005. **33**(8): p. 920-7.
188. Reddy, V., et al., *Low dendritic cell count after allogeneic hematopoietic stem cell transplantation predicts relapse, death, and acute graft-versus-host disease*. Blood, 2004. **103**(11): p. 4330-5.
189. Sato, K., et al., *Regulatory dendritic cells protect mice from murine acute graft-versus-host disease and leukemia relapse*. Immunity, 2003. **18**(3): p. 367-79.
190. Fagnoni, F.F., et al., *Reconstitution dynamics of plasmacytoid and myeloid dendritic cell precursors after allogeneic myeloablative hematopoietic stem cell transplantation*. Blood, 2004. **104**(1): p. 281-9.
191. Chan, G.W., et al., *Persistence of host dendritic cells after transplantation is associated with graft-versus-host disease*. Biol Blood Marrow Transplant, 2003. **9**(3): p. 170-6.
192. Mapara, M.Y., et al., *Donor lymphocyte infusion-mediated graft-versus-leukemia effects in mixed chimeras established with a nonmyeloablative conditioning regimen: extinction of graft-versus-leukemia effects after conversion to full donor chimerism*. Transplantation, 2003. **76**(2): p. 297-305.
193. MacDonald, K.P., et al., *Characterization of human blood dendritic cell subsets*. Blood, 2002. **100**(13): p. 4512-20.

Curriculum vitae

Name:	Weigl Roman
Academic Credentials:	Mag. rer. nat, Dipl.-Ing.
Present Address:	Neusiedlgasse 7, 2105 Oberrohrbach, Lower Austria
Date and Place of Birth:	June 10 th 1974, in Stockerau, Lower Austria
Family status:	unmarried
Nationality:	Austrian
Federal Army Force:	From July 1993 to March 1994
Education:	<p>Studies for the doctor's degree since Dec 2001</p> <p>Master's program in Teacher Training Program in Chemistry, Nutrition and Home Economics (Mag.rer.nat.) in 2005, University of Technology Vienna</p> <p>Diploma program in Technical Chemistry with concentration in Biotechnology, Biochemistry and Food Nutrition (Dipl.-Ing.) in 2001, University of Technology Vienna</p> <p>Matura 1993 at the De La Salle School, Anton-Böckgasse 37, Vienna</p>
Positions	<p>Since Sept 2005 teaching Chemistry and Nutrition at two secondary schools in Vienna</p> <p>Since Dec 2001 doctoral dissertation studies in the laboratories of the Bone Marrow Transplantation Unit, Medical University, Vienna</p> <p>Diploma studies from July 2000 to June 2001 at the Institute of Applied Microbiology, University of Natural Resources and Applied Life Sciences, Vienna</p>
Publications	<p>Buchta C, Hanslik-Schnabel B, Weigl R, <i>et al.</i> <i>Quality of drainage blood: Survival of red cells after re-transfusion and content of free hemoglobin and potassium.</i> Int J Surg 2005 Vol 4</p> <p>Development of a method for capturing secreted recombinant proteins on the cell surface of <i>Pichia pastoris</i>. Diploma Thesis, TU Vienna</p>
Professional Practice	<p>Jan. 2005: Design, Analyses and Interpretation of Clinical Studies; 21 training-points; MUW Vienna</p> <p>Nov. 2004: SAS Programming Manipulating Data with the DATA Step; SAS Center Vienna</p> <p>Nov. 2003: GKPRO Basic Knowledge for SAS Programmer and Data Warehouse Developer; SAS Center Vienna</p>